

Abundances in a Large Sample of Stars in M3 and M13¹

Judith G. Cohen² and Jorge Melendez²

ABSTRACT

We have carried out a detailed abundance analysis for 21 elements in a sample of 25 stars with a wide range in luminosity from luminous giants to stars near the main sequence turnoff in the globular cluster M13 ([Fe/H] -1.50 dex) and in a sample of 13 stars distributed from the tip to the base of the RGB in the globular cluster M3 ([Fe/H] -1.39 dex). The analyzed spectra, obtained with HIRES at the Keck Observatory, are of high dispersion ($R=\lambda/\Delta\lambda=35,000$). Most elements, including Fe, show no trend with T_{eff} , and low scatter around the mean between the top of the RGB and near the main sequence turnoff, suggesting that at this metallicity, non-LTE effects and gravitationally induced heavy element diffusion are not important for this set of elements over the range of stellar parameters spanned by our sample.

We have detected an anti-correlation between O and Na abundances, observed previously among the most luminous RGB stars in both of these clusters, in both M3 and in M13 over the full range of luminosity of our samples, i.e. in the case of M13 to near the main sequence turnoff. M13 shows a larger range in both O and Na abundance than does M3 at all luminosities, in particular having a few stars at its RGB tip with unusually strongly depleted O.

We detect a correlation between Mg abundance and O abundance among the stars in the M13 sample. We also find a decrease in the mean Mg abundance as one moves towards lower luminosity, which we tentatively suggest is due to our ignoring non-LTE effects in Mg.

Although CN burning must be occurring in both M3 and in M13, and ON burning is required for M13, we combine our new O abundances with published C and N abundances to confirm with quite high precision that the sum of C+N+O is constant near the tip of the giant branch, and we extend this down to the bump in the luminosity function. The same holds true for a smaller sample in M3, with somewhat larger variance.

Star I-5 in M13 has large excesses of Y and of Ba, with no strong enhancement of Eu, suggesting an *s*-process event contributed to its heavy element abundances.

The mean abundance ratios for M3 and for M13 are identical to within the errors. They show the typical pattern for metal-poor globular clusters of scatter among the

¹Based in part on observations obtained at the W.M. Keck Observatory, which is operated jointly by the California Institute of Technology, the University of California, and the National Aeronautics and Space Administration.

²Palomar Observatory, Mail Stop 105-24, California Institute of Technology, Pasadena, Ca., 91125, jlc(jorge)@astro.caltech.edu

light elements, with the odd atomic number elements appearing in the mean enhanced. The Fe-peak elements, where the odd atomic number elements are excessively depleted, do not show any detectable star-to-star variations in either cluster.

The abundance ratios for 13 Galactic globular clusters with recent detailed abundance analyses, obtained by combining our samples with published data, are compared to those of published large surveys of metal-poor halo field stars. For most elements, the agreement is very good, suggesting a common chemical history for the halo field and cluster stars.

Subject headings: globular clusters: general — globular clusters: individual (M3, M13) — stars: evolution – stars: abundances

1. Introduction

Abundance determinations of stars in Galactic globular clusters can provide valuable information about important astrophysical processes such as stellar evolution, stellar structure, Galactic chemical evolution and the formation of the Milky Way. Surface stellar abundances of C, N, O, and often Na, Mg, and Al are found to be variable among red giants within a globular cluster. The physical process responsible for these star-to-star element variations is still uncertain (see the reviews of Kraft 1994 and Pinsonneault 1997, as well as Cohen, Briley & Stetson 2002 and Ventura *et al.* 2001).

In order to study the origin of the star-to-star abundance variations, we started a program to determine chemical abundances of the nearer Galactic globular cluster stars. In previous papers in this series, we studied a sample of 25 stars in M71, the nearest globular cluster reachable from the northern hemisphere (Cohen, Behr & Briley 2001; Ramírez *et al.* 2001; Ramírez & Cohen 2002), followed by a similar sized sample in M5, the nearest intermediate metallicity globular cluster accessible from a northern hemisphere site (Ramírez & Cohen 2003). Our sample in each cluster includes stars over a large range in luminosity, in order to study in a consistent manner red giants, horizontal branch stars, and stars at the main sequence turnoff. We measured the iron abundance and the abundance ratios for ~ 20 elements with respect to Fe in each case, using high dispersion ($R=\lambda/\Delta\lambda=35,000$) optical spectra obtained with HIRES at the Keck Observatory. We found that the [Fe/H] abundances¹ from both Fe I and Fe II lines agree with each other and with earlier determinations and that the [Fe/H] obtained from Fe I and Fe II lines is constant within the rather small uncertainties over the full range in effective temperature (T_{eff}) and luminosity (Ramírez *et al.* 2001). We also found that the neutron capture, the iron peak and the α -element abundance ratios show no trend with T_{eff} , and low scatter around the mean between the top of the RGB and

¹The standard nomenclature is adopted; the abundance of element X is given by $\epsilon(X) = N(X)/N(H)$ on a scale where $N(H) = 10^{12}$ H atoms. Then $[X/H] = \log_{10}[N(X)/N(H)] - \log_{10}[N(X)/N(H)]_{\odot}$, and similarly for $[X/Fe]$.

near the main sequence turnoff in each cluster. We detected an anti-correlation between O and Na abundances in our sample of members of M71 which extends to the main sequence. We observed a statistically significant correlation in M5 between Al and Na abundances extending to $M_V = +1.8$, fainter than the luminosity of the RGB bump in M5. We merged our data with data compiled from the literature for the Na – O anticorrelation seen among globular cluster stars to find that the slope of this relation is the same for all clusters studied to date, but the amplitude of the effect varies from cluster to cluster.

In the present paper, we study a sample of stars in M3 and in M13, globular clusters of even lower metallicity than M5, again covering a wide range in luminosity. There are many photometric studies of these two clusters as they are the classic second parameter pair, having similar abundances yet very different horizontal branch morphologies. Those which were utilized in the present work are noted in §5.

The most important characteristic of the globular cluster M13 as compared to M71 and M5 is that M13 is well known to show unusually large star-to-star differences in abundance of Al, Mg, Na and O among its red giants (see, e.g. Kraft *et al.* 1997). A study of C and N variations among a large sample of M13 stars from the tip of the red giant branch to the main sequence turnoff is given in Briley, Cohen & Stetson (2002, 2004); large star-to-star differences in C and N abundances were found. M3, on the other hand, resembles M5 and M71 in being relatively inactive in this regard, although its metallicity is quite close to that of M13.

M3 and M13 have been the subject of several previous high dispersion analyses, beginning with that of Cohen (1978). Sneden *et al.* (2004) have recently presented a high dispersion study of 28 red giants in M3 to confirm the lower level of star-to-star variations in this cluster in contrast to M13; they compare their results with the older work of their group on both M3 and M13, see, e.g. Kraft *et al.* (1997).

M3 is more distant than M5 or M71, and we made no effort to reach the main sequence turnoff in this cluster, although our sample reaches far down the RGB. For M13, which is at a distance comparable to that of M5, we reach close to the main sequence turnoff.

2. Observations

To the maximum extent possible, the observing strategy, the atomic data and the analysis procedures used here are identical to those developed in our earlier papers on M71 and on M5 (Cohen, Behr & Briley 2001; Ramírez *et al.* 2001; Ramírez & Cohen 2002; Ramírez & Cohen 2003)

2.1. The Stellar Sample

Stars were chosen to span the range from the tip of the red giant branch to the base of the subgiant branch in M13 and to well below the RGB bump in M3. Both of these clusters lie far from the Galactic plane, hence field star contamination is minimal. The photometric database of Stetson, Hesser & Smecker-Hane (1998) and Stetson (2000), which is described in considerable detail in Cohen, Briley & Stetson (2002), was used to verify that the selected stars lie on the cluster locus in various color-magnitude diagrams. This database, in the form available at the time, only included small sections of the solid angle required to fully cover each of these two clusters.

Pairs were selected in M3 for which both stars lie below the luminosity of the RGB bump and appear, based on their broad band colors, to be members. A separation of less than 9 arcsec was required. Only reasonably isolated stars were selected. To this we added a sample of bright giants, most of which were selected to span the full range in Na and/or O abundances from Kraft *et al.* (1992). Throughout this paper, the star names are from Sandage (1953) for the brightest stars in M3, from Von Zeipel (1908) for the two bright stars near the center of M3 not included in the former work, or, for the stars previously not cataloged, are assigned based on the object’s J2000 coordinates, so that a star with RA, Dec of 13 hr 13 m 13.5 s +28° 15′ 15″ is identified in this paper with the name Crmrss_dmds. For M13, the primary source of star identifications is Arp (1955) (see also Kadla 1966). For the M13 stars not previously cataloged, names are assigned based on the object’s J2000 coordinates, so that a star with RA, Dec of 16 hr 16 m 16.5 s +36° 15′ 15″ is identified in this paper with the name Crmrss_dmds.

Our sample in M3 totals 13 stars, including 5 on the RGB well below the luminosity of the HB and one RHB star. Figure 1a shows the sample in M3 superposed on a color-magnitude diagram of this globular cluster.

Eight pairs of stars were selected for observation in M13 using criteria similar to those used for the M3 pairs. Two of the 16 stars turned out not to be members of M13, and two others are horizontal branch stars too hot to analyze. These members of M13 reach to $V=17.9$ mag. In addition, 13 bright giants were observed, chosen to have previous observations of [C/Fe] and of [N/Fe] from Suntzeff (1981) or from Smith *et al.* (1996). This sample include stars covering the full range of Na, Mg and Al abundances found in M13 by Kraft *et al.* (1997). Figure 1b shows the sample in M13 superposed on a color-magnitude diagram of this globular cluster.

Our sample in M13 totals 25 stars reaching from the tip of the RGB to almost the main sequence turnoff, plus two hot HB stars which we have not attempted to analyze.

2.2. Data Acquisition and Reduction

All spectra were obtained with HIRES (Vogt *et al.* 1994) at the Keck Observatory. In May 2001, we observed with an instrumental configuration similar to that used in our earlier globular

cluster work. The wavelength range from 5500 to 7800 Å was covered with gaps between the orders due to the undersized HIRES detector. We wanted to include key lines of critical elements, specifically the 6300, 6363 [OI] lines, the 7770 O triplet, the Na doublet at 6154, 6160Å, and the 6696, 6698Å Al I lines. However, it was impossible to create a single instrumental configuration which included all the desired spectral features in the wavelength range 6000 to 8000 Å, and a single compromise configuration had to be adopted. In particular, although the 6696, 6698Å Al I doublet is the most useful feature of that element in this spectral region, we could not get it to fit into a single HIRES setting together with the O lines. A 1.1 arcsec wide slit, corresponding to a spectral resolution of 34,000, was used. A maximum slit length of 14 arc sec can be used with this instrumental configuration without orders overlapping. However, we found that covering beyond 7000 Å, while highly desirable to reach the O I triplet, added little else of interest in the spectra of these low metallicity stars. Thus for the June 2003 observations (the spring 2002 run being totally lost to weather), we shifted the instrument configuration toward the blue, covering the range 4650 to 7010 Å, again with small gaps between the orders. The maximum slit length without orders overlapping at the blue end of the spectrum is then reduced to 7 arcsec. We call these two instrument configurations the “yellow” and the “red” configurations.

Since an image rotator for HIRES is available (built under the leadership of David Tytler), if we can find pairs of program stars with suitable separations, they can be observed together on a single exposure. Pairs were pre-selected as described above to contain two members of the fainter M3 stars. In May 2001, three (6) pairs of M3 (M13) stars² were observed with HIRES using the “red” setting. One of the six stars in the M3 pairs turned out to be a red horizontal branch star. In June 2003, two of the pairs in M3 as well as seven bright giants were reobserved at higher SNR using the “yellow” setting; the third pair was too far apart for this HIRES configuration. For M13, two of the pairs were reobserved in June or August 2003, as were two new pairs as well as several bright giants with the “yellow” HIRES configuration.

The desired minimum SNR was 75 over a 4 pixel resolution element for a wavelength near the center of the HIRES detector. This is calculated strictly from the counts in the object spectrum, and excludes noise from cosmic ray hits, sky subtraction, flattening problems, etc. Since the nights were relatively dark, sky subtraction is not an issue except at the specific wavelengths corresponding to strong night sky emission lines, such as the Na D doublet. This SNR goal was achieved for most of the stars reported here; see Table 1b for details regarding the faintest stars in the M13 sample. Note that for a fixed SNR in the continuum, for a star of a given luminosity, the lower metallicity of these clusters leads to weaker absorption lines, making it difficult to maintain the desired precision of the analysis. It is this which led to the repeat spectra with the “yellow” HIRES configuration.

The magnitude of the cluster radial velocity is large for both M3 and M13, and the cluster abundances are low. It was easy to tell after one integration whether or not a star is a member

²When values of a parameter are given simultaneously for both M3 and M13, the value for M3 is given, with that for M13 following in parentheses.

of the cluster. Approximate measurements of the radial velocity were made on line, and if a star was determined to be a non-member, the observations were terminated. Very few non-members turned up in this way. If the probable non-member was the second component in a pair, an attempt was made to switch to another position angle to pick up a different second star, when a possible candidate that was bright enough was available within the maximum allowed separation.

These data were reduced using a combination of Figaro scripts and the software package MAKEE³.

Table 1a gives details of the HIRES exposures for each star, with the total exposure time for each object. All long integrations were broken up into separate exposures, each 1200 sec long, to optimize cosmic ray removal. The last column of the table gives the heliocentric radial velocity for each star, measured from the HIRES spectra; see Ramírez & Cohen (2003) for the details of the procedure used to determine v_r . Based on their measured v_r , the 13 stars of our sample are all members of M3. They have a mean v_r of -147.6 km s^{-1} , which agrees exactly with the value of Harris (1996). The velocity dispersion of our sample in M3 is $\sigma = 4.7 \pm 1 \text{ km s}^{-1}$, which when the instrumental contribution is removed is about 4.4 km s^{-1} . This is comparable to the value of 5.6 km s^{-1} obtained by Gunn & Griffin (1979) and by Pryor, Latham & Hazen (1988). For the 27 stars in M13 in our sample, the mean v_r is -245.7 km s^{-1} , with $\sigma = 7.1 \text{ km s}^{-1}$. This is identical to the velocity dispersion obtained by Lupton, Gunn & Griffin (1989) from a sample of more than 130 bright giants.

Based on their HIRES spectra, stars C41262_2248 (V=15.6) and C40560_2847 are not members of M13.

3. EQUIVALENT WIDTHS

The search for absorption features present in our HIRES data and the measurement of their equivalent width (W_λ) was done automatically with a FORTRAN code, EWDET, developed for our globular cluster project. Details of this code and its features are described in Ramírez *et al.* (2001). Because M3 and M13 are considerably more metal poor than M5 or M71, the determination of the continuum level was easier, and the equivalent widths measured automatically should be more reliable.

The initial list of unblended atomic lines and their atomic parameters was adopted from our work on M5, where it was created by inspection of the spectra of M5 stars, as well as the online Solar spectrum taken with the FTS at the National Solar Observatory of Wallace *et al.* (1998) and the set of Solar line identifications of Moore *et al.* (1966). The list of lines identified and measured by EWDET was then correlated, taking the radial velocity into account, to the template list of suitable

³MAKEE was developed by T.A. Barlow specifically for reduction of Keck HIRES data. It is freely available on the world wide web at the Keck Observatory home page, <http://www2.keck.hawaii.edu:3636/>.

unblended lines to specifically identify the various atomic lines. The automatic identifications were accepted as valid for lines with $W_\lambda \geq 15$ mÅ. They were checked by hand for all lines with smaller W_λ and for all the rare earths. The equivalent widths of the O I lines were measured by hand, since they were generally very weak. The resulting W_λ for ~ 320 lines in the spectra of the 13 stars in M3 are listed in Table 5a. W_λ for the 25 stars in M13 are listed in Tables 5b and Table 5c. Note that lines with $W_\lambda > 200$ mÅ are not generally tabulated and are not used unless there are no other available lines of that species.

4. ATOMIC PARAMETERS

The provenance of the gf values and damping constants we adopt in our analysis of M3 and M13 stars is discussed below. In general, the atomic data and the analysis procedures used here are identical to those developed in our recent paper on M5 (Ramírez & Cohen 2003).

4.1. Transition Probabilities

Transition probabilities for the Fe I lines were obtained from several laboratory experiments, including studies of Fe I absorption lines produced by iron vapor in a carbon tube furnace (Blackwell *et al.* 1979, 1982a,b, 1986) (Oxford Group), measurement of radiative lifetimes of Fe I transitions by laser induced fluorescence (O’Brian *et al.* 1991; Bard *et al.* 1991; Bard & Kock 1994), Fe I emission line spectroscopy from a low current arc (May *et al.* 1974), and emission lines of Fe I from a shock tube (Wolnik *et al.* 1971). We also considered solar gf values from Thévenin (1989, 1990) when needed. The Fe I gf values obtained by the different experiments were placed into a common scale with respect to the results from O’Brian *et al.* (1991) (see Ramírez *et al.* (2001) for details). The gf values for our Fe II lines were taken from the solar analysis of Blackwell *et al.* (1980), Biémont *et al.* (1991), and from the semi-empirical calculations of Kurucz (1993b). For Fe I and Fe II gf values, we used the same priority order for the gf values from different experiments as in Ramírez *et al.* (2001).

Transition probabilities for the lines of atomic species other than iron were obtained from the NIST Atomic Spectra Database (NIST Standard Reference Database #78, see (Weise *et al.* 1969; Martin *et al.* 1988; Fuhr *et al.* 1988; Weise *et al.* 1996)) when possible. Nearly 80% of the lines selected as suitable from the HIRES spectra have transition probabilities from the NIST database. For the remaining lines the gf values come from the inverted solar analysis of Thévenin (1989, 1990), with the exception of La II, Nd II and Eu II lines, for which we have updated our values to those of Lawler, Bonvallet & Sneden (2001), Lawler *et al.* (2001) and Den Hartog *et al.* (2003).

Six elements show hyperfine structure splitting (Sc II, V I, Mn I, Co I, Cu I, and Ba II). The corresponding hyperfine structure constants were taken from Prochaska *et al.* (2000). For Ba II, we adopt the HFS from McWilliam (1998). We use the laboratory spectroscopy of Lawler, Bonvallet

& Sneden (2001) and Lawler *et al.* (2001) to calculate the HFS patterns for La II and for Eu II.

We use the damping constants of Barklem, Piskunov & O’Mara (2000) which were calculated based on the theory of Anstee, Barklem & O’Mara (Barklem, Anstee & O’Mara 2000) when available. If there is no entry in their database, as in our earlier work, the damping constants were set to twice that of the Unsöld approximation for van der Waals broadening following Holweger *et al.* (1991).

4.2. Solar Abundances

The regime in which we are operating is so metal poor that we cannot in general attempt to calculate Solar abundances corresponding to our particular choices of atomic data because the lines seen in these metal poor globular cluster stars are far too strong in the Sun. We must therefore rely on the accuracy of the *gf* values for each element across the large relevant range of line strength and wavelength. We adopt the Solar abundances of Anders & Grevesse (1989) for most elements. For Ti and for Sr, we adopt the slightly modified values given in Grevesse & Sauval (1998). For the special cases of La II, Nd II and Eu II we use the results found by the respective recent laboratory studies cited above. For Mg, we adopt the slightly updated value suggested by Holweger (2001), ignoring the small suggested non-LTE and granulation corrections, since we do not implement such in our analyses.

There is considerable controversy regarding the abundances of the CNO elements in the Sun, with the recent results of Allende-Prieto, Lambert & Asplund (2002), Asplund (2003) and Asplund *et al.* (2004) being considerably (~ 0.2 dex) lower than those of Anders & Grevesse (1989) and somewhat lower than those of Grevesse & Sauval (1998). We have derived an inverse Solar O abundance for our particular choice of atomic data and of model atmospheres using both the forbidden doublet at 6300,6363 Å and the triplet at 7770 Å. The equivalent widths of these lines in the Sun were measured from the Solar atlas of Kurucz *et al.* (1984), and checked in the McDonald Observatory Solar spectrum used by Allende-Prieto *et al.* (2004). Corrections for the contribution of the Ni I line for the 6300 Å line (Allende Prieto, Lambert & Asplund 2001) and the CN lines for the 6363 Å line (Asplund *et al.* 2004) were made. We adopted the O abundance from [OI]; after applying a non-LTE correction interpolated from the calculations of Gratton *et al.* (1999), the O abundance from the triplet lines is only 0.05 dex smaller than derived from the forbidden lines.

We adopt $\log\epsilon(\text{Fe}) = 7.45$ dex for iron following the revisions in the Solar photospheric abundances suggested by Asplund *et al.* (2000) and by Holweger (2001). This value is somewhat lower than that given by Grevesse & Sauval (1998) and considerably lower than that recommended by Anders & Grevesse (1989). Some papers in the literature use the Grevesse & Sauval (1998) value and some older ones use 7.67 dex, the value recommended by Anders & Grevesse (1989). In such cases, their values of [Fe/H] will be 0.1 to 0.2 dex smaller than ours while their abundance ratios [X/Fe] the same amount larger than ours.

Table 2 gives the Solar abundances used here.

5. Stellar Parameters

We follow the philosophy developed in our earlier work on globular cluster stars and described in Cohen, Behr & Briley (2001). T_{eff} is derived by comparing reddening-corrected broad band colors with the predictions of grids of model atmospheres. We utilize here the grid of predicted broad band colors and bolometric corrections of Houdashelt, Bell & Sweigart (2000) based on the MARCS stellar atmosphere code of Gustafsson *et al.* (1975). In Cohen, Behr & Briley (2001) we demonstrated that the Kurucz and MARCS predicted colors are essentially identical, at least for the specific colors used here. We adopt current values from the on-line database of Harris (1996) for the distances of 10.4 (7.5) kpc for M3 (M13) with a reddening of $E(B-V) = 0.01$ (0.02) mag. The relative extinction in various passbands is taken from Cohen *et al.* (1981) (see also Schlegel, Finkbeiner & Davis 1998). Based on the earlier high dispersion analyses of Kraft *et al.* (1997) and Sneden *et al.* (2004), we adopt as an initial guess $[Fe/H] = -1.5$ dex for these two globular clusters.

Our primary source for optical photometry is the BVI database of Stetson (Stetson, Hesser & Smecker-Hane 1998; Stetson 2000). All the bright giants in M3 except VZ 1000 and VZ 1397, which are too close to the center of this cluster, are included there. All components of the pairs except V-30 + V-31, which are too far from the center of M3, are included as well. Photometry for the missing stars was obtained from Sandage (1953), Johnson & Sandage (1956), Buonanno *et al.* (1994) or Ferraro *et al.* (1997), with preference given to the most recent study.

For M13, we used (in order of preference) the optical photometry of Cudworth (1979), Rey *et al.* (2001) Buonanno *et al.* (1994), and Stetson (Stetson, Hesser & Smecker-Hane 1998; Stetson 2000). After a small adjustment in the zero point of the (uncalibrated) photometry of Buonanno *et al.* (1994), the agreement between the various datasets is reasonable. The area in M13 covered by the work of Johnson & Bolte (1998), Rosenberg *et al.* (2000) and by Piotto *et al.* (2002) does not overlap with our stars, nor does that of the IR photometry of Davidge & Courteau (1999) and of Valenti *et al.* (2004).

We only used V and I magnitudes from these sources, combining them with J and K photometry from 2MASS (Skrutskie *et al.* 1997; Cutri *et al.* 2003). This worked extremely well for the bright giants, with a scatter in deduced T_{eff} from V-I, V-J and V-K of under 40 K. The fainter stars in our sample (i.e. the pairs) show much larger scatter in their deduced T_{eff} from the various colors. These stars are too crowded (and in some cases rather faint) for 2MASS, which uses an aperture size of 2 arcsec. This problem is more serious in M13, as our sample reaches fainter there than in M3; a large fraction of the pairs observed in M13 had no entry or only a single entry in the 2MASS database.

To get around this problem, in April, 2004 we observed the fields of the fainter stars in our samples in both M3 and M13 with the Wide Field Infrared Camera (Wilson *et al.* 2003) at the 5-m

Hale Telescope for the purpose of establishing reliable J,K magnitudes for the fainter stars in our sample. The 2MASS colors of nearby isolated somewhat brighter stars were used to calibrate our WIRC photometry. This new infrared photometry for only the pairs in M3 and M13 is listed in Table 3. The agreement with 2MASS is very good for the brighter, wider pairs.

With improved infrared photometry in hand, the observed broad band colors V-I, V-J and V-K for each program star from the sources listed above, corrected for extinction, were used to determine T_{eff} . The set of models with metallicity of -1.5 dex, nearest to our initial estimate of $[Fe/H]$, is used. Table 4a (Table 4b) lists the T_{eff} thus deduced for the sample in M3 and in M13. The reddening to each of these clusters is small, making possible extinction variations across the cluster irrelevant. We assume a random photometric error of 0.02 mag applies to $V - I$ from Stetson (2000). Following Cohen, Behr & Briley (2001), this translates into a total uncertainty in T_{eff} of 75 K for giants rising to 150 K for main sequence stars using only $V - I$. The errors in T_{eff} deduced from V-J or V-K are about a factor of two smaller.

We have slightly smoothed the T_{eff} for the fainter stars in our sample by small amounts to ensure that stars at the approximately same evolutionary stage have approximately the same stellar parameters.

Once an initial guess at T_{eff} has been established from a broad band color, it is possible with minimal assumptions to evaluate $\log(g)$ using observational data. The adopted distance modulus for the cluster, initial guess at T_{eff} for the star, and an assumed stellar mass (we adopt $0.8 M_{\odot}$ for the stars in M3 and in M13) are combined with the known interstellar absorption, the bolometric corrections predicted by the model atmosphere grid, as well as a broad band observed V mag to calculate $\log(g)$. An iterative scheme is used to correct for the small dependence of the predictions of the model atmosphere grid on $\log(g)$ itself. Rapid convergence is achieved.

It is important to note that because of the constraint of a known distance to each cluster, the uncertainty in $\log(g)$ for any star in our sample is small, ≤ 0.1 dex when comparing two members of the same cluster. Propagating an uncertainty of 15% in the cluster distance, 5% in the stellar mass, and a generous 3% in T_{eff} , and ignoring any covariance, leads to a potential systematic error of ± 0.2 dex for $\log(g)$.

6. Abundance Analysis

We rely heavily in the present work on the procedures and atomic data for abundance analyses of metal-poor stars described in our earlier papers referenced above reporting analyses of globular cluster stars.

Given the derived stellar parameters from Table 4a (4b), we determined the abundances using the equivalent widths obtained as described above. The abundance analysis is carried out using a current version of the LTE spectral synthesis program MOOG (Snedden 1973). We employ the

grid of stellar atmospheres from Kurucz (1993a) without convective overshoot, when available. We compute the abundances of the species observed in each star using the four stellar atmosphere models with the closest T_{eff} and $\log(g)$ to each star’s parameters. The abundances were interpolated using results from the closest stellar model atmospheres to the appropriate T_{eff} and $\log(g)$ for each star given in Table 4a (4b).

The microturbulent velocity (v_t) of a star is determined spectroscopically by requiring the abundance to be independent of the strength of the lines. The uncertainty in our derived v_t is estimated to be $+0.4, -0.2$ km s $^{-1}$ based on repeated trials with the same line list for several stars varying v_t . We apply this technique here to the large sample of detected Fe I lines in each star; the results are listed with the stellar parameters in Table 4a (4b).

Iron is the only element with more than a few detected lines in each of two different stages of ionization, hence useful for determining the ionization equilibrium. Figure 2 (9) shows the Fe abundance as inferred from lines of Fe I as well as the Fe ionization equilibrium for the stars in our sample in M3 (M13). The ionization equilibrium for Fe I versus Fe II is satisfactory in each of these globular clusters. The average difference between $[\text{Fe}/\text{H}]$ as inferred from Fe II lines and from Fe I lines for the 8 luminous RGB stars in M3 is 0.00 dex, while the largest difference (in absolute value) is only 0.11 dex. For the 5 low luminosity giants in M3, the range is somewhat larger, but the average difference is only 0.01 dex. Over the full M13 sample, the average difference is only 0.04 dex. The Fe ionization equilibrium shifts by 0.2 dex for a 100 K change in T_{eff} in this temperature regime, so our ± 50 K uncertainty in T_{eff} is capable of producing the observed dispersion in Fe ionization equilibrium. For Ti, which has far fewer detected lines of the neutral species than does Fe, the mean difference in $[\text{Ti}/\text{Fe}]$ as deduced from the neutral lines and from the ionized lines for the stars in our sample in M3 (M13) is only 0.10 (0.15) dex.

Following upon our previous work, no non-LTE corrections have been applied for the specific ions studied in the M3 and M13 stars, with the exception of O, where we rely on the calculations of Gratton *et al.* (1999). The detailed non-LTE calculations of Gratton *et al.* (1999) and of Takeda *et al.* (2003) for the two Na I doublets we use suggest that for this regime of T_{eff} , the non-LTE correction is about +0.15 dex. For Ba II, the non-LTE calculations of Mashonkina & Gehren (1999) and of Mashonkina, Gehren & Bikmaev (2000) suggest that a non-LTE correction of -0.1 dex is appropriate for the metallicity of M3 and M13 and the set of Ba II lines we used. In comparing with other abundance analyses, the issue of implementing non-LTE corrections and their adopted values must be considered.

The resulting abundance ratios for 13 (25) stars in M3 (M13) are given in Tables 6a to 6e (Tables 9a to 9e). The abundance ratio for a species with only one detected line in a particular star is assigned an uncertainty of 0.10 dex. Table 7 indicates the changes in derived abundance ratios for small changes in the adopted stellar parameters, the $[\text{Fe}/\text{H}]$ for the adopted model atmosphere, or the set of W_λ for the lines of each species. Table 8 (Table 10) gives the mean abundance and 1σ variance for the species observed in M3 (M13).

6.1. Comments on Individual Elements

The oxygen abundance is derived from the forbidden lines at 6300 and 6363 Å and from the triplet lines at 7770 Å when these were included within the wavelength range and were detected. The subtraction of the night sky emission lines for the forbidden lines was reasonably straightforward given that the radial velocities of M3 and of M13 sufficiently different from 0 km s⁻¹ that their W_λ can be reliably measured. The C/O ratio was assumed to be Solar. Small non-LTE corrections, calculated from Gratton *et al.* (1999), were applied for abundances deduced from the O I triplet. Since $N(\text{CN})/N(\text{H})$ is roughly $\propto \{N(\text{Fe})/N(\text{H})\}^2$, CN lines are much weaker relative to O lines in metal poor stars, so that the correction for CN contamination to the 6363 Å [OI] line for the M3 and M13 stars is negligible. Finally, the contribution of the Ni I line to the 6300 Å forbidden line of O can be ignored in M3 and M13, as we will see that O/Fe (and O/Ni) is larger than the Solar value⁴. The O abundance from the triplet lines is given with respect to [Fe/H] deduced from lines of Fe I, while that from the forbidden lines is given with respect to Fe II; the mean [O/Fe] becomes 0.04 dex larger if expressed using the Fe II lines instead.

The usual lines of Al in this wavelength region, in particular the 6696,6698 Å doublet, can not be reached with our HIRES configuration as they fall in an interorder gap. We have detected the much weaker Al I line at 5557 Å in the coolest M13 giants only. There is a difference of 0.4 dex between the Al abundance we deduce and that obtained by Sneden *et al.* (2004) (see also Kraft *et al.* 1997; Shetrone 1996) for the two M13 luminous giants in common. The *gf* value adopted for this rarely used line (−1.67 dex) may be wrong, or non-LTE may play a role; Baumüller & Gehren (1997) have demonstrated that non-LTE effects can be very strong for Al I features in this T_{eff} range, and the effect varies a lot from multiplet to multiplet.

The Na abundance was obtained from the 5680 Å doublet in general. For the faintest, hottest stars in M13, these lines become very weak, and so the Na abundance was checked using the D lines (after a small empirical correction not exceeding 0.08 dex to put them on the same abundance scale as for the weak Na lines).

The abundances of the elements with respect to Fe, [X/Fe], as a function of T_{eff} are shown in Figures 3 (10), covering O, Na, Mg and Si, Figures 4 (11), which include Ca, Sc, Ti and V, Figures 5 (12), which include Cr, Mn, Co and Ni, Figures 6 (13), which include Cu, Zn, Y and Zr, and Figure 7 (14), for Ba, La, Nd, Eu and Dy. Note the apparent star-to-star variation in [O/Fe] and in [Na/Fe], which becomes undetectably small, if it exists at all, for the elements heavier than Na. The scatter for Ni, which is detected with several lines in every star, is remarkably small. Even the rare earths, for which in general only a few weak lines are detected only in the more luminous stars, show very small variations in general.

⁴Sneden *et al.* (2004) estimate that W_λ for this Ni I lines is less than 0.5 mÅ.

6.2. Abundance Spreads

Detection and quantitative measurement of star-to-star variations in abundance ratios within a single Galactic globular cluster is one of the primary goals of this effort. As a global indicator of the presence of such effects we use a parameter we call the “spread ratio” (SR). The numerator of SR is the 1σ rms variance for the sample of 13 (25) stars in M3 (M13) about that mean abundance for each atomic species (X) with detected absorption lines, denoted σ . The mean abundance and σ for each species observed are given in the first three columns of Table 8 (Table 10). The denominator of SR is the total expected uncertainty, $\sigma(tot)$, which is the sum in quadrature of the known contributing terms. Included are a term corresponding to an uncertainty of 50 K in T_{eff} , the same for an uncertainty of 0.2 dex in $\log(g)$, and for an uncertainty of 0.2 km s⁻¹ in v_t , and the observed uncertainty [$\sigma(obs)$]. The parameter $\sigma(obs)$, which is calculated from data given in Tables 6a to 6e (Tables 9a to 9e), is taken as the variance about the mean abundance for a given species in a given star, i.e. the 1σ rms value about the mean abundance of species X in a given star/ \sqrt{N} , where N is the number of observed lines of species X . It includes contributions from errors in the measured W_λ , random errors (i.e. between lines of a given species) in the adopted gf values, etc. Some species, an example being Fe I with its very large value of N , have unrealistically small values of $\sigma(obs)$; we adopt a minimum of 0.05 dex for this parameter.

The ratio $\sigma/\sigma(tot)$ is an indication of whether there is any intrinsic star-to-star variation in [X/Fe]. A high value of this “spread ratio”, tabulated in the fifth column of this table, suggests a high probability of intrinsic scatter for the abundance of the species X . Ideally the mean SR for those elements with no star-to-star variation should be unity. However, we use the entries in Table 7 for the lowest T_{eff} , i.e. for giants near the RGB tip, to calculate $\sigma(tot)$. Since the abundance sensitivities in general decrease as T_{eff} increases, we will slightly overestimate $\sigma(tot)$, and hence underestimate SR , thus explaining why the deduced values for SR tend to be slightly less than 1. A second indication of the reality of the star-to-star variation in [X/Fe] for any species X is deduced using a χ^2 analysis, and evaluating the probability of exceeding by chance the measured value of χ^2 from our sample of stars in a globular cluster. Only O I and Na I have values of χ^2 much higher than the number of degrees of freedom ($N(star) - 1$), where $N(star)$ is the number of stars in which that species was detected.

Inspection of Table 8 shows that for all but two species the SR in M3 ranges from 0.5 to 1.1, indicating little sign of an intrinsic star-to-star range in abundance. O I and Na I, however, have SR exceeding 2.0 and their χ^2 are very large. Note that SR for Mg I is 0.7, suggesting no real star-to-star abundance variations for this element in M3. For M13, O I and Na I again have by far the largest values of SR , exceeding 2.5 in both cases, with no other species having a value exceeding 1.5. We therefore assume that the range of abundances seen in our M3 and in our M13 samples for Na I and O I represent real star-to-star abundance variations; while no other element shows definite evidence for such variations from this simple analysis, but see §7.

We have also examined whether one can discern a difference in the mean $\langle [Fe/H] \rangle$ between

stars with high and low O abundances in M13 and between stars with high and low Na abundances in M13. No statistically significant difference was found.

6.3. The Peculiar Star M13 I–5

With regard to the heavy elements, astute readers will have noticed that there is one star (M13 I–5) with anomalously high Y and Ba (see Table 9d). This star, which is too faint to have been included in any previous high dispersion analyses in this globular cluster, stands out (and is marked) in Figure 13 (Y panel) and in Figure 14 (Ba panel). It has the highest abundance of each of these two elements in the entire M13 sample; its deduced $\epsilon(Y)$ is five times the mean of the remaining 24 stars in the M13 sample. Y II has the fourth largest values of SR ($SR = 1.27$) in M13, but eliminating this star would reduce it to below 0.5. Figure 15 shows a section of the spectrum of this star compared with one of similar luminosity and T_{eff} in M13. This figure demonstrates convincingly that the very high abundance of Y measured for star M13 I–5 is definitely real.

With regard to the other heavy elements, in the spectrum of star M13 I–5 there is one weak and uncertain detection for La II, and several weak lines ascribed to Nd II; these give $[La/Fe]$ at the upper end of those for the other M13 stars and the largest (but only by ~ 0.05 dex) $[Nd/Fe]$ for any star in our sample in M13. An upper limit to the 6645 Å line of Eu II of 10.5 mÅ yields an upper limit to $[Eu/Fe]$ of +0.7 dex. Since the M13 mean for $[Eu/Fe]$ is +0.57 dex, Eu is not significantly enhanced in this star, consistent with a *s*-process enhancement. A better spectrum for this peculiar star has just been acquired, and results will be reported in a future publication.

6.4. Comparison With Previous Analyses

Since M3 and M13 are key globular clusters, there have been several previous high dispersion analyses of the most luminous stars in them. A comparison of the T_{eff} determined in the present work with those from previous investigations (most of which relied on B–V colors) for the stars in common in M3 and in M13 with the analyses of Cohen (1978), Kraft *et al.* (1992), Kraft *et al.* (1997), Cavallo & Nagar (2000) and Sneden *et al.* (2004) is shown in Table 11. The agreement is very gratifying. No difference exceeds 100 K, and most are 50 K or less.

A comparison of the mean abundance ratios of large sample of bright giants in M3 (M13) analyzed by Sneden *et al.* (2004) with our determinations is given in Table 12. The results are encouraging. The differences are given in the last column of the table. The deduced $[Fe/H]$ (Fe I) between the current work and that of Sneden *et al.* (2004) differ by 0.23 (0.13) dex, while the difference using Fe II is only 0.12 (0.03) dex. The largest difference in abundance ratios $[X/Fe]$ for M3 is 0.24 dex (for Sc II), with only 3 species (O I, Mg I and Sc II) having differences exceeding 0.15 dex. For M13, $[O/Fe]$ and $[Mg/Fe]$ both have differences exceeding 0.15 dex. Part of the difference in O arises as Sneden *et al.* (2004) adopt a Solar O abundance of 8.93 dex, 0.08 dex higher than

we do. It could also in principle, at least partially, be produced if the amplitude of the star-to-star variations of O were a function of stellar luminosity or equivalently T_{eff} , given the differences in mean luminosity of the two samples. Other differences in the details of the analysis may enter as well. For example, the difference in Ca appears to be due to difference in the absolute scaling of the Ca I *gf* values adopted by the Lick-Texas group and by us. This may also play a role for Sc II, but there are not sufficient lines in common to be certain. The HFS corrections for Sc II in these stars are probably not large enough to contribute significantly to this difference.

Because we are interested in star-to-star variations in abundance, we also carry out a comparison of our derived O and Na abundances for the individual stars in common with the sample of bright giants of Sneden *et al.* (2004), rather than comparing the mean of the samples in M3 as was done in Table 12. We choose to compare only to the most recent detailed abundance analysis for stars in these two clusters, ignoring earlier work, in the hopes of demonstrating good agreement. The results are shown in Table 13a (Table 13b); the mean differences for each species have been removed, thus removing the systematic differences in the analyses. The table reveals the scatter about the mean, i.e. the non-systematic differences, whose variance is given as the final column in each table. There are three stars in common in M3 and five in M13. For these stars in common, the Na abundances as analyzed by Sneden *et al.* (2004) and by us are in extremely good agreement, ignoring a constant offset between us and the Lick-Texas group, but the O abundances are not. Overall, for M3, the agreement is pretty good, with $\sigma \leq 0.15$ dex for 9 of the 12 species; only for [O/Fe], [Sc/Fe] and [Eu/Fe] is it larger. O has only a few weak lines in the relevant wavelength region, and difficulties in determining the O abundance are notorious. [Eu/Fe] has essentially the same mean in our analysis of M3 and of M13 as was found by Sneden *et al.* (2004). There is only one line used by both analyses, that of Eu II at 6645 Å, which is very weak. The derived Sc abundances might be affected by differences in the treatment of HFS. The largest σ is 0.22 dex, for [Eu/Fe]. In M13 two of the 8 differences have $\sigma > 0.3$ dex ([O/Fe] and [La/Fe]), again two species with only a few weak lines. (Sc is not included in Sneden *et al.*'s analysis for M13, while there are no stars in common in M3 with [La/Fe] measurements.)

Having already removed the systematic differences, one might admit “random” variations in deduced abundance ratios of up to 0.15 dex as resulting from different assumptions made in these two independent analyses. However, the larger differences found for M13, with $\sigma > 0.3$ dex for two species, suggest that the abundance errors in one or both of these analyses are being underestimated. We have compared our measured W_λ with those of the Lick-Texas group, when available. The agreement is extremely good; $W_\lambda(\text{us: Keck}) - W_\lambda(\text{Sneden et al 2004, Keck})$ has a mean of 7% with $\sigma = 7\%$, while $W_\lambda(\text{us: Keck}) - W_\lambda(\text{Kraft et al 1992, Lick})$ has a mean of -5% with $\sigma = 8\%$ ⁵.

To summarize, there is very good agreement on a star-by-star basis for the derived [Na/Fe] in M3 and in M13 for the sample of stars in common with Sneden *et al.* (2004). The agreement in de-

⁵This good agreement suggests that our adoption of the uncertainty in W_λ as 10% is reasonable.

rived $[O/Fe]$ is not as good, but fortunately the star-to-star variations in O are large. Furthermore, we believe we understand the origin of most of the discrepancies, and believe that our analysis is sound. Hence we have some confidence that we may proceed to analyze the abundance spreads in terms of star-to-star variations in $[X/Fe]$.

7. Correlated Abundance Variations of the Light Elements

C, N, O, Na, Mg, and Al are known to show correlated abundance variations from star-to-star among the most luminous stars in globular clusters; see, e.g. the review of Kraft (1994). Our simple spread ratio analysis (see §6.2) shows definite star-to-star variations in abundance of both O and Na in both M3 and in M13. Variations in Mg, if present are smaller and subtle. Al is not effectively covered in our spectra⁶.

It is well established that O and Na are anti-correlated among luminous giants in globular clusters, see, e.g. Kraft (1994). Furthermore, Ramírez & Cohen (2002) compiled the data from the literature, combined it with their own, and showed that the same linear relation can be used to fit the O and Na data for all globular clusters studied in detail thus far. The latest addition to the clusters studied in detail, NGC 2808, by Carretta, Bragaglia & Cacciari (2004), does so as well. The question of interest is what happens when we look at lower luminosity stars.

Figure 8 shows the relationship between Na and O abundances (both with respect to Fe) for our sample in M3. Also superposed is the line representing the fit for this anti-correlation determined by Sneden *et al.* (2004) for the luminous giants in M13, shifted by +0.07 dex in $[O/Fe]$. The first and last quartiles of the O–Na anti-correlation seen by Sneden *et al.* (2004) in their sample of luminous giants in M3 are indicated. There is a reasonably clear anti-correlation even for the faintest stars in our M3 sample, which agrees well with that of Sneden *et al.* (2004), given a small shift in O abundance scale. Thus the anti-correlation between O and Na persists in M3 from the RGB to at least $V = 16.6$ mag, which is about 2 mag fainter than the regime over which Sneden *et al.* (2004) established this relationship. The anti-correlation between O and Na has approximately the same slope and extends over approximately the same range among the fainter stars in M3 as it does among the most luminous M3 giants.

Although Sneden *et al.* (2004) claim a marginal detection of variations in $[Mg/Fe]$ among their sample of luminous giants in M3, with increasing Mg abundance being correlated with increasing Na abundance, we fail to find any credible evidence of such in M3; it might be only slightly larger than $\sigma(tot)$.

For M13, there is a much richer phenomenology. Figure 16 shows the relationship between Na and O abundances (both with respect to Fe) for our sample. Also superposed is the line representing

⁶Our spectra only include the line at 5557 Å, which is very weak and only detected in a few stars; they do not include the most commonly used Al lines.

the fit for this anti-correlation we determined for the luminous giants in M3, shifted vertically by +0.22 dex. The anti-correlation is immediately apparent. It contains a regime extending to very strong depletion of O at the highest values of [Na/Fe], which is not seen in M3, but was seen by Kraft *et al.* (1997) in M13. This regime is populated only by the most luminous giants in M13. It is also immediately apparent that the anti-correlation holds to the lowest luminosities probed in the present dataset, i.e. to the regime just above the main sequence turnoff in M13. With the exception of the extremely O-depleted RGB tip stars, the amplitude of the Na-O anti-correlation in M13 appears to be constant over the full range of luminosities in the present sample.

Figure 17 shows the behavior of Mg as a function of [O/Fe]. The general previously observed small trend of increasing Mg as O increases or Na decreases is present with an amplitude of ~ 0.4 dex, as was found by Kraft *et al.* (1997). This trend is present at all luminosities probed. However the mean abundance ratio [Mg/Fe] appears to decrease with decreasing luminosity along the RGB. The effect is small, ~ 0.2 dex in [Mg/Fe] over the range of our sample, but is clearly seen in this figure and also in Figure 18, which shows [Mg/Fe] as a function of [Na/Fe]. A similar difference between [Mg/Fe] for dwarfs and for subgiants for stars in metal-poor GCs was noted by Gratton *et al.* (2001). We are using the same three Mg lines for each star (the Mg triplet lines are not used), and in all but the three faintest stars, all three lines are detected. We use the same atomic parameters throughout. Given the strong increase in Mg I line strength with luminosity along the RGB, a systematic error in the choice of v_t with T_{eff} could in principle produce this increase in Mg abundance with luminosity along the M13 RGB. However, a more likely culprit is non-LTE effects in Mg. These, as calculated by Zhao & Gehren (2000) (see also Gehren *et al.* 2004) increase with T_{eff} and with decreasing [Fe/H] and have the right amplitude and sign to produce this effect.

7.1. Correlations of C, N and O

Correlated C and N variations in M13 have been studied in detail by Briley, Cohen & Stetson (2002, 2004). They determined C abundances from the G band of CH for a large sample of stars reaching from the RGB to below the main sequence turnoff in M13. Combining their results with the earlier work of Smith *et al.* (1996) and Suntzeff (1981) who cover the most luminous RGB stars in M13, they evaluated the variation from star-to-star of [C/Fe] from the RGB tip to very low luminosities. They find big spreads in [C/Fe] at all luminosities probed, with [C/Fe] ranging from -0.8 to -0.2 dex among the lower luminosity giants. There is a marked decline in [C/Fe] towards higher luminosities among the upper RGB M13 stars, found originally by Suntzeff (1981). Briley, Cohen & Stetson also see a large range in [N/Fe] of 0.0 to +1.5 dex.

A crucial test is to determine whether just CN burning is occurring, C being transformed into N, in which case $\epsilon(\text{C+N})$ will be constant, or if ON burning is also occurring. In either case, the sum $\epsilon(\text{C+N+O})$ should be approximately constant, as nucleosynthesis of even heavier elements proceeds only at very high temperatures. Such a test was carried out by Brown, Wallerstein & Oke (1991) for a small sample of stars; we carry it out for a considerably larger sample of 5 (12) stars

using our new O abundances and the C and N abundances of Smith *et al.* (1996) or Suntzeff (1981). Figure 19 shows the result for M13; $\log[\epsilon(\text{C+N+O})]$ is constant at -1.24 dex with a relatively small σ of 0.12 dex; this value is ~ 0.3 dex higher than $[\text{Fe/H}]$ for M13. The sum of C+N is not constant, and O burning, especially near the RGB tip of M13, is required. For M3, the necessary data exists for five stars, combining our new determination of $[\text{O/Fe}]$ with the C,N measurements of Smith *et al.* (1996), Suntzeff (1981) or of Bell & Dickens (1980). We find a value of -1.2 dex for the mean of sum of $\log[\epsilon(\text{C+N+O})]$, identical to that of M13.

7.2. Comments on Nucleosynthesis

We now turn to what we can learn about the chemical history of the two globular clusters M3 and M13 from our work. Figure 20 shows the abundance $[X/\text{Fe}]$ we have derived for these two populous Galactic GCs. The light elements are characterized by very large ranges of star-to-star abundance variations. Since the odd atomic number elements among the light elements normally are of lower abundance (in terms of X/H), a small increment of these elements can lead to large enhancements in $[X/\text{Fe}]$. Such behavior is seen throughout this range of atomic number. The correlations among the elements showing such star-to-star variations suggest that CN and, especially for M13, ON burning, as well NaMg burning are required. These spreads have been widely discussed in the literature for the luminous giants in these and other Galactic GCs.

Our main contributions are twofold. We have confirmed with quite high precision that the sum of C+N+O is constant near the tip of the giant branch as shown by Smith *et al.* (1996) but we extend this down to the bump in the luminosity function. Second we have demonstrated that the correlations and anti-correlations among these light elements extend with the same amplitude seen on the upper RGB (but not with the extreme ratios characteristic of the tip of the RGB in M13) to the faintest luminosities probed, which for our sample in M13, is near the main sequence turnoff. The range of luminosities for our sample in each of these two GCs reaches well below their RGB bump, which is at $V = 15.45$ for M3 and at $V=14.75$ for M13 (Ferraro *et al.* 1999), and is where the first dredge up is believed to begin. Stars less luminous than this cannot have mixed significantly according to current theory (see, e.g. Charbonnel 1995; Pinsonneault 1997; Palacios *et al.* 2003).

This behavior demonstrates yet again that intrinsic nuclear processes within these low mass, and in some cases relatively unevolved, stars is not capable of explaining the observed phenomena. In this context, we note the work of Gratton *et al.* (2000) on metal-poor field stars, which do not show these phenomena, but rather a much more orderly and smaller amplitude change in abundance ratios with luminosity. Thus these phenomena seem restricted to globular clusters, where the stellar density is high, and the gas density presumably was also quite high in the past. Since internal nucleosynthesis has been ruled out, some form of external pollution onto the low mass stars we currently see in GCs is required. This could be from a companion AGB star or from mass loss into the ISM of the cluster itself by higher mass stars presumably in the AGB phase,

followed by accretion as the low mass star passes through the denser regions near the cluster core, or by incomplete mixing of the cluster ISM prior to the formation of the generation of stars we see today. The problems with this general type of mechanism have been discussed at length by many, see, e.g. Cohen, Briley & Stetson (2002), and basically involve whether enough mass can be accreted, whether with the additional accreted material the observed abundance ratios can be reproduced (see, e.g. Fenner *et al.* 2004, for a discussion regarding massive AGB stars), and over what mass zones and how deeply down from the surface does the accreting star mix and hence dilute the accreted material.

All this exotic behavior ceases with Si, whose abundance appears to be constant, with a small range consistent with the observational and modeling uncertainties. The regime from Si through the Fe-peak is characterized by no detectable star-to-star variations, and by strong over-depletion of the odd atomic number elements, expected for Fe-peak nuclei from considerations of explosive nucleosynthesis (Arnett 1971, 1996). (Recall that among the lightest elements, the odd atomic numbers show large enhancements in $[X/Fe]$.)

The heaviest elements are not well sampled by our data. However, the $[Ba/Eu]$ ratio is -0.35 (-0.31) dex in M3 (M13), which value is intermediate between the Solar ratio and that of the pure r -process, presumably reflecting the increased dominance of the r -process contribution at low metallicities.

The heaviest elements also show the first signs of star-to-star variations again, not surprising since their abundances X/H are so low that any small addition of material could raise $[X/Fe]$. In particular, M13 I-5 shows strong excesses of Y and of Ba, presumably from a s -process event, but we need, and have already obtained, better spectra with more complete wavelength coverage to verify this. Ignoring ω Cen⁷, star-to-star variations among the heavy elements have been previously detected only in M15 (Snedden *et al.* 1997), and there they appear quite different in character.

8. The Evolution of Abundances Within the GC System

While it is clear that the GCs differ from the field stars in the amplitude of their star-to-star variation of the light elements, we need to establish whether this difference persists in their average abundance ratios. If so, this would provide evidence for a difference in the chemical history and/or formation mechanisms for globular clusters from those of the halo field stars. With the advent of our program at the Keck Observatory and similar programs at ESO using UVES, there are now a substantial number of Galactic GCs for which detailed abundance analyses using high precision,

⁷We ignore ω Cen in discussing star-to-star variations among globular clusters for the rest of this paper as it has been known for more than 20 years to have a wide range of heavy element abundance (see, e.g. the latest such work, Pancino *et al.* 2002) and has been repeatedly suggested recently as the remnant of the nucleus of an accreted dwarf galaxy.

high resolution spectra have been published. We collect those carried out at Keck and at the VLT, and add in only recent analyses of relatively nearby GCs using 4-m telescopes. We impose a minimum of 4 stars per cluster. Ignoring the GCs associated with the Sgr dwarf galaxy, we find 13 clusters with suitable analyses, which in order of decreasing metallicity are NGC 6528 (Carretta *et al.* 2001), NGC 6553 (Cohen *et al.* 1999; Carretta *et al.* 2001), 47 Tuc (Carretta *et al.* 2004; James *et al.* 2004), M71 (Ramírez & Cohen 2002, 2003), M5 (Ramírez & Cohen 2003), NGC 288 (Shetrone & Keane 2000), NGC 362 (Shetrone & Keane 2000), NGC 6752 (James *et al.* 2004), M3 (this paper, see also Sneden *et al.* 2004), M13 (this paper, see also Sneden *et al.* 2004), NGC 7492 (Cohen & Melendez, in preparation), NGC 6397 (Thévenin *et al.* 2001; Gratton *et al.* 2001; James *et al.* 2004) and M15 (Sneden *et al.* 1997). There are at least 10 more Galactic GCs which have been observed at Keck or at the VLT within the past two years with analyses in progress, so a significant fraction of the total Galactic population of GCs has been covered.

This strict selection of GC analyses guarantees the maximum possible accuracy of the abundance ratios, without of course guaranteeing consistency between the various analyses. Although the first author has been associated with seven of the 13, we have not tried to homogenize the details of the procedures adopted by other groups.

To characterize the behavior of the metal-poor halo field stars, we adopt abundance ratios from recent large surveys of such by Gratton & Sneden (1991), McWilliam *et al.* (1995), Fulbright (2000), Nissen *et al.* (2000) and by Johnson (2002). No effort has been made to homogenize these analyses either, but since they were carried out over the course of more than a decade, we have corrected for the difference in the Solar Fe abundance adopted by each.

For both the field star surveys and the GCs, we have looked at the differences between the transition probabilities used for each of these analyses, and set them to the same absolute scale. Such differences are small for most species, but are large (up to 0.2 dex) for Ca I, with substantial scatter in the difference from line to line.

When one examines the resulting relations between $[X/H]$ and $[Fe/H]$ for the Galactic globular clusters and for the halo field stars, one is struck by the similarity for many elements of the trends between the two systems, present in spite of completely independent analyses on very different samples (the halo stars being mostly dwarfs, while the GC samples focus on giants in many cases). Two typical cases are illustrated; for Ti (Figure 21) and for Ba (Figure 22), as for most elements, the relations of abundance ratio with metallicity of the GCs and of the halo field are indistinguishable.

The most credible difference we notice is shown by the α -elements Mg and Ca (we show that of $[Ca/Fe]$ versus $[Fe/H]$ in Figure 23). The most metal poor GC appears to be deficient in Mg and in Ca at $[Fe/H] \leq -1.5$ dex by ~ 0.3 dex as compared to the field. One explanation for this could be that the luminous giants usually analyzed in the GCs are slightly depleted in Mg, an element which shows modest star-to-star variations in GCs, or perhaps non-LTE effects in Mg are playing a role. The notoriously uncertain Mg *gf* values could also be relevant if the same lines are not used by all the groups, and there are also problems in the *gf* values for Ca I at the level of ~ 0.2 dex

which may not have been completely removed. This difference in behavior between the GCs and the halo field is at present smaller than 2σ and involves just the most metal poor GC. We await publication of analyses for more of the most metal deficient halo GCs to confirm the reality of this potential difference.

9. Summary

We have carried a detailed abundance analysis for 21 elements in a sample of 25 stars with a wide range in luminosity from luminous giants to stars near the main sequence turnoff in the globular cluster M13 ($[\text{Fe}/\text{H}] -1.50$ dex) and in a sample of 13 stars distributed from the tip to the base of the RGB in the globular cluster M3 ($[\text{Fe}/\text{H}] -1.39$ dex). The analyzed spectra, obtained with HIRES at the Keck Observatory, are of high dispersion ($R=\lambda/\Delta\lambda=35,000$). Most elements, including Fe, but excluding the elements lighter than Si, show no trend in abundance ratio $[\text{X}/\text{Fe}]$ with T_{eff} , and scatter around the mean between the top of the RGB and near the main sequence turnoff consistent with observational uncertainties. This suggests that at this metallicity, non-LTE effects and gravitationally induced heavy element diffusion are not important for this set of elements over the range of stellar parameters spanned by our sample.

The elements lighter than Si that have been studied in detail, i.e. C and N (by Briley, Cohen & Stetson 2002, 2004), O, Na, Mg, and Al (see Sneden *et al.* 2004) all show strong star-to-star variations and correlations among each other. We have detected an anti-correlation between O and Na abundances, observed previously only among the most luminous RGB stars in both of these clusters. We find these anti-correlations to persist in both M3 and in M13 over the full range of luminosity of our samples, i.e. in the case of M13 to near the main sequence turnoff. M13 shows a larger range in both O and Na abundance than does M3 at all luminosities, in particular having a few stars at its RGB tip with very strongly depleted O.

We detect a correlation between Mg abundance and O abundance among the stars in the M13 sample, but no credible star-to-star variation in $[\text{Mg}/\text{Fe}]$ within the M3 sample. We also find a decrease in the mean Mg abundance as one moves towards lower luminosity, which we tentatively suggest is due to ignoring non-LTE effects in Mg.

Although CN burning must be occurring in both M3 and in M13, and ON burning is required for M13, we have confirmed with quite high precision that the sum of C+N+O is constant, $\log[\epsilon(\text{C}+\text{N}+\text{O})] = -1.24$ dex with a relatively small σ of 0.12 dex, previously shown near the tip of the giant branch by Smith *et al.* (1996) for luminous giants, but we extend this down to the bump in the luminosity function. The same holds true for a smaller sample in M3, with somewhat larger variance.

We have shown that these star-to-star abundance variations among the light elements continue well below the RGB bump in both M3 and M13. The low luminosity at which these phenomena are now detected in M3 and M13, and from our previous work, in M71 and in M5 (Ramírez &

Cohen 2003), as in other published analyses (see, e.g. Gratton *et al.* 2001; Carretta *et al.* 2004) has effectively ruled out the possibility of generating the spreads through internal nucleosynthesis and mixing within the stars we observe today. Instead some form of external pollution involving a previous generation of stars, combined with binaries or accretion of gas from the cluster ISM, must be involved. But as discussed most recently by Fenner *et al.* (2004), the details do not fit (yet).

Star I-5 in M13 has large excesses of Y and of Ba, with no strong enhancement of Eu, suggesting an *s*-process event contributed to its heavy element abundances. This is the first star we have found in the present long term effort that shows any credible deviation from the cluster mean for any heavy element.

The mean abundance ratios we derive for M3 and for M13 are identical to within the errors. They show the typical pattern of scatter among the light elements, with the odd atomic number elements appearing enhanced, then no star-to-star variations among the Fe-peak elements, where the odd atomic number elements are excessively depleted. The mean [Eu/Ba] ratio is essentially the same in both clusters; it is intermediate between the Solar ratio and that of the *r*-process, suggesting the additional *r*-process contribution characteristic of metal-poor populations. It does not appear possible to explain the significant differences in horizontal branch characteristics of M3 and M13, the classic second parameter pair, through differences in abundances (unless He is the culprit), since we have shown that these two clusters have essentially identical values of [Fe/H] and of mean [X/Fe], for all elements studied here.

The abundance ratios for 13 Galactic globular clusters with recent detailed abundance analyses, obtained by combining our samples with published data, are compared to those of published large surveys of metal-poor halo field stars. For most elements, the agreement is very good, suggesting a common chemical history for the halo field and for the Galactic globular clusters.

We see yet again that the abundances of the Fe-peak elements in M3 and in M13, which are rather massive globular clusters ($\sim 6 \times 10^5 M_{\odot}$) are single valued, with extremely narrow peaks. It is ironic that such intense theoretical and observational effort has in recent years focused on the correlations and anti-correlations among the light elements C, N, O, Na, Mg and Al in globular clusters, and the mixing and nuclear processes that might produce these, and so little has focused on the amazingly narrow range of abundances of the Fe-peak elements characteristic of the Galactic globular clusters.

The entire Keck/HIRES user communities owes a huge debt to Jerry Nelson, Gerry Smith, Steve Vogt, and many other people who have worked to make the Keck Telescope and HIRES a reality and to operate and maintain the Keck Observatory. We are grateful to the W. M. Keck Foundation for the vision to fund the construction of the W. M. Keck Observatory. The authors wish to extend special thanks to those of Hawaiian ancestry on whose sacred mountain we are privileged to be guests. Without their generous hospitality, none of the observations presented herein would have been possible. This publication makes use of data from the Two Micron All-Sky

Survey, which is a joint project of the University of Massachusetts and the Infrared Processing and Analysis Center, funded by the National Aeronautics and Space Administration and the National Science Foundation. We are grateful to the National Science Foundation for partial support under grant AST-0205951 to JGC.

REFERENCES

- Allende Prieto, C., Lambert, D. L., & Asplund, M., 2001, *ApJ*, 556, L63
- Allende-Prieto, C., Lambert, D. L. & Asplund, M., 2002, *ApJ*, 573, L137
- Allende Prieto, C., Barklem, P. S., Lambert, D. L. & Cunha, K., 2004, *A&A*, 420, 183
- Anders, E. & Grevesse, N., 1989, *Geochim. Cosmochim. Acta*, 53, 197
- Arnett, W. D., 1971, *ApJ*, 166, 153
- Arnett, D., *Supernovae and Nucleosynthesis*, Princeton U. Press, 1996, page 275
- Arp, H. C., 1955, *AJ*, 60, 317
- Asplund, M., Nordlund, A., Trampedach, R., Prieto, C. A. & Stein, R. F., 2000, *A&A*, 359, 729
- Asplund, M., 2003, in *CNO in the Universe*, ed. G. Charbonnel, D. Schaerer & G. Meynet, ASP Conf. Series Vol. 304, pg. 275
- Asplund, M., Grevesse, N., Sauval, A. J., Allende Prieto, C. & Kiselman, D., 2004, *A&A*, 417, 751
- Bard, A., Kock, A., & Kock, M., 1991, *A&A*, 248, 315
- Bard, A., & Kock, M., 1994, *A&A*, 282, 1014
- Barklem, P. S., Anstee, S. D. & O’Mara, B. J., 1998, *Pub. Astr. Soc. Australia*, 15, 336
- Barklem, P. S., Piskunov, N. & O’Mara, B. J., 2000, *A&AS*, 142, 467
- Baumüller, D. & Gehren, T., 1997, *A&A*, 325, 108
- Bell, R. A. & Dickens, R. J., 1980, *ApJ*, 242, 657
- Biémont, E., Baudoux, M., Kurucz, R. L., Ansbacher, W., & Pinnington, E. H., 1991, *A&A*, 249, 539
- Blackwell, D. E., Petford, A. D., & Shallis, M. J., 1979, *MNRAS*, 186, 657
- Blackwell, D. E., Shallis, M. J., & Simmons, G. J., 1980, *A&A*, 81, 340
- Blackwell, D. E., Petford, A. D., Shallis, M. J., & Simmons, G. J., 1982*a*, *MNRAS*, 199, 43
- Blackwell, D. E., Petford, A. D., & Simmons, G. J., 1982*b*, *MNRAS*, 201, 595
- Blackwell, D. E., Booth, A. J., Haddock, D. J., Petford, A. D., & Leggett, S. K., 1986, *MNRAS*, 220, 549
- Briley, M. M., Cohen, J. G. & Stetson, P. B., 2002, *ApJ*, 579, L17

- Briley, M. M., Cohen, J. G. & Stetson, P. B., 2004, *AJ*, 127, 1579
- Brown, J. A., Wallerstein, G. & Oke, J. B., 1991, *AJ*, 101, 1693
- Buonanno, R., Corsi, C. E., Buzzoni, A., Cacciari, C., Ferraro, F. R. & Fusi Pecci, F., 1994, *A&A*, 290, 69
- Carretta, E., Cohen, J. G., Gratton, R. G. & Behr, B. B., 2001, *AJ*, 122, 1469
- Carretta, E., Gratton, R., Bragaglia, A., Bonifacio, P. & Pasquini, L., 2004, *A&A*, 416, 925
- Carretta, E., Bragaglia, A. & Cacciari, C., 2004, *A&A*, in press
- Cavallo, R. M. & Nagar, N. M., 2000, *AJ*, 120, 1364
- Charbonnel, C., 1995, *ApJ*, 453, L41
- Cohen, J. G., 1978, *ApJ*, 223, 487
- Cohen, J. G., Frogel, J. A., Persson, S. E. & Elias, J. H., 1981, *ApJ*, 249, 481, 1981
- Cohen, J. G., Gratton, R. G., Behr, B. B. & Carretta, E., 1999, *ApJ*, 523, 739
- Cohen, J. G., Behr, B. B. & Briley, M. M., 2001, *AJ*, 122, 1420
- Cohen, J. G., Briley, M. M. & Stetson, P. B., 2002, *AJ*, 123, 2525
- Cudworth, K. C., 1979, *AJ*, 84, 1312
- Cudworth, K. C. & Monet, D. M., 1979, *AJ*, 84, 774
- Cutri, R. M. *et al.*, 2003, “Explanatory Supplement to the 2MASS All-Sky Data Release, <http://www.ipac.caltech.edu/2mass/releases/allsky/doc/explsup.html>
- Davidge, T. J. & Courteau, S., 1999, *AJ*, 117, 129
- Den Hartog, E.A., Lawler, J.E., Sneden, C. & Cowan J.J., 2003, *ApJS*, 148, 543
- Fenner, Y. Campbell, S., Karakas, A. I., Lattanzio, J. C. & Gibson, B. K., 2004, *MNRAS*, in press
- Ferraro, F. R., Carretta, E., Corsi, C.E., Fusi Pecci, F., Cacciari, C., Buonanno, R., Paltrinieri, B. & Hamilton, D., 1997, *A&A*, 320, 757
- Ferraro, F. R., Messineo, M., Fusi Pecci, F., Da Palo, M. A. D., Straniero, O., Chieffi, A. & Limongi, M., 1999, *AJ*, 118, 1738
- Fuhr, J. R., Martin, G. A., & Wiese, W. L., 1988, *J. Phys. Chem. Ref. Data* 17, Suppl. 4
- Fulbright, J. P., 2000, *AJ*, 120, 1841

- Gehren, T., Liang, Y. C., Shi, J. R., Zhang, H. W. & Zhao, G., 2004, *A&A*, 413, 1045
- Gratton, R. G. & Sneden, C., 1991, *A&A*, 241, 501
- Gratton, R. G., Carretta, E., Eriksson, K. & Gustafsson, B., 1999, *A&A*, 350, 955
- Gratton, R. G., Sneden, C., Carretta, E. & Bragaglia, A., 2000, *A&A*, 354, 169
- Gratton, R. G., *et al.*, 2001, *A&A*, 369, 87
- Grevesse, N. & Sauval, A. J., 1998, *Space Science Reviews*, 85, 161
- Gunn, J. E. & Griffin, R. F., 1979, *AJ*, 84, 752
- Gustafsson, B., Bell, R.A., Eriksson, K. & Nordlund, A&A, 1975, *A&A*, 42, 407
- Harris, W. E., 1996, *AJ*, 112, 1487
- Harris, W. E. & Canterna, R., 1980, *ApJ*, 239, 815
- Holweger, H., Bard, A., Kock, A., & Kock, M., 1991, *A&A*, 249, 545
- Holweger, H., 2001, in *Solar and Galactic Composition*, ed R.F.Wimmer-Schweingruber, AIP Conf. Proceedings, (see Astro-ph/0107426)
- Houdashelt, M. L., Bell, R. A. & Sweigart, A. V., 2000, *AJ*, 119, 1448
- James, G. *et al.*, 2004, *A&A*, 414, 1071
- James, G., Francois, P., Bonifacio, P. Carretta, E., Gratton, R. G. & Spite, F., 2004, *A&A*, in press
- Johnson, J. A., 2002, *ApJS*, 139, 219
- Johnson, J. A. & Bolte, M. M., 1998, *AJ*, 115, 693
- Johnson, H. L. & Sandage, A. R., 1956, *ApJ*, 124, 379
- Kadla, Z. I., 1966, *Common. Pulkova Obs.*, 24, No.181, 93
- Kraft, R. P., 1994, *PASP*, 106, 553
- Kraft, R. P., Sneden, C., Langer, G. E. & Prosser, C. F., 1992, *AJ*, 105, 645
- Kraft, R. P., Sneden, C., Smith, G. H., Shetrone, M. D., Langer, G. E. & Pilachowski, C. A., 1997, *AJ*, 113, 279
- Kurucz, R. L., Furenlid, I., Brault, J. & Testerman L., 1984, *Solar Flux Atlas From 296 to 1300 Nm*, National Solar Observatory Atlas No. 1 (Harvard University).

- Kurucz, R. L., 1993*a*, ATLAS9 Stellar Atmosphere Programs and 2 km/s Grid, (Kurucz CD-ROM No. 13)
- Kurucz, R. L., 1993*b*, SYNTHE Spectrum Synthesis Programs and Line Data (Kurucz CD-ROM No. 18)
- Lawler, J. E., Bonvallet, G. & Sneden, C., 2001, ApJ, 556, 452
- Lawler, J. E., Wickliffe, M. E., den Hartog, E. A. & Sneden, C., 2001, ApJ, 563, 1075
- Lupton, R. H., Gunn, J. E. & Griffin, R. F., 1989, AJ, 93, 1114
- Martin, G. A., Fuhr, J. R., & Wiese, W. L., 1988, J. Phys. Chem. Ref. Data 17, Suppl. 3
- Mashonkina, L. & Gehren, T., 1999, A&A, 364, 249
- Mashonkina, L., Gehren, T. & Bikmaev, I., 2000, A&A, 343, 519
- May, M., Richter, J., & Wichelmann, J., 1974, A&AS, 18, 405
- McWilliam, A., Preston, G. W., Sneden, C. & Searle, L., 1995, AJ, 109, 2757
- McWilliam, A., 1998, AJ, 115, 1640
- Moore, C. E., Minnaert, M. G. J., & Houtgast, J., 1966, *The Solar Spectrum 2935 Å to 8770 Å*, National Bureau of Standards Monograph, Washington: US Government Printing Office (USGPO).
- Nissen, P. E., Chen, Y. Q., Schuster, W. J. & Zhao, G., 2000, A&A, 353, 722
- O'Brian, T. R., Wickliffe, M. E., Lawler, J. E., Whaling, W., & Brault, J. W., 1991, J. Opt. Soc. Am., B8, 1185
- Palacios, A., Talon, S., Charbonnel, C. & Forestini, M., 2003, A&A, 399, 603
- Pancino, E., Pasquini, L., Hill, V., Ferraro, F. R. & Bellazzini, M., 2002, ApJ, 568, L101
- Pinsonneault, M., 1997, ARA&A, 35, 557
- Piotto, G. *et al.*, 2002, A&A, 391, 945
- Prochaska, J. X., Naumov, S. O., Carney, B. W., McWilliam, A., & Wolfe, A. M., 2000, ApJ, 120, 2513
- Pryor, C., Latham, D. W. & Hazen, M. L., 1988, AJ, 96, 123
- Ramírez, S. V., Cohen, J. G., Buss, J., & Briley, M. M., 2001, AJ, 122, 1429
- Ramírez, S. V. & Cohen, J. G., 2002, AJ, 123, 3277

- Ramírez, S. V. & Cohen, J. G., 2003, *AJ*, 125, 224
- Rosenberg, A., Aparicio, A., Saviane, I. & Piotto, G., 2000, *A&AS*, 145, 451
- Rey, S.-C., Yoon, S.-J., Lee, Y. W., Chaboyer, B. & Sarajedini, A., 2001, *AJ*, 122, 3219
- Sandage, A. R., 1953, *AJ*, 58, 61
- Schlegel, D. J., Finkbeiner, D. P. & Davis, M., 1998, *ApJ*, 500, 525
- Shetrone, M. D., 1996, *AJ*, 112, 1517
- Shetrone, M. & Keane, 2000, *AJ*, 119, 840
- Skrutskie, M. F., Schneider, S.E., Stiening, R., Strom, S.E., Weinberg, M.D., Beichman, C., Chester, T. *et al.*, 1997, in *The Impact of Large Scale Near-IR Sky Surveys*, ed. F.Garzon *et al.* (Dordrecht: Kluwer), p. 187
- Smith, G. H., Shetrone, M. D., Bell, R. A., Churchill, C. & Briley, M. M., 1996, *AJ*, 112, 1511
- Snedden, C., 1973, Ph.D. thesis, Univ. of Texas
- Snedden, C., Kraft, R. P., Shetrone, M. D., Smith, G. H., Langer, G. E. & Prosser, C. F., 1997, *AJ*, 114, 1964
- Snedden, C., Kraft, R. P., Guhathakurta, P., Peterson, R. C. & Fulbright, J. P., 2004, *AJ*, 127, 2162
- Stetson, P.B., Vandenberg, D. A., Bolte, M., Hesser, J. E. & Smith, G. H., 1989, *AJ*, 97, 1360
- Stetson, P. B., Hesser, J. E. & Smecker-Hane, T., 1998, *PASP*, 110, 533
- Stetson, P. B., 2000, *PASP*, 112, 925
- Suntzeff, N. B., 1981, *ApJS*, 47, 1
- Takeda, Y., Zhao, G., Takada-Hidai, M., Chen, Y.-Q., Saito, Y. & Zhang, H.-W., 2003, *Chinese Jrl. Astron. & Astrophys.*, 3, 316
- Thévenin, F., 1989, *A&AS*, 77, 137
- Thévenin, F., 1990, *A&AS*, 82, 179
- Thévenin, F. & Idiart, T. P., 1999, *ApJ*, 521, 753
- Thevenin, F., Carbonnel, C., de Freitas Pacheco, J. A., Idiart, T. P., Jasniewszyc, G., de Lavery, P. & Plez, B., 2001, *A&A*, 373, 905
- Valenti, E., Ferraro, F. R., Perina, S. & Origlia, L., 2004, *A&A*, 419, 139
- Ventura, J., D’Antona, F., Mazzitelli, I. & Gratton, R., 2001, *ApJ*, 550, L65

Vogt, S. E. *et al.* 1994, SPIE, 2198, 362

Von Zeipel, M. H., 1908, Ann. Obs. Paris. Mem. 25, 108

Wallace, L., Hinkle, K. & Livingston, W.C., 1998, N.S.O. Technical Report 98-001,
<http://ftp.noao.edu.fts/visatl/README>

Weise, W. L., Smith, M. W., & Miles, B. M., 1969, Natl Stand. Ref. Data Ser., Natl Bur. Stand.
(U.S.), NSRDS-NBS 22, Vol. II

Weise, W. L., Fuhr, J. R., & Deters, T. M., 1996, J. Phys. Chem. Ref. Data Monograph No. 7

Wilson, W. C. *et al.*, 2003, SPIE, 484, 4157

Wolnik, S. J., Berthel, R. O., & Wares, G. W., 1971, ApJ, 166, L31

Zhao, G. & Gehren, T., 2000, A&A, 362, 1077

Table 1a. The Sample of Stars in M3

ID ^a	V ^b (mag)	Date Obs.	Exp. Time (sec)	SNR ^c	v_r (km s ⁻¹)
VZ1397	12.65	6/2003	600	>100	-146.1
II-46	12.68	6/2003	600	>100	-151.4
III-28	12.73	6/2003	800	>100	-154.0
VZ1000	13.01	6/2003	400	>100	-151.8
IV-25	13.60	6/2003	1000	>100	-150.4
C41303_2217	13.75	6/2003	1000	>100	-144.5
IV-27	13.95	6/2003	1000	>100	-151.4
C41543_2334	15.71	5/2001	4800	>100	-139.9
C41543_2334	15.71	6/2003	7200	100	-145.7
III-61	16.33	5/2001	3600	80	-148.7
III-60	16.44	5/2001	3600	75	-141.4
V-30	16.58	5/2001	4800	85	-143.6
V-30	16.58	6/2003	8400	90	-143.7
C41544_2336	16.65	5/2001	4800	80	-150.4
C41544_2336	16.65	6/2003	7200	90	-153.8
V-31	16.65	5/2001	4800	80	-138.6
V-31	16.65	6/2003	8400	90	-149.8

^aIdentifications are from Sandage (1953) or from Von Zeipel (1908), or are based on J2000 coordinates (Cmmsss_mmsss means R.A. 13 mm ss.s, Dec. +28 mm ss.s)

^bV photometry from Sandage (1953), Buonanno *et al.* (1994), Ferraro *et al.* (1997), Stetson (2000)

^cSignal to noise ratio in the continuum near 6380 Å for the 2001 spectra and near 5865 Å for the 2003 spectra per 4 pixel spectral resolution element.

Table 1b. The Sample of Stars in M13

ID ^a	V ^b (mag)	Date Obs.	Exp. Time (sec)	SNR ^c	v_r (km s ⁻¹)
II-67	12.12	8/2003	200	>100	-244.0
IV-25	12.19	8/2003	200	>100	-252.3
II-76	12.51	6/2003	400	>100	-240.7
III-18	12.77	6/2003	800	>100	-234.9
K188	13.39	6/2003	800	100	-246.3
III-7	13.47	8/2003	1200	>100	-261.5
I-18	13.91	6/2003	1000	>100	-247.1
I-49	14.03	8/2003	1200	>100	-261.2
J37	14.51	6/2003	1200	95	-249.3
C41196_2632	14.52	8/2003	2400	>100	^d
II-4	14.59	6/2003	1200	100	-241.3
IV-29	14.90	6/2003	1800	100	-245.1
J45	14.93	8/2003	2400	100	-243.7
C41155_3103	15.24	5/2001	3000	>100	-237.8
I-5	15.44	8/2003	2700	90	-249.8
C41148_3103	16.33	5/2001	3000	80	-235.7
C40559_2839	16.76	5/2001	1800	50	-241.2
C41134_3056	17.21	6,8/2003	10800	90	-256.6
C41134_3056	17.21	5/2001	8400	90	-252.2
C41099_3046	17.27	6/2003	7200	85	-252.6
C41099_3046	17.27	5/2001	6000	70	-250.4
C40535_2813	17.27	5/2001	7200	65	-244.9
C41101_3050	17.28	6/2003	7200	85	-241.8
C41101_3050	17.28	5/2001	6000	65	-239.8
C41135_3053	17.66	6,8/2003	10800	75	-248.7
C41135_3053	17.66	5/2001	8400	75	-244.4
C41133_2750	17.62	5/2001	7200	65	-237.2
C40535_2819	17.82	5/2001	7200	65	-242.4
C41135_2753	17.92	5/2001	7200	60	-238.2
HB Stars					
C41195_2635	15.1	8/2003	2400	85	
C41265_2249	15.9	8/2003	1550	70	

Table 1b—Continued

ID ^a	V ^b (mag)	Date Obs.	Exp. Time (sec)	SNR ^c	v_r (km s ⁻¹)
-----------------	-------------------------	-----------	--------------------	------------------	--------------------------------

^aIdentifications are from Arp (1955), Kadla (1966) or, if not included in the above, based on J2000 coordinates (Cmmsss_mmsss means R.A. 16 mm ss.s, Dec. +36 mm ss.s)

^bV photometry from Stetson’s database (Stetson, Hesser & Smecker-Hane 1998; Stetson 2000), from a 1990 update of Cudworth & Monet (1979) (private communication from K. Cudworth), or from Rey *et al.* (2001).

^cSignal to noise ratio in the continuum near 6380 Å for the 2001 spectra and near 5865 Å for the 2003 spectra per 4 pixel spectral resolution element.

^d v_r for this star not measured due to technical issues. Star is a member of M13.

Table 2. Adopted Solar Abundances

Element	[X/H] ^a	Element	[X/H] ^a
O	8.85	Fe	7.45
Na	6.33	Ni	6.25
Mg	7.54	Cu	4.21
Al	6.47	Zn	4.60
Si	7.55	Ba	2.13
Ca	6.36	Y	2.24
Sc	3.10	Zr	2.60
Ti	4.99	La	1.14
V	4.00	Nd	1.45
Cr	5.67	Eu	0.51
Mn	5.39	Dy	1.10

^aGiven on a scale where $\log(N(\text{H}))=12.0$; values in dex.

Table 3. New IR Photometry for the Fainter Stars

ID ^a	<i>J</i> (mag) ^b	<i>K</i> (mag) ^b
M 3		
C41544_2336	15.16	14.68
C41543_2334	14.67	14.38
III-60	15.03	14.52
III-61	14.92	14.41
V-31	15.33	14.74
V-30	15.18	14.61
M 13		
C41134_3056	15.73	15.32
C41135_3053	16.29	15.91
C41101_3050	15.88	15.40
C41099_3046	15.88	15.44
C40539_2813	16.49	16.08
C40535_2819	16.58	16.19
C41135_2753	16.87	16.44
C41133_2750	16.30	15.86
C41148_3103	14.87	14.30
C41155_3103	13.64	13.09
C40559_2839	12.84	12.20
C41196_2632	12.84	12.20
C41195_2635	14.72	14.82

^aIdentifications as in notes to Table 1a (1b).

^b 1σ uncertainties are ± 0.03 mag.

Table 4a. Stellar Parameters for the M3 Sample.

ID ^a	T_{eff} (K)	$\log(g)$ (dex)	v_t (km/s)
VZ1397	3985	0.40	1.90
II-46	3998	0.40	1.90
VZ1000	4175	0.70	1.85
III-28	4200	0.60	1.80
IV-25	4408	1.10	1.60
C41303_2217	4436	1.20	1.60
IV-27	4547	1.30	1.60
III-61	5140	2.70	1.35
III-60	5170	2.65	1.30
C41544_2336	5170	2.70	1.25
V-30	5170	2.75	1.40
V-31	5170	2.80	1.20
C41543_2334 ^b	6090	2.70	2.05

^aIdentifications as in notes to Table 1a.

^bThis is a RHB star

Table 4b. Stellar Parameters for the M13 Sample.

ID ^a	T_{eff} (K)	$\log(g)$ (dex)	v_t (km/s)
II-67	3900	0.45	1.9
IV-25	3985	0.50	1.95
II-76	4300	0.85	1.95
III-18	4350	1.00	1.65
K188	4535	1.37	1.45
III-7	4550	1.40	1.35
I-18	4690	1.65	1.5
I-49	4745	1.75	1.55
J37	4895	2.00	1.45
C41196_2632	4900	2.00	1.5
II-4	4910	2.05	1.5
IV-29	5007	2.22	1.55
J45	5055	2.25	1.55
C41155_3103	5068	2.37	1.55
I-5	5070	2.45	1.5
C41148_3103	5247	2.89	1.55
C40559_2839	5349	3.10	1.6
C41134_3056	5305	3.25	1.0
C41099_3046	5414	3.35	1.05
C40535_2813	5718	3.60	2.3
C41101_3050	5370	3.30	1.2
C41135_3053	5500	3.50	1.15
C41133_2750	5520	3.50	1.65
C40535_2819	5722	3.65	2.05
C41135_2753	6045	3.80	2.3

^aIdentifications as in notes to Table 1b.

Table 5a. Equivalent Widths for the M3 Stars

Ion	λ (Å)	χ (eV)	$\log gf$	VZ 1397 (mÅ)	II 46 (mÅ)	III 28 (mÅ)	VZ 1000 (mÅ)	IV 25 (mÅ)	C41303 2217 (mÅ)	IV 27 (mÅ)	41543 2334 (mÅ)	III 61 (mÅ)	III 60 (mÅ)	V 30 (mÅ)	41 2 (mÅ)
OI	6300.30	0.00	-9.78	77.2	66.5	55.0	28.5	39.0	37.0	16.0
OI	6363.78	0.02	-10.30	41.0	27.5	28.1	14.6	14.0	15.7	7.0
OI	7771.94	9.15	0.37	111.0	32.0	27.0	≤14.0	...
OI	7774.17	9.15	0.22	90.0	30.0	20.0
OI	7775.39	9.15	0.00	71.0
NaI	5682.63	2.10	-0.70	72.1	58.0	30.2	73.9	46.3	33.0	55.9	41.0	...

Table 5b. Equivalent Widths for the Brighter M13 Stars

Ion	λ (Å)	χ (eV)	$\log gf$	II 67 (mÅ)	IV 25 (mÅ)	II 76 (mÅ)	III 18 (mÅ)	K 188 (mÅ)	III 7 (mÅ)	I 18 (mÅ)	I 49 (mÅ)	J 37 (mÅ)	41196 2632 (mÅ)	II 4 (mÅ)	IV 29 (mÅ)	J 45 (mÅ)
OI	6300.30	0.00	-9.78	6.1	20.0	55.0	10.0	26.0	30.0	16.0	30.0	9.0	6.5	10.0	14.0	7.0
OI	6363.78	0.02	-10.30	...	7.0	23.8	...	11.7	14.0	...	9.0
NaI	5682.63	2.10	-0.70	109.2	112.0	30.0	83.7	36.0	40.7	55.0	39.4	56.0	42.3	43.5	15.5	41.0
NaI	5688.19	2.10	-0.42	124.0	138.0	52.8	106.4	59.0	57.8	80.4	53.0	75.6	61.7	63.4	29.4	57.3
NaI	6154.23	2.10	-1.53	45.7	46.9	6.6	27.0	10.0	...	14.5	...	19.0	...	8.5
NaI	6160.75	2.00	-1.23	...	67.9	11.0	44.0	18.1	...	29.6	17.0	23.5	20.0	21.0	...	16.0

Table 5c. Equivalent Widths for the Fainter M13 Stars

Ion	λ (Å)	χ (eV)	$\log gf$	I 5 (mÅ)	41155 _3103 (mÅ)	41148 _3103 (mÅ)	41134 _3056 (mÅ)	40559 _2839 (mÅ)	41101 _3050 (mÅ)	41099 _3046 (mÅ)	41135 _3053 (mÅ)	41133 _2750 (mÅ)	40535 _2819 (mÅ)	40539 _2813 (mÅ)	41135 _2753 (mÅ)
OI	7771.94	9.15	0.37	...	12.0	34.0	16.0	25.0	22.5	20.0	20.0	20.0	25.0	19.0	16.5
OI	7774.17	9.15	0.22	25.0	14.0	17.0	...	15.0	18.0	14.0	25.0	19.0	20.0
NaI	5682.63	2.10	-0.70	56.0	49.0	20.0	21.7	26.0	30.3	29.0	14.0	...	19.0	20.0	...
NaI	5688.19	2.10	-0.42	76.5	69.0	29.0	44.3	33.0	44.3	48.0	23.3	27.0	26.0	35.0	27.0
NaI	6160.75	2.00	-1.23	26.6	22.0

Table 6a. Abundance Ratios for M3: O to Mg

Star	$[\text{Fe}/\text{H}]_{\text{I}}$ $\pm\sigma/\sqrt{N}$ (dex)	N	$[\text{Fe}/\text{H}]_{\text{II}}$ $\pm\sigma/\sqrt{N}$ (dex)	N	$[\text{O}/\text{Fe}]$ $\pm\sigma/\sqrt{N}$ (dex)	N	$[\text{Na}/\text{Fe}]$ $\pm\sigma/\sqrt{N}$ (dex)	N	$[\text{Mg}/\text{Fe}]$ $\pm\sigma/\sqrt{N}$ (dex)	N
VZ1397	$-1.36 \pm 0.05^*$	149	-1.36 ± 0.06	13	$0.52 \pm 0.05^*$	2	-0.16 ± 0.05	4	0.59 ± 0.13	3
II-46	$-1.50 \pm 0.05^*$	148	-1.39 ± 0.05	13	$0.37 \pm 0.05^*$	2	-0.23 ± 0.07	4	0.56 ± 0.15	3
VZ1000	$-1.43 \pm 0.05^*$	143	-1.40 ± 0.05	13	0.08 ± 0.10	2	$+0.10 \pm 0.06$	4	0.44 ± 0.10	3
III-28	$-1.54 \pm 0.05^*$	134	-1.54 ± 0.05	10	0.55 ± 0.07	2	-0.33 ± 0.06	2	0.49 ± 0.15	3
IV-25	$-1.39 \pm 0.05^*$	141	$-1.45 \pm 0.05^*$	14	$0.38 \pm 0.05^*$	2	-0.10 ± 0.05	4	0.41 ± 0.11	3
C41303_2217	$-1.37 \pm 0.05^*$	126	$-1.34 \pm 0.05^*$	14	$0.33 \pm 0.05^*$	2	-0.39 ± 0.09	3	0.40 ± 0.11	3
IV-27	$-1.35 \pm 0.05^*$	129	-1.45 ± 0.05	10	0.08 ± 0.08	2	$+0.11 \pm 0.06$	4	0.31 ± 0.17	3
III-61	$-1.38 \pm 0.05^*$	61	-1.29 ± 0.07	3	0.60 ± 0.05	2	-0.45 ± 0.09	2	0.29 ± 0.10	1
III-60	$-1.33 \pm 0.05^*$	65	-1.49 ± 0.10	3	$0.29 \pm 0.05^*$	2	-0.23 ± 0.13	2	0.25 ± 0.10	1
C41544_2336	$-1.26 \pm 0.05^*$	85	-1.50 ± 0.07	8	$0.39 \pm 0.05^*$	2	$-0.20 \pm 0.05^*$	2	0.48 ± 0.09	2
V-30	$-1.34 \pm 0.05^*$	80	-1.43 ± 0.06	8	$\leq -0.03 \pm 0.10$	1	$+0.16 \pm 0.05^*$	2	0.35 ± 0.22	2
V-31	$-1.44 \pm 0.05^*$	76	$-1.46 \pm 0.04^*$	8	0.35 ± 0.10	1	$-0.20 \pm 0.05^*$	2	0.22 ± 0.11	2
C41543_2334	$-1.34 \pm 0.05^*$	43	-1.15 ± 0.06	8	0.50 ± 0.07	3	$+0.25 \pm 0.05^*$	2	0.51 ± 0.08	2

*The minimum value of 0.05 dex has been adopted; the nominal calculated value is smaller.

Table 6b. Abundance Ratios for M3: Si to V

Star	$[\text{Si}/\text{Fe}]$ $\pm\sigma/\sqrt{N}$ (dex)	N	$[\text{Ca}/\text{Fe}]$ $\pm\sigma/\sqrt{N}$ (dex)	N	$[\text{Sc}/\text{Fe}]$ $\pm\sigma/\sqrt{N}$ (dex)	N	$[\text{Ti}/\text{Fe}]$ $\pm\sigma/\sqrt{N}$ (dex)	N	$[\text{V}/\text{Fe}]$ $\pm\sigma/\sqrt{N}$ (dex)	N
VZ1397	$0.35 \pm 0.05^*$	11	$0.09 \pm 0.05^*$	16	0.10 ± 0.06	7	$0.30 \pm 0.05^*$	35	0.05 ± 0.06	9
II-46	0.28 ± 0.06	9	$-0.02 \pm 0.05^*$	15	$0.13 \pm 0.05^*$	7	$0.08 \pm 0.05^*$	33	-0.21 ± 0.05	9
VZ1000	$0.35 \pm 0.05^*$	9	$0.11 \pm 0.05^*$	15	0.19 ± 0.05	7	$0.13 \pm 0.05^*$	32	$-0.10 \pm 0.05^*$	10
III-28	0.19 ± 0.08	3	$0.05 \pm 0.05^*$	15	0.15 ± 0.07	7	$0.11 \pm 0.05^*$	29	$-0.20 \pm 0.05^*$	10
IV-25	$0.25 \pm 0.05^*$	9	$0.12 \pm 0.05^*$	15	0.11 ± 0.05	7	$0.10 \pm 0.05^*$	26	$-0.17 \pm 0.05^*$	8
C41303_2217	$0.20 \pm 0.05^*$	9	$0.08 \pm 0.05^*$	15	0.15 ± 0.05	7	$0.10 \pm 0.05^*$	25	-0.18 ± 0.06	8
IV-27	$0.23 \pm 0.05^*$	12	$0.10 \pm 0.05^*$	15	0.18 ± 0.06	7	$0.10 \pm 0.05^*$	27	$-0.15 \pm 0.05^*$	8
III-61	0.23 ± 0.13	4	0.18 ± 0.05	17	0.21 ± 0.11	7	0.13 ± 0.06	3	...	0
III-60	$0.29 \pm 0.05^*$	5	$0.14 \pm 0.05^*$	17	0.08 ± 0.08	7	0.26 ± 0.06	5	...	0
C41544_2336	0.32 ± 0.06	8	$0.12 \pm 0.05^*$	17	0.04 ± 0.05	7	0.27 ± 0.06	13	...	0
V-30	0.19 ± 0.05	5	$0.05 \pm 0.05^*$	17	0.13 ± 0.06	7	0.21 ± 0.05	11	...	0
V-31	0.30 ± 0.06	4	$0.12 \pm 0.05^*$	16	0.10 ± 0.05	7	$0.19 \pm 0.05^*$	10	...	0
C41543_2334	$0.32 \pm 0.05^*$	2	0.22 ± 0.05	9	-0.07 ± 0.25	2	$0.18 \pm 0.05^*$	3	...	0

*The minimum value of 0.05 dex has been adopted; the nominal calculated value is smaller.

Table 6c. Abundance Ratios for M3: Cr to Cu

Star	$\frac{[\text{Cr}/\text{Fe}]}{\pm\sigma/\sqrt{N}}$ (dex)	N	$\frac{[\text{Mn}/\text{Fe}]}{\pm\sigma/\sqrt{N}}$ (dex)	N	$\frac{[\text{Co}/\text{Fe}]}{\pm\sigma/\sqrt{N}}$ (dex)	N	$\frac{[\text{Ni}/\text{Fe}]}{\pm\sigma/\sqrt{N}}$ (dex)	N	$\frac{[\text{Cu}/\text{Fe}]}{\pm\sigma/\sqrt{N}}$ (dex)	N
VZ1397	0.03 ± 0.06	8	-0.11 ± 0.14	5	-0.01 ± 0.05	4	$-0.10 \pm 0.05^*$	24	-0.55 ± 0.09	3
II-46	-0.06 ± 0.05	8	-0.20 ± 0.15	5	-0.08 ± 0.06	4	$-0.13 \pm 0.05^*$	21	-0.55 ± 0.09	3
VZ1000	-0.10 ± 0.09	9	-0.25 ± 0.09	5	-0.07 ± 0.09	4	$-0.14 \pm 0.05^*$	20	-0.51 ± 0.06	3
III-28	0.10 ± 0.08	8	-0.34 ± 0.12	3	-0.02 ± 0.09	4	$-0.18 \pm 0.05^*$	13	$-0.66 \pm 0.05^*$	3
IV-25	0.05 ± 0.06	10	-0.30 ± 0.12	5	-0.06 ± 0.08	4	$-0.14 \pm 0.05^*$	20	-0.62 ± 0.11	2
C41303_2217	0.01 ± 0.06	9	-0.27 ± 0.14	4	-0.11 ± 0.03	3	$-0.16 \pm 0.05^*$	15	-0.56 ± 0.21	2
IV-27	$-0.03 \pm 0.05^*$	9	-0.17 ± 0.05	3	-0.16 ± 0.06	3	$-0.16 \pm 0.05^*$	14	$-0.71 \pm 0.05^*$	2
III-61	...	0	...	0	...	0	-0.32 ± 0.08	6	...	0
III-60	...	0	...	0	...	0	-0.24 ± 0.10	6	...	0
C41544_2336	-0.32 ± 0.09	4	-0.32 ± 0.17	3	...	0	-0.08 ± 0.05	4	-0.46 ± 0.10	1
V-30	-0.26 ± 0.07	3	-0.44 ± 0.05	3	...	0	-0.17 ± 0.09	4	-0.56 ± 0.10	1
V-31	-0.17 ± 0.12	4	-0.33 ± 0.09	3	...	0	$-0.13 \pm 0.05^*$	6	-0.57 ± 0.10	1
C41543_2334	-0.07 ± 0.17	3	-0.43 ± 0.06	3	...	0	...	0	...	0

*The minimum value of 0.05 dex has been adopted; the nominal calculated value is smaller.

Table 6d. Abundance Ratios for M3: Zn to La

Star	$\frac{[\text{Zn}/\text{Fe}]}{\pm\sigma/\sqrt{N}}$ (dex)	N	$\frac{[\text{Y}/\text{Fe}]}{\pm\sigma/\sqrt{N}}$ (dex)	N	$\frac{[\text{Zr}/\text{Fe}]}{\pm\sigma/\sqrt{N}}$ (dex)	N	$\frac{[\text{Ba}/\text{Fe}]}{\pm\sigma/\sqrt{N}}$ (dex)	N	$\frac{[\text{La}/\text{Fe}]}{\pm\sigma/\sqrt{N}}$ (dex)	N
VZ1397	$-0.14 \pm 0.05^*$	2	-0.56 ± 0.07	3	0.13 ± 0.05	3	0.13 ± 0.05	3	0.07 ± 0.05	3
II-46	0.09 ± 0.08	2	-0.27 ± 0.10	3	$-0.12 \pm 0.05^*$	3	0.12 ± 0.05	3	0.03 ± 0.08	3
VZ1000	$-0.12 \pm 0.05^*$	2	-0.25 ± 0.09	4	$-0.11 \pm 0.05^*$	3	0.15 ± 0.06	3	0.01 ± 0.05	3
III-28	$-0.12 \pm 0.05^*$	2	-0.14 ± 0.13	4	-0.03 ± 0.06	3	0.08 ± 0.09	3	0.17 ± 0.08	2
IV-25	-0.10 ± 0.07	2	-0.25 ± 0.09	4	0.05 ± 0.05	3	$0.15 \pm 0.05^*$	3	-0.02 ± 0.05	3
C41303_2217	$-0.10 \pm 0.05^*$	2	-0.15 ± 0.10	4	0.22 ± 0.10	3	0.16 ± 0.05	3	-0.02 ± 0.15	2
IV-27	$-0.13 \pm 0.05^*$	2	-0.35 ± 0.09	4	...	0	0.14 ± 0.06	3	0.05 ± 0.05	3
III-61	...	0	...	0	...	0	$-0.09 \pm 0.05^*$	3	...	0
III-60	...	0	...	0	...	0	$0.12 \pm 0.05^*$	3	...	0
C41544_2336	$-0.19 \pm 0.05^*$	2	-0.29 ± 0.06	3	...	0	0.24 ± 0.09	3	...	0
V-30	-0.10 ± 0.28	2	-0.38 ± 0.20	3	...	0	0.34 ± 0.10	3	...	0
V-31	0.02 ± 0.18	2	-0.26 ± 0.09	3	...	0	0.20 ± 0.08	3	...	0
C41543_2334	$-0.15 \pm 0.05^*$	2	$-0.12 \pm 0.05^*$	2	...	0	0.38 ± 0.15	3	...	0

*The minimum value of 0.05 dex has been adopted; the nominal calculated value is smaller.

Table 6e. Abundance Ratios for M3: Nd to Dy

Star	[Nd/Fe] $\pm\sigma/\sqrt{N}$ (dex)	N	[Eu/Fe] $\pm\sigma/\sqrt{N}$ (dex)	N	[Dy/Fe] $\pm\sigma/\sqrt{N}$ (dex)	N
VZ1397	0.12 ± 0.07	5	0.46 ± 0.10	1	-0.04 ± 0.10	1
II-46	0.16 ± 0.05	5	0.51 ± 0.10	1	0.12 ± 0.10	1
VZ1000	0.29 ± 0.05	7	0.44 ± 0.10	1	-0.09 ± 0.10	1
III-28	$0.15 \pm 0.05^*$	7	0.52 ± 0.10	1	0.08 ± 0.10	1
IV-25	$0.16 \pm 0.05^*$	7	0.46 ± 0.10	1	0.19 ± 0.10	1
Stet189	0.28 ± 0.06	5	0.51 ± 0.10	1	...	0
IV-27	$0.21 \pm 0.05^*$	5	0.55 ± 0.10	1	...	0
III-61	...	0	...	0	...	0
III-60	...	0	...	0	...	0
C41544_2336	-0.06 ± 0.10	1	0.53 ± 0.10	1	...	0
V-30	...	0	...	0	...	0
V-31	...	0	...	0	...	0
C41543_2334	...	0	...	0	...	0

*The minimum value of 0.05 dex has been adopted; the nominal calculated value is smaller.

Table 7. Sensitivity of Abundances

	$\Delta(\text{EW})$ 10% ^a (dex)	$\Delta(T_{\text{eff}})$ +100 K ^b (dex)	$\Delta(\log g)$ +0.2 dex (dex)	$\Delta(vt)$ +0.4/−0.2 km s ^{−1} (dex)	$\Delta([\text{Fe}/\text{H}])$ +0.2 dex (dex)
O I :					
4250/1.0/1.6	0.05	−0.01	0.09	−0.01/0.00	0.08
5250/3.0/1.3	0.06	−0.09	0.07	−0.01/+0.01	−0.01
5750/3.5/2.0	0.06	−0.08	0.07	−0.02/+0.01	−0.01
Na I :					
4250/1.0/1.6	0.07	0.09	−0.02	−0.02/+0.02	−0.01
5250/3.0/1.3	0.06	0.06	−0.03	−0.01/+0.01	0.00
5750/3.5/2.0	0.05	0.04	0.00	−0.01/0.00	0.00
Mg I :					
4250/1.0/1.6	0.17	0.10	−0.05	−0.16/+0.07	0.00
5250/3.0/1.3	0.12	0.08	−0.05	−0.06/+0.03	0.01
Si I :					
4250/1.0/1.6	0.06	0.01	0.03	−0.02/+0.01	−0.03
5250/3.0/1.3	0.06	0.03	0.01	−0.01/+0.01	0.01
Ca I :					
4250/1.0/1.6	0.16	0.13	−0.02	−0.16/+0.10	−0.02
5250/3.0/1.3	0.10	0.07	−0.02	−0.08/+0.04	0.00
5750/3.5/2.0	0.09	0.06	−0.01	−0.06/+0.03	0.00
Sc II:					
4250/1.0/1.6	0.13	−0.02	0.08	−0.12/+0.07	0.06
5250/3.0/1.3	0.09	0.03	0.08	−0.05/+0.04	0.04
5750/3.5/2.0	0.06	0.03	0.07	−0.02/+0.02	0.02
Ti I :					
4250/1.0/1.6	0.11	0.19	−0.01	−0.09/+0.06	−0.02
5250/3.0/1.3	0.08	0.11	−0.01	−0.05/+0.03	0.00
Ti II :					
4250/1.0/1.6	0.20	−0.02	0.06	−0.21/+0.14	0.12
5250/3.0/1.3	0.10	0.03	0.08	−0.05/+0.04	0.04
V I :					
4250/1.0/1.6	0.06	0.22	0.00	−0.03/+0.02	−0.02
Cr I :					
4250/1.0/1.6	0.13	0.14	−0.02	−0.15/+0.08	−0.02
5250/3.0/1.3	0.14	0.12	−0.02	−0.12/+0.08	0.00
Mn I :					
4250/1.0/1.6	0.19	0.16	−0.02	−0.23/+0.13	−0.01

Table 7—Continued

	$\Delta(\text{EW})$ 10% ^a (dex)	$\Delta(T_{\text{eff}})$ +100 K ^b (dex)	$\Delta(\log g)$ +0.2 dex (dex)	$\Delta(vt)$ +0.4/−0.2 km s ^{−1} (dex)	$\Delta([\text{Fe}/\text{H}])$ +0.2 dex (dex)
5250/3.0/1.3	0.12	0.10	−0.01	−0.10/+0.06	0.00
Fe I :					
4250/1.0/1.6	0.12	0.11	0.00	−0.13/+0.07	0.01
5250/3.0/1.3	0.11	0.10	−0.02	−0.09/+0.05	0.00
5750/3.5/2.0	0.09	0.08	0.00	−0.05/+0.03	0.01
Fe II:					
4250/1.0/1.6	0.11	−0.08	0.08	−0.12/+0.06	0.07
5250/3.0/1.3	0.08	−0.01	0.08	−0.05/+0.03	0.03
Co I :					
4250/1.0/1.6	0.05	0.13	0.02	−0.02/+0.01	0.02
Ni I :					
4250/1.0/1.6	0.08	0.09	0.03	−0.07/+0.04	0.02
5250/3.0/1.3	0.07	0.10	0.00	−0.05/+0.02	0.00
5750/3.5/2.0	0.06	0.06	0.00	−0.02/+0.02	0.01
Cu I :					
4250/1.0/1.6	0.16	0.14	0.03	−0.17/+0.12	0.02
Zn I :					
4250/1.0/1.6	0.14	−0.05	0.04	−0.13/+0.10	0.04
5250/3.0/1.3	0.07	0.04	0.04	−0.05/+0.03	0.02
Y II :					
4250/1.0/1.6	0.17	−0.01	0.07	−0.18/+0.13	−0.06
5250/3.0/1.3	0.07	0.04	0.08	−0.03/+0.03	0.04
Zr I :					
4250/1.0/1.6	0.05	0.25	0.00	0.00/+0.01	−0.02
Ba II:					
4250/1.0/1.6	0.23	0.04	0.06	−0.36/+0.20	0.06
5250/3.0/1.3	0.17	0.07	0.05	−0.23/+0.15	0.04
5750/3.5/2.0	0.12	0.06	0.06	−0.10/+0.07	0.02
La II:					
4250/1.0/1.6	0.06	0.02	0.08	−0.02/+0.02	0.07
Nd II:					
4250/1.0/1.6	0.09	0.03	0.07	−0.07/+0.06	0.06
Eu II:					
4250/1.0/1.6	0.06	−0.01	0.08	−0.03/+0.02	0.07
Dy II:					

Table 7—Continued

	$\Delta(\text{EW})$ 10% ^a (dex)	$\Delta(T_{eff})$ +100 K ^b (dex)	$\Delta(\log g)$ +0.2 dex (dex)	$\Delta(vt)$ +0.4/−0.2 km s ^{−1} (dex)	$\Delta([\text{Fe}/\text{H}])$ +0.2 dex (dex)
4250/1.0/1.6	0.05	0.03	0.08	−0.01/+0.01	0.07

^aThis is an underestimate of the uncertainty for the weakest lines.

^bThe T_{eff} uncertainty is a function of T_{eff} ; see §5.

Table 8. Mean Abundances and Abundance Spreads for Stars in M3

Species	Mean Abund. [X/Fe] (dex)	σ (dex)	$\sigma(\text{tot})^{\text{a}}$ (dex)	Spread Ratio ^b (dex)	No. of Stars ^e	x^2 ^c	$p(x)^{\text{d}}$ %	Variation ^e
OI	0.33	0.20	0.07	2.26	12	56.1	<0.1	Yes
NaI	-0.16	0.20	0.08	2.32	12	55.4	<0.1	Yes
MgI	0.40	0.12	0.17	0.71	12	5.5	90.7	No
SiI	0.27	0.06	0.07	0.88	12	7.6	75.0	No
CaI	0.10	0.05	0.12	0.43	12	2.1	99.8	No
ScII	0.13	0.05	0.12	0.41	12	1.7	99.9	No
TiI	0.17	0.08	0.12	0.65	12	4.2	95.7	No
TiII	0.27	0.11	0.15	0.74	10	4.6	86.6	No
VI	-0.14	0.09	0.23	0.40	7	0.9	98.8	No
CrI	-0.08	0.14	0.14	1.04	10	9.4	40.4	No
MnI	-0.27	0.10	0.18	0.55	10	2.5	98.2	No
FeI	-1.39	0.08	0.09	0.85	12	7.3	77.2	No
FeII	-1.43	0.07	0.12	0.57	12	3.8	97.6	No
CoI	-0.07	0.05	0.10	0.51	7	1.7	94.8	No
NiI	-0.16	0.06	0.09	0.67	12	5.4	90.9	No
CuI	-0.58	0.07	0.16	0.45	10	1.9	99.2	No
ZnI	-0.09	0.08	0.12	0.65	10	3.6	93.7	No
YII	-0.29	0.12	0.16	0.76	10	5.1	82.3	No
ZrI	0.02	0.14	0.14	1.01	6	4.8	44.6	No
BaII	0.15	0.10	0.21	0.48	12	2.5	99.5	No
LaII	0.04	0.07	0.11	0.65	7	2.1	91.0	No
NdII	0.16	0.11	0.10	1.08	8	8.1	32.8	No
EuII	0.50	0.04	8	1.1	99.2	No
DyII	0.05	0.12	5	5.3	25.7	No

^a $\sigma(\text{tot})$ is defined in §6.2.

^bThis is the ratio of σ for the M3 sample stars to $\sigma(\text{tot})$. See text.

^c $x^2 = \sum(y_i - \bar{y})^2 / \sigma_i^2$, where $\bar{y} = \sum(y_i / \sigma_i^2) / \sum(1 / \sigma_i^2)$. A minimum $\sigma_i = \sigma(\text{tot})$ was adopted

^d $p(x)$ is the probability of exceeding x^2 by chance

^eIf $p(x) < 0.1\%$ there is abundance variation; if $p(x) > 0.5\%$ there is no variation.

^eThe number of stars in the M3 sample in which lines of this species were detected.

Table 9a. Abundance Ratios for M13: O to Mg

Star	$[\text{Fe}/\text{H}]_{\text{I}}$ $\pm\sigma/\sqrt{N}$ (dex)	N	$[\text{Fe}/\text{H}]_{\text{II}}$ $\pm\sigma/\sqrt{N}$ (dex)	N	$[\text{O}/\text{Fe}]$ $\pm\sigma/\sqrt{N}$ (dex)	N	$[\text{Na}/\text{Fe}]$ $\pm\sigma/\sqrt{N}$ (dex)	N	$[\text{Mg}/\text{Fe}]$ $\pm\sigma/\sqrt{N}$ (dex)	N
II-67	$-1.45 \pm 0.05^*$	110	-1.14 ± 0.06	12	-1.14 ± 0.10	1	0.32 ± 0.05	3	0.29 ± 0.19	3
IV-25	$-1.47 \pm 0.05^*$	128	-1.35 ± 0.05	12	$-0.33 \pm 0.05^*$	2	0.41 ± 0.09	4	0.35 ± 0.21	3
II-76	$-1.56 \pm 0.05^*$	123	$-1.49 \pm 0.05^*$	13	$0.55 \pm 0.05^*$	2	-0.32 ± 0.05	4	0.49 ± 0.17	3
III-18	$-1.43 \pm 0.05^*$	123	$-1.46 \pm 0.05^*$	13	-0.35 ± 0.10	1	0.36 ± 0.06	4	0.29 ± 0.14	3
K188	$-1.45 \pm 0.05^*$	111	$-1.44 \pm 0.05^*$	13	0.33 ± 0.07	2	$-0.08 \pm 0.05^*$	4	0.39 ± 0.17	3
III-7	$-1.60 \pm 0.05^*$	93	$-1.46 \pm 0.05^*$	13	0.46 ± 0.08	2	$0.10 \pm 0.05^*$	2	0.52 ± 0.14	3
I-18	$-1.49 \pm 0.05^*$	88	$-1.45 \pm 0.05^*$	13	0.17 ± 0.10	1	$0.32 \pm 0.05^*$	4	0.31 ± 0.18	3
I-49	$-1.45 \pm 0.05^*$	87	$-1.52 \pm 0.05^*$	12	$0.58 \pm 0.05^*$	2	$0.00 \pm 0.05^*$	3	0.38 ± 0.12	3
J37	$-1.44 \pm 0.05^*$	79	$-1.52 \pm 0.05^*$	11	0.15 ± 0.10	1	0.37 ± 0.06	4	0.09 ± 0.10	3
C41196_2632	$-1.45 \pm 0.05^*$	69	-1.51 ± 0.05	9	-0.01 ± 0.10	1	$0.17 \pm 0.05^*$	3	0.29 ± 0.12	3
II-4	$-1.54 \pm 0.05^*$	69	-1.56 ± 0.06	10	0.26 ± 0.10	1	$0.28 \pm 0.05^*$	4	0.32 ± 0.09	3
IV-29	$-1.42 \pm 0.05^*$	69	$-1.56 \pm 0.05^*$	10	0.52 ± 0.10	1	$-0.33 \pm 0.05^*$	2	0.30 ± 0.12	3
J45	$-1.44 \pm 0.05^*$	69	-1.49 ± 0.05	10	0.16 ± 0.10	1	$0.18 \pm 0.05^*$	3	0.03 ± 0.13	3
I-5	$-1.51 \pm 0.05^*$	65	-1.59 ± 0.06	6	...	0	$0.49 \pm 0.05^*$	3	0.27 ± 0.13	3
C41155_3103	$-1.47 \pm 0.05^*$	70	-1.52 ± 0.06	3	-0.06 ± 0.10	1	$0.35 \pm 0.05^*$	3	-0.06 ± 0.10	1
C41148_3103	$-1.49 \pm 0.05^*$	59	-1.53 ± 0.07	2	$0.55 \pm 0.05^*$	2	$-0.09 \pm 0.05^*$	2	0.10 ± 0.10	1
C41134_3056	$-1.44 \pm 0.05^*$	60	-1.36 ± 0.06	7	$0.24 \pm 0.05^*$	2	-0.02 ± 0.07	2	0.26 ± 0.17	3
C40559_2839	$-1.51 \pm 0.05^*$	42	-1.58 ± 0.10	1	0.37 ± 0.06	2	0.15 ± 0.08	2	0.27 ± 0.10	1
C41101_3050	$-1.46 \pm 0.05^*$	56	-1.41 ± 0.05	6	0.37 ± 0.10	1	$0.18 \pm 0.05^*$	2	0.05 ± 0.20	3
C41099_3046	$-1.39 \pm 0.05^*$	53	-1.33 ± 0.06	7	$0.19 \pm 0.05^*$	2	$0.04 \pm 0.05^*$	2	0.09 ± 0.14	3
C41135_3053	$-1.51 \pm 0.05^*$	44	-1.42 ± 0.09	4	$0.35 \pm 0.05^*$	2	$-0.05 \pm 0.05^*$	2	0.11 ± 0.14	3
C41133_2750	$-1.53 \pm 0.05^*$	33	...	0	$0.26 \pm 0.05^*$	2	-0.04 ± 0.10	1	...	0
C40535_2819	$-1.55 \pm 0.05^*$	30	...	0	0.38 ± 0.07	2	0.05 ± 0.06	2	...	0
C40539_2813	$-1.61 \pm 0.05^*$	33	...	0	0.25 ± 0.07	2	$0.31 \pm 0.05^*$	2	...	0
C41135_2753	-1.72 ± 0.05	15	...	0	0.14 ± 0.13	2	0.30 ± 0.10	1	...	0

*The minimum value of 0.05 dex has been adopted, the nominal calculated value is smaller.

Table 9b. Abundance Ratios for M13: Al to Ti

Star	$\frac{[\text{Al}/\text{Fe}]}{\pm\sigma/\sqrt{N}}$ (dex)	N	$\frac{[\text{Si}/\text{Fe}]}{\pm\sigma/\sqrt{N}}$ (dex)	N	$\frac{[\text{Ca}/\text{Fe}]}{\pm\sigma/\sqrt{N}}$ (dex)	N	$\frac{[\text{Sc}/\text{Fe}]}{\pm\sigma/\sqrt{N}}$ (dex)	N	$\frac{[\text{Ti}/\text{Fe}]}{\pm\sigma/\sqrt{N}}$ (dex)	N
II-67	0.64 ± 0.10	1	0.56 ± 0.05	9	$-0.10 \pm 0.05^*$	13	0.31 ± 0.06	7	$-0.13 \pm 0.05^*$	28
IV-25	0.85 ± 0.10	1	0.44 ± 0.07	8	$0.04 \pm 0.05^*$	13	$0.27 \pm 0.05^*$	7	$0.04 \pm 0.05^*$	27
II-76	≤ 0.59	1	0.41 ± 0.05	8	$0.03 \pm 0.05^*$	13	$0.20 \pm 0.05^*$	7	$0.07 \pm 0.05^*$	24
III-18	0.74 ± 0.10	1	$0.36 \pm 0.05^*$	8	$0.10 \pm 0.05^*$	13	$0.21 \pm 0.05^*$	7	$0.09 \pm 0.05^*$	22
K188	≤ 0.57	1	$0.27 \pm 0.05^*$	9	$0.11 \pm 0.05^*$	13	$0.16 \pm 0.05^*$	7	$0.13 \pm 0.05^*$	15
III-7	≤ 0.70	1	$0.37 \pm 0.05^*$	8	$0.16 \pm 0.05^*$	13	$0.19 \pm 0.05^*$	7	$0.04 \pm 0.05^*$	11
I-18	≤ 0.76	1	$0.39 \pm 0.05^*$	7	$0.15 \pm 0.05^*$	13	$0.21 \pm 0.05^*$	7	$0.16 \pm 0.05^*$	10
I-49	≤ 0.67	1	$0.32 \pm 0.05^*$	7	$0.15 \pm 0.05^*$	13	0.13 ± 0.06	7	0.15 ± 0.05	10
J37	≤ 0.97	1	$0.31 \pm 0.05^*$	6	$0.12 \pm 0.05^*$	12	$0.09 \pm 0.05^*$	7	0.11 ± 0.07	7
C41196_2632	...	0	0.28 ± 0.06	6	$0.12 \pm 0.05^*$	12	0.14 ± 0.05	7	0.17 ± 0.07	5
II-4	...	0	0.35 ± 0.05	6	$0.13 \pm 0.05^*$	12	$0.12 \pm 0.05^*$	7	0.31 ± 0.08	6
IV-29	...	0	0.30 ± 0.07	6	0.03 ± 0.05	12	0.04 ± 0.05	7	$0.20 \pm 0.05^*$	6
J45	...	0	$0.30 \pm 0.05^*$	6	$0.11 \pm 0.05^*$	12	0.13 ± 0.06	7	0.24 ± 0.05	5
I-5	...	0	0.28 ± 0.06	5	$0.12 \pm 0.05^*$	12	0.12 ± 0.05	7	0.25 ± 0.08	5
C41155_3103	...	0	0.32 ± 0.06	5	$0.22 \pm 0.05^*$	16	0.11 ± 0.05	7	0.24 ± 0.08	6
C41148_3103	...	0	$0.15 \pm 0.05^*$	4	$0.20 \pm 0.05^*$	16	0.09 ± 0.09	5	0.30 ± 0.07	4
C41134_3056	...	0	0.22 ± 0.07	5	$0.08 \pm 0.05^*$	13	0.05 ± 0.09	2	-0.02 ± 0.09	4
C40559_2839	...	0	0.09 ± 0.05	3	0.07 ± 0.06	14	0.10 ± 0.08	2	0.23 ± 0.05	2
C41101_3050	...	0	0.35 ± 0.06	5	$0.06 \pm 0.05^*$	14	$-0.02 \pm 0.05^*$	2	0.22 ± 0.10	3
C41099_3046	...	0	$0.10 \pm 0.05^*$	2	$0.14 \pm 0.05^*$	13	$0.11 \pm 0.05^*$	2	$0.29 \pm 0.05^*$	6
C41135_3053	...	0	0.34 ± 0.11	2	0.20 ± 0.05	12	-0.08 ± 0.11	2	0.25 ± 0.08	3
C41133_2750	...	0	...	0	0.20 ± 0.06	13	0.00 ± 0.10	1	...	0
C40535_2819	...	0	...	0	0.24 ± 0.05	12	-0.03 ± 0.10	1	...	0
C40539_2813	...	0	...	0	$0.12 \pm 0.05^*$	13	-0.02 ± 0.10	1	...	0
C41135_2753	...	0	...	0	0.18 ± 0.08	9	0.36 ± 0.10	1	...	0

*The minimum value of 0.05 dex has been adopted, the nominal calculated value is smaller.

Table 9c. Abundance Ratios for M13: V to Ni

Star	$\frac{[\text{V}/\text{Fe}]}{\pm\sigma/\sqrt{N}}$ (dex)	N	$\frac{[\text{Cr}/\text{Fe}]}{\pm\sigma/\sqrt{N}}$ (dex)	N	$\frac{[\text{Mn}/\text{Fe}]}{\pm\sigma/\sqrt{N}}$ (dex)	N	$\frac{[\text{Co}/\text{Fe}]}{\pm\sigma/\sqrt{N}}$ (dex)	N	$\frac{[\text{Ni}/\text{Fe}]}{\pm\sigma/\sqrt{N}}$ (dex)	N
II-67	-0.33 ± 0.05	9	0.04 ± 0.08	10	-0.20 ± 0.10	4	-0.03 ± 0.09	4	$-0.09 \pm 0.05^*$	19
IV-25	$-0.14 \pm 0.05^*$	9	0.10 ± 0.07	9	-0.26 ± 0.13	4	0.00 ± 0.05	4	$-0.06 \pm 0.05^*$	18
II-76	-0.19 ± 0.05	8	-0.11 ± 0.07	7	-0.36 ± 0.05	4	$-0.03 \pm 0.05^*$	4	$-0.12 \pm 0.05^*$	18
III-18	$-0.11 \pm 0.05^*$	8	-0.01 ± 0.05	7	-0.25 ± 0.08	4	-0.02 ± 0.06	4	$-0.09 \pm 0.05^*$	18
K188	$-0.16 \pm 0.05^*$	7	-0.04 ± 0.05	7	-0.16 ± 0.06	4	-0.05 ± 0.07	3	$-0.12 \pm 0.05^*$	15
III-7	-0.09 ± 0.10	1	-0.06 ± 0.06	7	-0.14 ± 0.05	4	-0.02 ± 0.08	2	-0.19 ± 0.05	11
I-18	0.05 ± 0.10	1	-0.12 ± 0.07	5	-0.25 ± 0.09	4	-0.07 ± 0.10	1	-0.10 ± 0.08	11
I-49	-0.17 ± 0.10	1	-0.02 ± 0.05	5	-0.25 ± 0.07	3	0.08 ± 0.10	1	$-0.08 \pm 0.05^*$	11
J37	-0.07 ± 0.10	1	-0.06 ± 0.05	5	-0.44 ± 0.09	3	...	0	-0.13 ± 0.06	7
C41196_2632	...	0	-0.03 ± 0.05	3	$-0.25 \pm 0.05^*$	3	...	0	-0.14 ± 0.10	5
II-4	...	0	-0.11 ± 0.09	3	$-0.55 \pm 0.05^*$	3	...	0	-0.21 ± 0.12	5
IV-29	...	0	0.02 ± 0.08	3	$-0.29 \pm 0.05^*$	3	...	0	-0.02 ± 0.09	5
J45	...	0	-0.14 ± 0.08	3	-0.31 ± 0.08	3	...	0	-0.06 ± 0.09	5
I-5	...	0	-0.07 ± 0.06	3	-0.40 ± 0.06	3	...	0	-0.10 ± 0.10	5
C41155_3103	...	0	...	0	...	0	...	0	-0.08 ± 0.06	12
C41148_3103	...	0	...	0	...	0	...	0	-0.16 ± 0.05	8
C41134_3056	...	0	$-0.11 \pm 0.05^*$	3	-0.41 ± 0.12	3	...	0	0.08 ± 0.14	4
C40559_2839	...	0	...	0	...	0	...	0	0.09 ± 0.09	4
C41101_3050	...	0	-0.19 ± 0.06	3	$-0.50 \pm 0.05^*$	3	...	0	-0.18 ± 0.12	4
C41099_3046	...	0	-0.15 ± 0.11	3	-0.38 ± 0.10	3	...	0	-0.05 ± 0.10	3
C41135_3053	...	0	0.06 ± 0.05	3	-0.38 ± 0.13	3	...	0	$-0.01 \pm 0.05^*$	2
C41133_2750	...	0	...	0	...	0	...	0	-0.34 ± 0.10	1
C40535_2819	...	0	...	0	...	0	...	0	-0.14 ± 0.10	1
C40539_2813	...	0	...	0	...	0	...	0	-0.10 ± 0.09	2
C41135_2753	...	0	...	0	...	0	...	0	...	0

*The minimum value of 0.05 dex has been adopted, the nominal calculated value is smaller.

Table 9d. Abundance Ratios for M13: Cu to Ba

Star	$[\text{Cu}/\text{Fe}]$ $\pm\sigma/\sqrt{N}$ (dex)	N	$[\text{Zn}/\text{Fe}]$ $\pm\sigma/\sqrt{N}$ (dex)	N	$[\text{Y}/\text{Fe}]$ $\pm\sigma/\sqrt{N}$ (dex)	N	$[\text{Zr}/\text{Fe}]$ $\pm\sigma/\sqrt{N}$ (dex)	N	$[\text{Ba}/\text{Fe}]$ $\pm\sigma/\sqrt{N}$ (dex)	N
II-67	-0.55 ± 0.13	2	0.17 ± 0.14	2	-0.08 ± 0.11	5	-0.37 ± 0.05	3	$0.43 \pm 0.05^*$	3
IV-25	-0.62 ± 0.06	2	$0.02 \pm 0.05^*$	2	-0.18 ± 0.07	5	$-0.12 \pm 0.05^*$	3	0.28 ± 0.05	3
II-76	-0.62 ± 0.12	2	$0.04 \pm 0.05^*$	2	$-0.26 \pm 0.05^*$	4	0.06 ± 0.06	3	0.38 ± 0.06	3
III-18	-0.61 ± 0.13	2	$-0.05 \pm 0.05^*$	2	-0.26 ± 0.06	5	0.05 ± 0.07	2	0.36 ± 0.05	3
K188	$-0.70 \pm 0.05^*$	2	$0.08 \pm 0.05^*$	2	-0.13 ± 0.05	4	...	0	$0.44 \pm 0.05^*$	3
III-7	$-0.73 \pm 0.05^*$	2	$0.16 \pm 0.05^*$	2	$-0.21 \pm 0.05^*$	5	...	0	0.44 ± 0.05	3
I-18	-0.61 ± 0.08	2	$0.09 \pm 0.05^*$	2	-0.25 ± 0.05	4	...	0	0.37 ± 0.06	3
I-49	-0.68 ± 0.11	2	$0.06 \pm 0.05^*$	2	-0.33 ± 0.09	4	...	0	0.28 ± 0.05	3
J37	-0.80 ± 0.10	1	-0.02 ± 0.06	2	-0.16 ± 0.08	4	...	0	0.30 ± 0.05	3
C41196_2632	-0.68 ± 0.10	1	-0.14 ± 0.05	2	-0.26 ± 0.08	4	...	0	0.33 ± 0.10	3
II-4	-0.79 ± 0.10	1	$-0.28 \pm 0.05^*$	2	-0.17 ± 0.05	4	...	0	0.37 ± 0.09	3
IV-29	-0.63 ± 0.10	1	-0.04 ± 0.07	2	-0.26 ± 0.05	4	...	0	$0.20 \pm 0.05^*$	3
J45	-0.52 ± 0.10	1	$0.00 \pm 0.05^*$	2	$-0.29 \pm 0.05^*$	4	...	0	$0.15 \pm 0.05^*$	3
I-5	-0.56 ± 0.10	1	$0.12 \pm 0.05^*$	2	$0.53 \pm 0.05^*$	3	...	0	0.58 ± 0.06	3
C41155_3103	...	0	...	0	...	0	...	0	0.12 ± 0.08	3
C41148_3103	...	0	...	0	...	0	...	0	0.01 ± 0.08	3
C41134_3056	...	0	-0.11 ± 0.10	1	-0.14 ± 0.07	4	...	0	0.37 ± 0.05	3
C40559_2839	...	0	...	0	...	0	...	0	0.06 ± 0.08	3
C41101_3050	...	0	-0.11 ± 0.10	1	-0.29 ± 0.07	4	...	0	0.22 ± 0.06	3
C41099_3046	...	0	-0.09 ± 0.10	1	$-0.13 \pm 0.05^*$	3	...	0	0.39 ± 0.05	3
C41135_3053	...	0	0.00 ± 0.10	1	-0.19 ± 0.10	1	...	0	$0.27 \pm 0.05^*$	3
C41133_2750	...	0	...	0	...	0	...	0	0.16 ± 0.13	2
C40535_2819	...	0	...	0	...	0	...	0	-0.04 ± 0.11	2
C40539_2813	...	0	...	0	...	0	...	0	0.03 ± 0.06	2
C41135_2753	...	0	...	0	...	0	...	0	0.09 ± 0.08	2

*The minimum value of 0.05 dex has been adopted, the nominal calculated value is smaller.

Table 9e. Abundance Ratios for M13: La to Dy

Star	$\frac{[\text{La}/\text{Fe}]}{\pm\sigma/\sqrt{N}}$ (dex)	N	$\frac{[\text{Nd}/\text{Fe}]}{\pm\sigma/\sqrt{N}}$ (dex)	N	$\frac{[\text{Eu}/\text{Fe}]}{\pm\sigma/\sqrt{N}}$ (dex)	N	$[\text{Dy}/\text{Fe}]$	N
II-67	0.12 ± 0.06	3	0.41 ± 0.05	7	0.56 ± 0.10	1	-0.03 ± 0.10	1
IV-25	0.20 ± 0.10	3	$0.40 \pm 0.05^*$	7	0.59 ± 0.10	1	0.09 ± 0.10	1
II-76	0.11 ± 0.10	3	$0.21 \pm 0.05^*$	7	0.30 ± 0.10	1	0.10 ± 0.10	1
III-18	0.09 ± 0.09	3	0.31 ± 0.06	7	0.58 ± 0.10	1	0.22 ± 0.10	1
K188	0.09 ± 0.09	3	$0.27 \pm 0.05^*$	7	0.67 ± 0.10	1	...	0
III-7	0.21 ± 0.05	3	0.24 ± 0.07	6	0.71 ± 0.10	1	...	0
I-18	0.11 ± 0.10	2	0.12 ± 0.07	6	0.67 ± 0.10	1	...	0
I-49	0.06 ± 0.14	2	$0.23 \pm 0.05^*$	7	0.52 ± 0.10	1	...	0
J37	-0.05 ± 0.10	1	0.33 ± 0.06	5	0.68 ± 0.10	1	...	0
C41196_2632	0.04 ± 0.10	1	0.16 ± 0.07	5	0.48 ± 0.10	1	...	0
II-4	0.28 ± 0.10	1	0.16 ± 0.09	3	...	0	...	0
IV-29	$0.28 \pm 0.05^*$	2	$0.35 \pm 0.05^*$	6	0.59 ± 0.10	1	...	0
J45	...	0	0.28 ± 0.05	5	0.51 ± 0.10	1	...	0
I-5	0.23 ± 0.10	1	0.47 ± 0.05	5	...	0	...	0
C41155_3103	...	0	...	0	...	0	...	0
C41148_3103	...	0	...	0	...	0	...	0
C41134_3056	...	0	...	0	...	0	...	0
C40559_2839	...	0	...	0	...	0	...	0
C41101_3050	...	0	...	0	...	0	...	0
C41099_3046	...	0	...	0	...	0	...	0
C41135_3053	...	0	...	0	...	0	...	0
C41133_2750	...	0	...	0	...	0	...	0
C40535_2819	...	0	...	0	...	0	...	0
C40539_2813	...	0	...	0	...	0	...	0
C41135_2753	...	0	...	0	...	0	...	0

*The minimum value of 0.05 dex has been adopted, the nominal calculated value is smaller.

Table 10. Mean Abundances and Abundance Spreads for Stars in M13

Species	Mean Abund. [X/Fe] (dex)	σ (dex)	$\sigma(\text{tot})^{\text{a}}$ (dex)	Spread Ratio ^b (dex)	No. of Stars ^f	x^2 ^c	$p(x)^{\text{d}}$ %	Variation ^e
OI	0.18	0.37	0.10	3.70	24	319	<0.1	Yes
NaI	0.14	0.22	0.08	2.75	25	174	<0.1	Yes
MgI	0.24	0.15	0.18	0.83	21	14.2	81.9	No
AlI	0.74 ^g	0.11	3
SiI	0.31	0.11	0.08	1.37	21	36.9	1.9	No
CaI	0.12	0.07	0.12	0.58	25	9.1	99.7	No
ScII	0.12	0.11	0.12	0.92	25	19.2	74.4	No
TiI	0.16	0.11	0.13	0.85	21	15.4	75.4	No
TiII	0.31	0.12	0.15	0.80	18	9.6	92.0	No
VI	-0.13	0.10	0.23	0.43	9	1.6	99.1	No
CrI	-0.06	0.08	0.14	0.57	18	5.3	99.7	No
MnI	-0.32	0.11	0.18	0.61	18	6.8	98.6	No
FeI	-1.50	0.07	0.09	0.78	25	15.6	90.1	No
FeII	-1.46	0.10	0.12	0.83	21	15.1	77.1	No
CoI	-0.02	0.04	0.11	0.36	8	11.5	99.2	No
NiI	-0.10	0.09	0.10	0.90	24	16.1	85.2	No
CuI	-0.65	0.08	0.17	0.47	14	3.2	99.7	No
ZnI	-0.01	0.11	0.13	0.85	18	13.0	73.9	No
YII	-0.17	0.19	0.15	1.27	18	26.6	10.1	No
ZrI	-0.09	0.20	0.14	1.43	4	6.2	14.4	No
BaII	0.26	0.16	0.21	0.76	25	13.7	95.4	No
LaII	0.14	0.10	0.13	0.77	13	6.8	87.2	No
NdII	0.28	0.10	0.11	0.91	14	11.5	56.9	No
EuII	0.57	0.11	12	14.0	33.2	No
DyII	0.10	0.10	4	3.1	37.2	No

^a $\sigma(\text{tot})$ is defined in §6.2.

^bThis is the ratio of σ for the M13 sample stars to $\sigma(\text{tot})$. See text.

^c $x^2 = \sum(y_i - \bar{y})^2/\sigma_i^2$, where $\bar{y} = \sum(y_i/\sigma_i^2)/\sum(1/\sigma_i^2)$. A minimum $\sigma_i = \sigma(\text{tot})$ was adopted

^d $p(x)$ is the probability of exceeding x^2 by chance

^eIf $p(x) < 0.1\%$ there is abundance variation; if $p(x) > 0.5\%$ there is no variation.

^fThe number of stars in the M13 sample in which lines of this species were detected.

^g[Al/Fe] is based on the weak and rarely used line at 5557 Å, detected in only three of the most luminous stars of M13.

Table 11. Comparison with Atmospheric Parameters From the Literature

ID	This work		Literature		
	T_{eff}	$\log g$	T_{eff}	$\log g$	Reference
M 3					
VZ 1397	3985	0.40	3950	0.40	Sneden et al. (2004), photometric
			3925	0.10	Sneden et al. (2004), spectroscopic
			3950	0.40	Kraft et al. (1992)
			4000	0.6	Cohen (1978)
II-46	3998	0.40	4050	0.40	Sneden et al. (2004)
			4000	0.60	Kraft et al. (1992)
			4000	0.6	Cohen (1978)
III-28	4200	0.60	4175	0.55	Cavallo & Nagar (2000)
			4160	0.75	Kraft et al. (1992)
			4100	0.7	Cohen (1978)
VZ 1000	4175	0.70	4125	0.60	Sneden et al. (2004)
			4200	0.65	Cavallo & Nagar(2000)
			4175	0.45	Kraft et al. (1992)
M 13					
II-67	3900	0.45	3900	0.37	Sneden et al. (2004)
			3950	0.20	Kraft et al. (1997)
			3950	0.30	Kraft et al. (1992)
IV-25	3985	0.50	3975	0.38	Sneden et al. (2004)
			4000	0.15	Kraft et al. (1997)
			4000	0.30	Kraft et al. (1992)
			4000	0.5	Cohen (1978)
II-76	4300	0.85	4285	0.80	Sneden et al. (2004)
			4350	1.00	Kraft et al. (1992)
III-18	4350	1.00	4330	0.95	Sneden et al. (2004)
			4350	1.20	Kraft et al. (1992)
A1 K188	4535	1.35	4550	1.34	Sneden et al. (2004)
			4550	1.50	Kraft et al. (1997)

Table 12. Comparison of Deduced Abundance Ratios with Sneden et al. (2004)

Species	This work		Sneden et al. (2004)		Us – Sneden
	[X/Fe] (dex)	σ_N^a (dex)	[X/Fe] (dex)	σ_N^a (dex)	$\Delta([X/Fe])$ (dex)
M 3					
OI	+0.33	0.05	+0.15	0.03	+0.18
NaI	−0.16	0.06	+0.01	0.04	−0.17
MgI	+0.40	0.03	+0.22	0.03	+0.18
SiI	+0.27	0.02	+0.30	0.01	−0.03
CaI	+0.10	0.01	+0.23	0.01	−0.13
ScII	+0.13	0.01	−0.11	0.02	+0.24
TiI	+0.17	0.02	+0.21	0.01	−0.04
TiII	+0.27	0.03	+0.16	0.02	+0.11
VI	−0.14	0.03	−0.04	0.02	−0.10
MnI	−0.27	0.03	−0.37	0.01	+0.10
FeI ^b	−1.39	0.02	−1.62	0.01	+0.23
FeII ^b	−1.43	0.02	−1.55	0.02	+0.12
NiI	−0.16	0.02	−0.05	0.01	−0.11
BaII	+0.15	0.03	+0.21	0.02	−0.06
LaII	+0.04	0.02	+0.09	0.02	−0.05
EuII	+0.50	0.01	+0.54	0.03	−0.04
M 13					
OI	+0.18	0.08	−0.13	0.06	+0.31
NaI	+0.14	0.04	+0.21	0.04	−0.07
MgI	+0.24	0.03	+0.11	0.03	+0.21
AlI	+0.74	0.06	+0.75	0.11	−0.01
FeI ^b	−1.50	0.01	−1.63	0.03	+0.13
FeII ^b	−1.46	0.02	−1.49	0.06	+0.03
BaII	+0.26	0.03	+0.24	0.03	+0.02
LaII	+0.14	0.03	+0.11	0.03	+0.03
EuII	+0.57	0.03	+0.49	0.03	+0.08

^a σ_N is the uncertainty in the mean value of [X/Fe] for the cluster, i.e. $\sigma/\sqrt{N_{stars}}$

^bThese values are [Fe/H].

Table 13a. Star by Star Comparison of Abundances for M3^a

Species	VZ 1397	II-46	VZ1000	σ
[O/Fe]	0.21	-0.13	0.02	0.17
[Na/Fe]	0.09	0.14	0.17	0.04
[Mg/Fe]	0.09
[Si/Fe]	0.03	0.10	0.09	0.04
[Ca/Fe]	-0.04	-0.04	0.01	0.03
[Sc/Fe]	-0.12	0.09	0.19	0.16
[Ti/Fe]	0.03	-0.09	0.05	0.08
[V/Fe]	0.15	-0.10	-0.04	0.13
[Mn/Fe]	0.09	0.10	-0.05	0.08
[Fe/H]	-0.06	-0.16	-0.08	0.05
[Ni/Fe]	0.08	0.12	0.00	0.06
[Ba/Fe]	0.21	0.24	0.15	0.05
[La/Fe]	0.16
[Eu/Fe]	0.07	0.24	-0.20	0.22

^a[X/Fe](this work) – [X/Fe](Sneden *et al.* 2004)
– (mean Δ from Table 12).

Table 13b. Star by Star Comparison of Abundances for M13^a

Species	II-67	IV-25	II-76	III-18	K188	σ
[O/Fe]	0.17	0.44	-0.06	-0.40	-0.28	0.34
[Na/Fe]	-0.03	-0.04	0.02	-0.01	-0.02	0.02
[Mg/Fe]	0.06	0.06	-0.16	0.13
[Al/Fe]	-0.51	-0.35	0.11
[Fe/H]	0.05	0.04	-0.04	-0.04	0.14	0.07
[Ba/Fe]	0.29	0.14	0.14	0.09
[La/Fe]	0.20	0.30	-0.32	0.33
[Eu/Fe]	0.09	0.17	-0.10	0.14

^a[X/Fe](this work) – [X/Fe](Sneden *et al.* 2004) – (mean Δ
from Table 12).

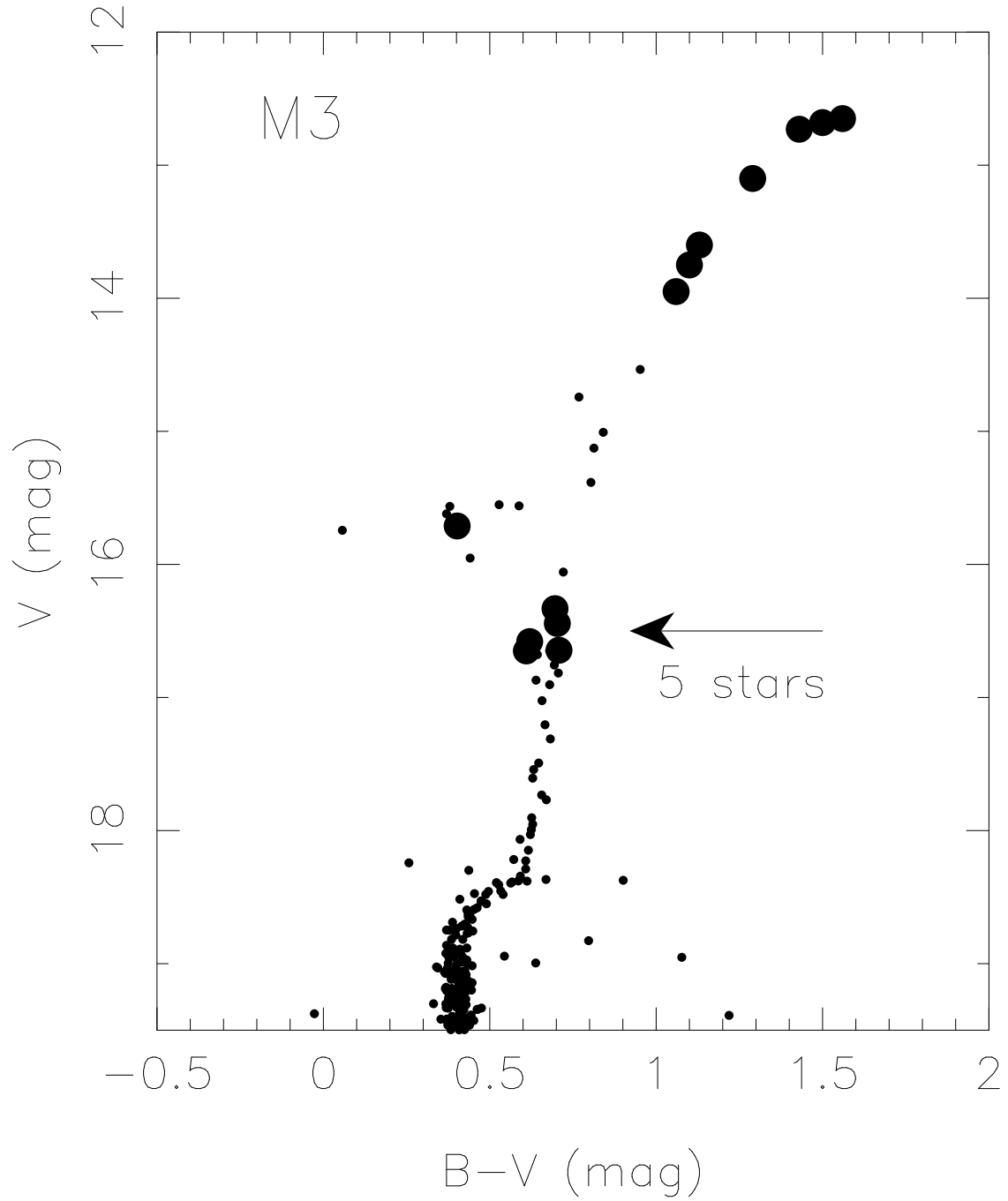


Fig. 1a.— The $B - V$ CMD for a sector of M3 is shown with data from the database of Stetson (2000). The 13 stars observed with HIRES are indicated by large filled circles.

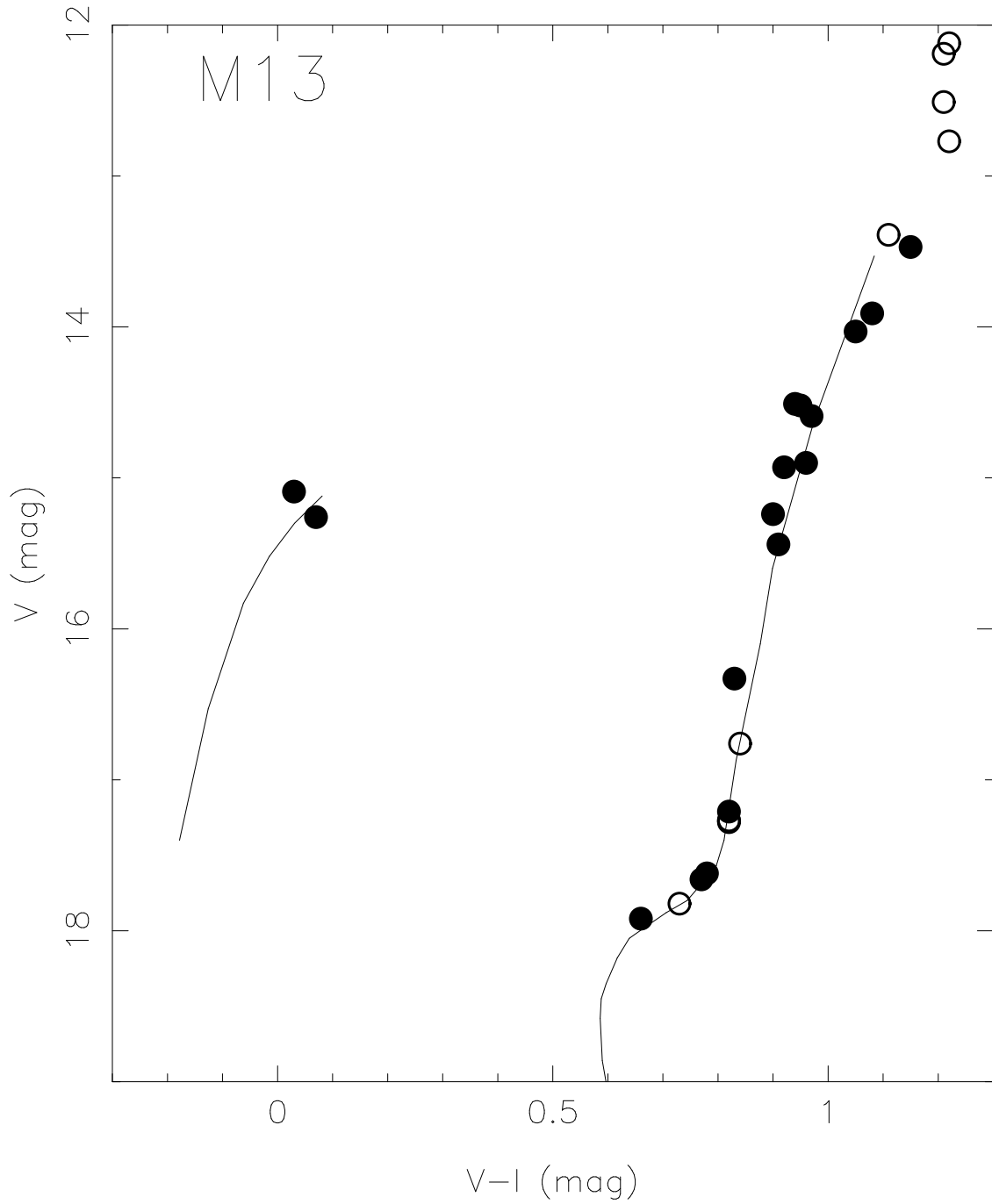


Fig. 1b.— The $V - I$ locus for M13 from Johnson & Bolte (1998) is shown with the 27 cluster members observed with HIRES superposed (large circles). Open circles denote those sample stars without I photometry from the database of Stetson (2000).

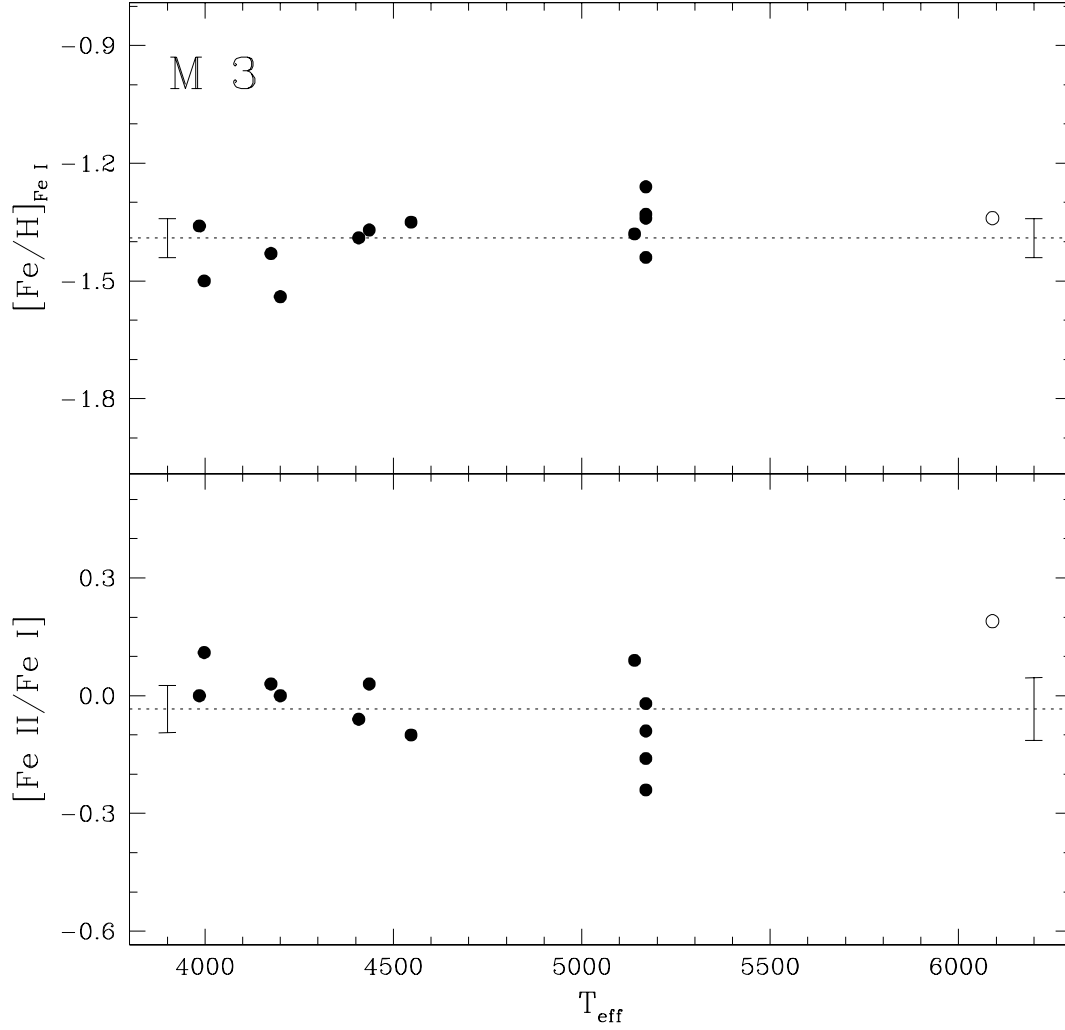


Fig. 2.— The $[\text{Fe}/\text{H}]$ from lines of Fe I is shown as a function of T_{eff} in the upper panel, while the lower panel shows the ionization equilibrium of Fe for our sample of 13 stars in M3. The open circle indicates the HB star. The error bars on the left margin are those of the most luminous giants, while the error bars on the right margin are those of the faintest stars in our sample. The dotted horizontal line indicates the mean value for our sample in this globular cluster.

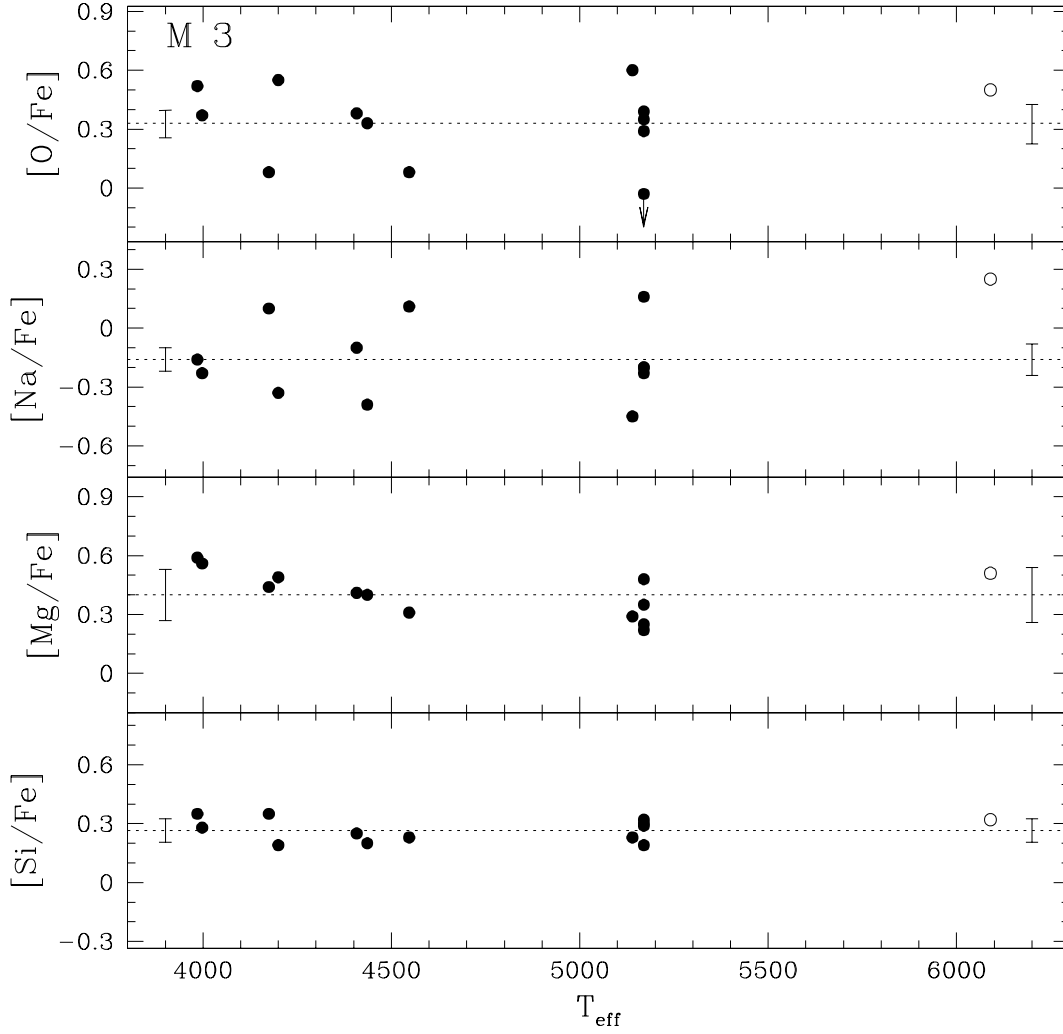


Fig. 3.— $[X/Fe]$ for the elements O, Na, Mg and Si are shown as a function of T_{eff} for our sample of 13 stars in M3. The open circle indicates the HB star. The error bars for the most luminous and least luminous stars, as well as the cluster mean, are indicated as in Figure 2.

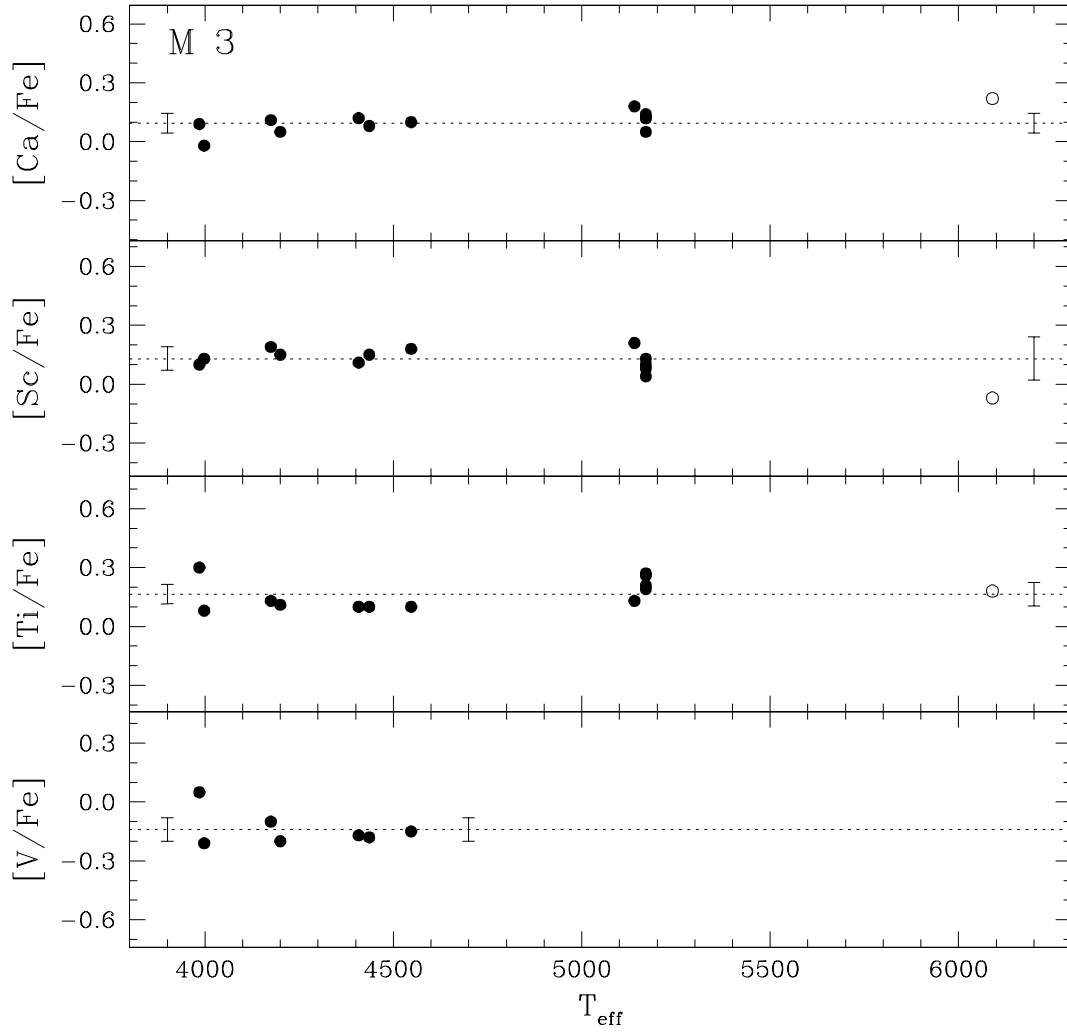


Fig. 4.— Same as Figure 3 for the elements Ca, Sc, Ti and V in M3.

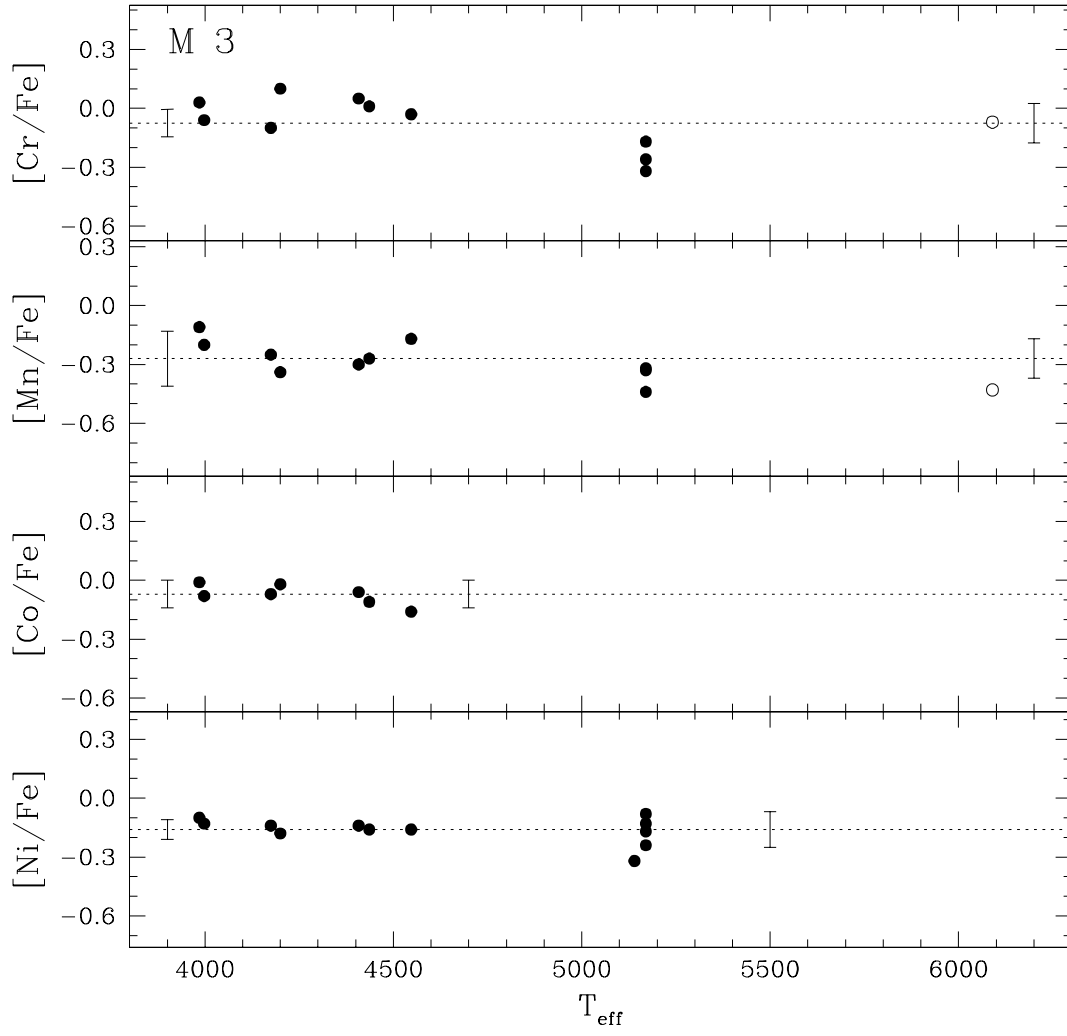


Fig. 5.— Same as Figure 3 for the elements Cr, Mn, Co and Ni in M3.

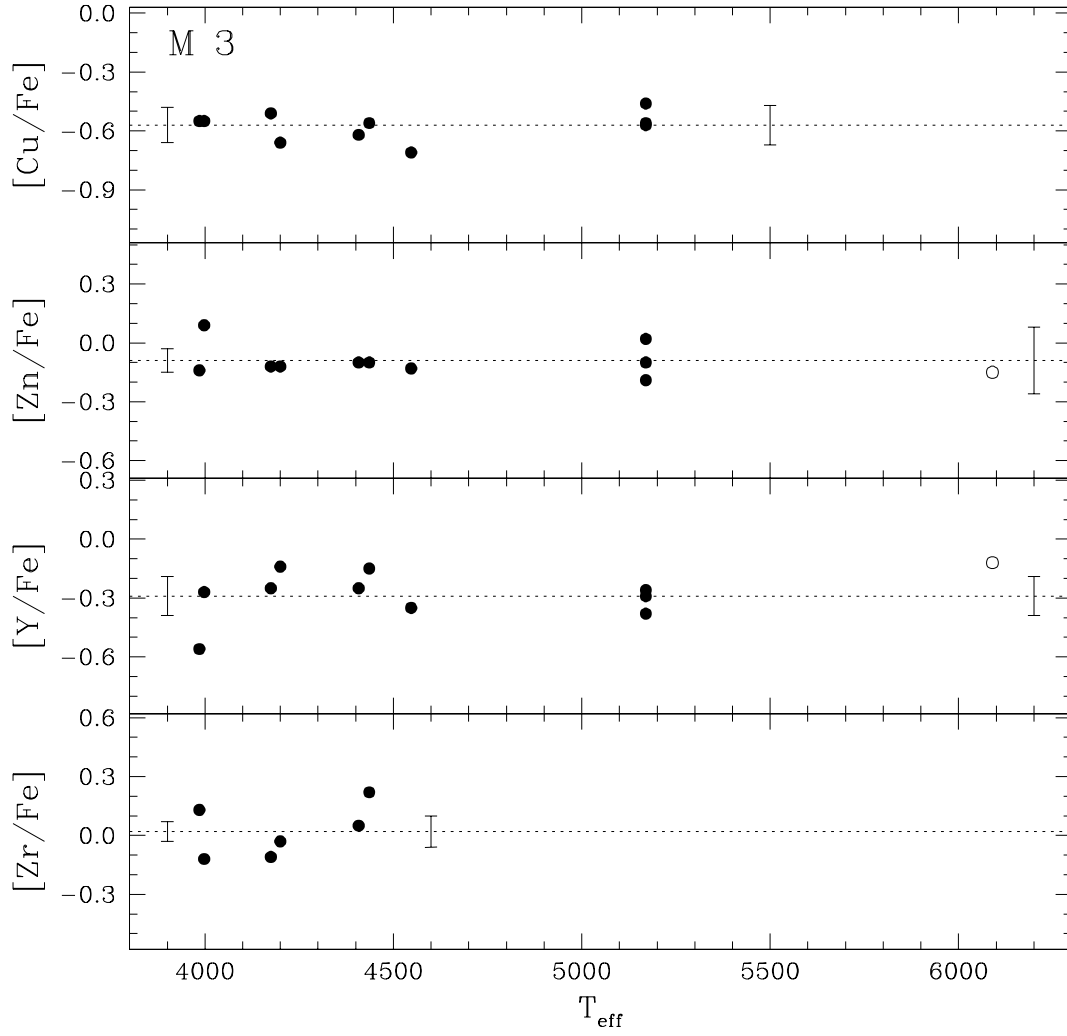


Fig. 6.— Same as Figure 3 for the elements Cu, Zn, Y and Zr in M3.

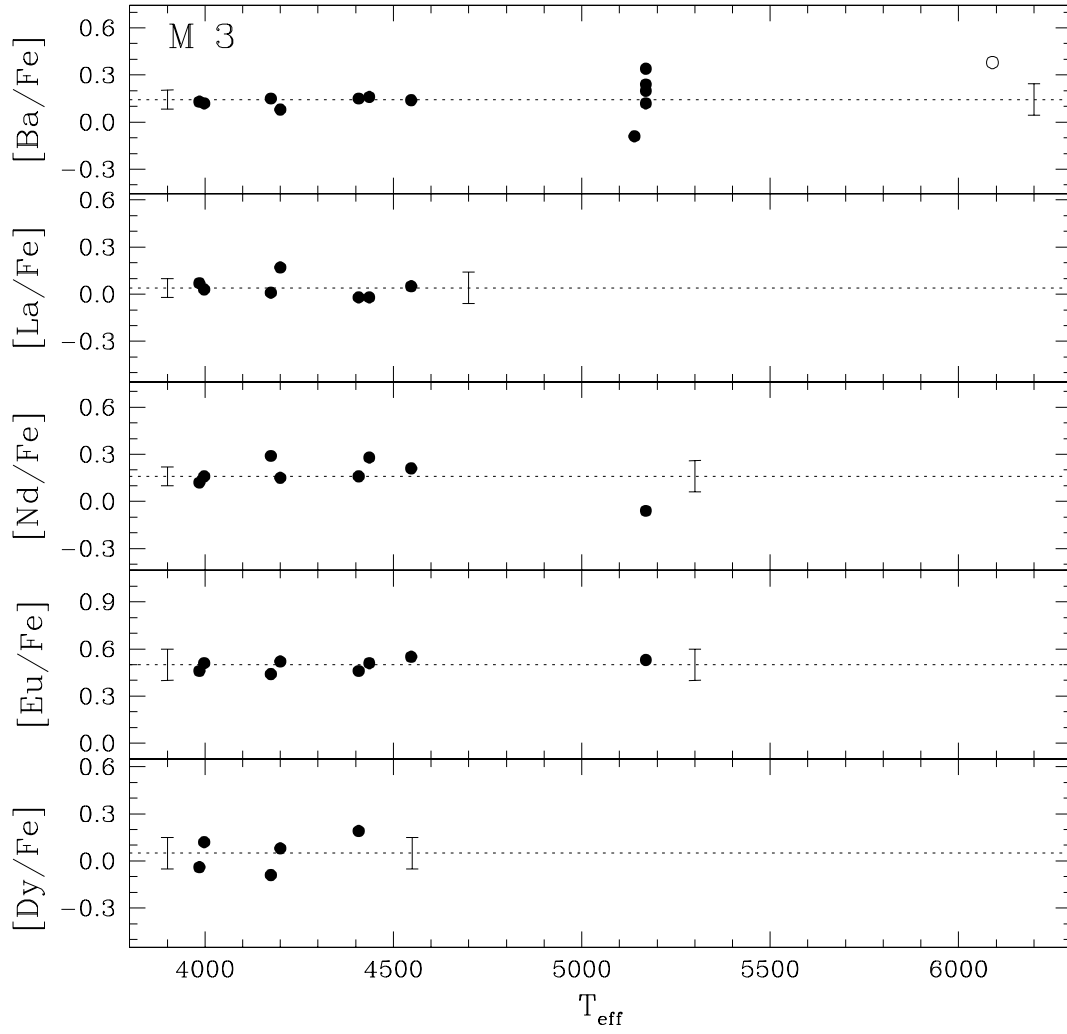


Fig. 7.— Same as Figure 3 for the elements Ba, La, Nd, Eu and Dy in M3.

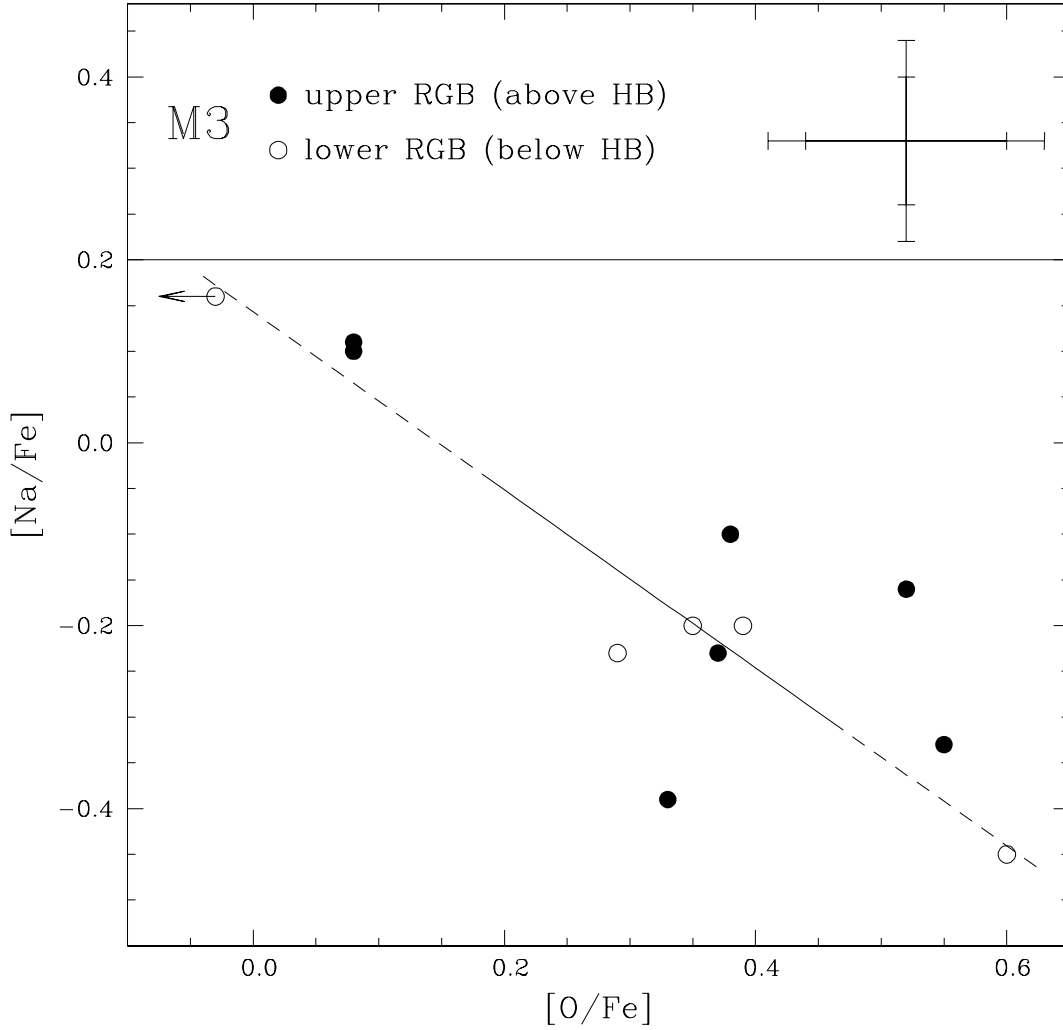


Fig. 8.— The ratio $[\text{Na}/\text{Fe}]$ is shown as a function of $[\text{O}/\text{Fe}]$ for our sample of 13 stars in M3. The filled circles denote the luminous RGB stars; the open circles the lower luminosity giants. The error bars typical of the most luminous and least luminous stars in our sample are indicated. The line represents the relationship found by Sneden *et al.* (2004), with a shift of +0.07 dex in $[\text{O}/\text{Fe}]$ applied; the line is solid between the first and third quartiles of his sample and is dashed outside that regime.

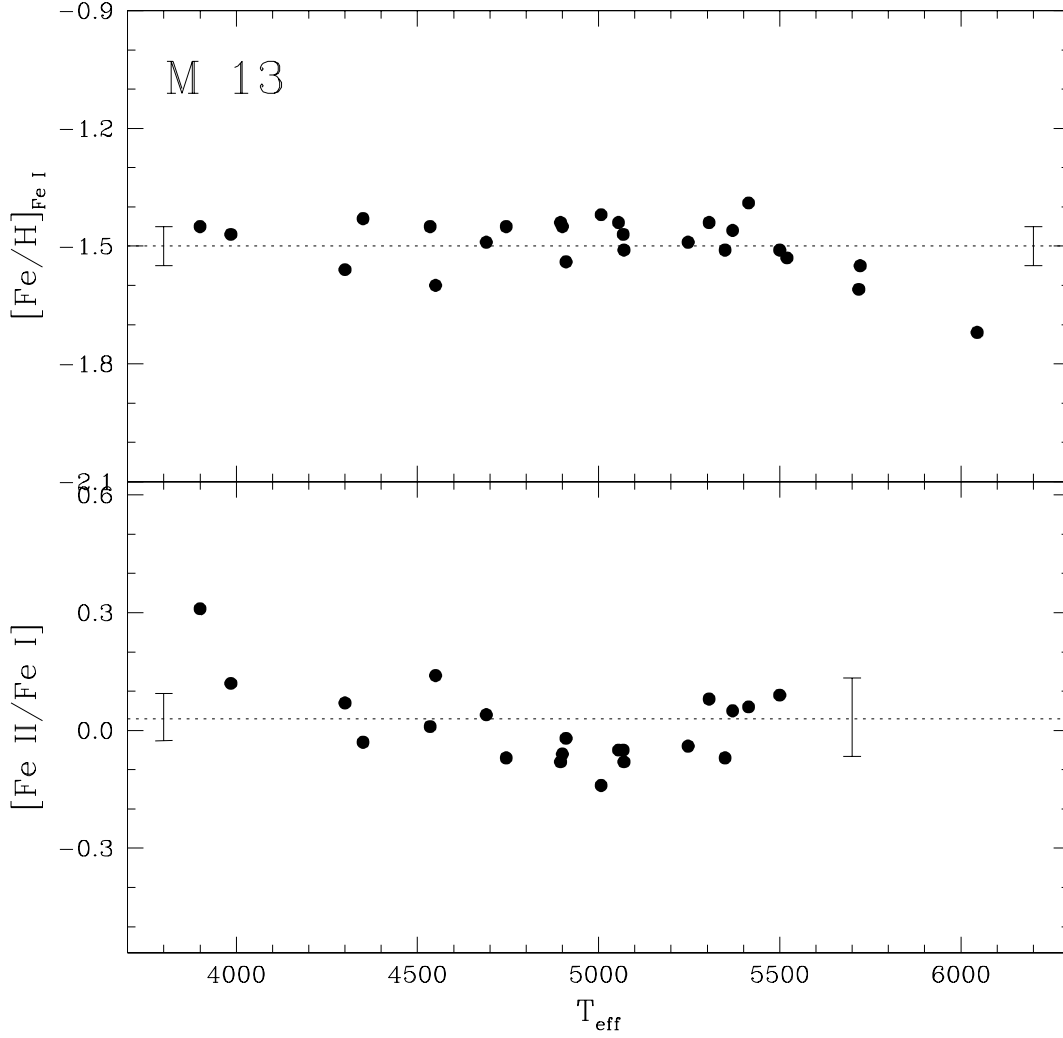


Fig. 9.— The $[\text{Fe}/\text{H}]$ from lines of Fe I is shown as a function of T_{eff} in the upper panel, while the lower panel shows the ionization equilibrium of Fe for our sample of 25 stars in M13. The error bars on the left margin are those of the most luminous giants, while the error bars on the right margin are those of the faintest stars in our sample. The dotted horizontal line indicates the mean value for our sample in this globular cluster.

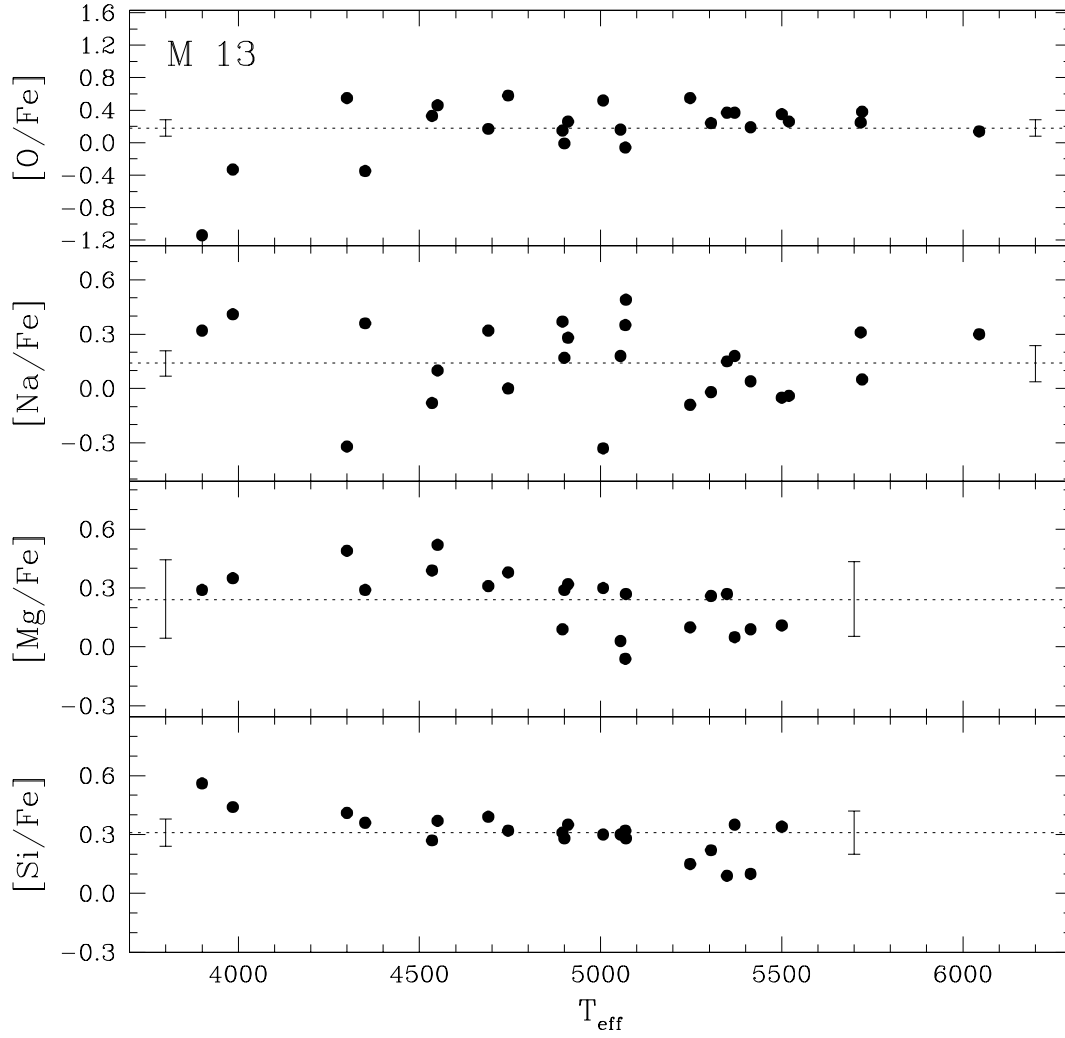


Fig. 10.— $[X/Fe]$ for the elements O, Na, Mg and Si are shown as a function of T_{eff} for our sample of 13 stars in M13. The error bars for the most luminous and least luminous stars, as well as the cluster mean, are indicated as in Figure 2.

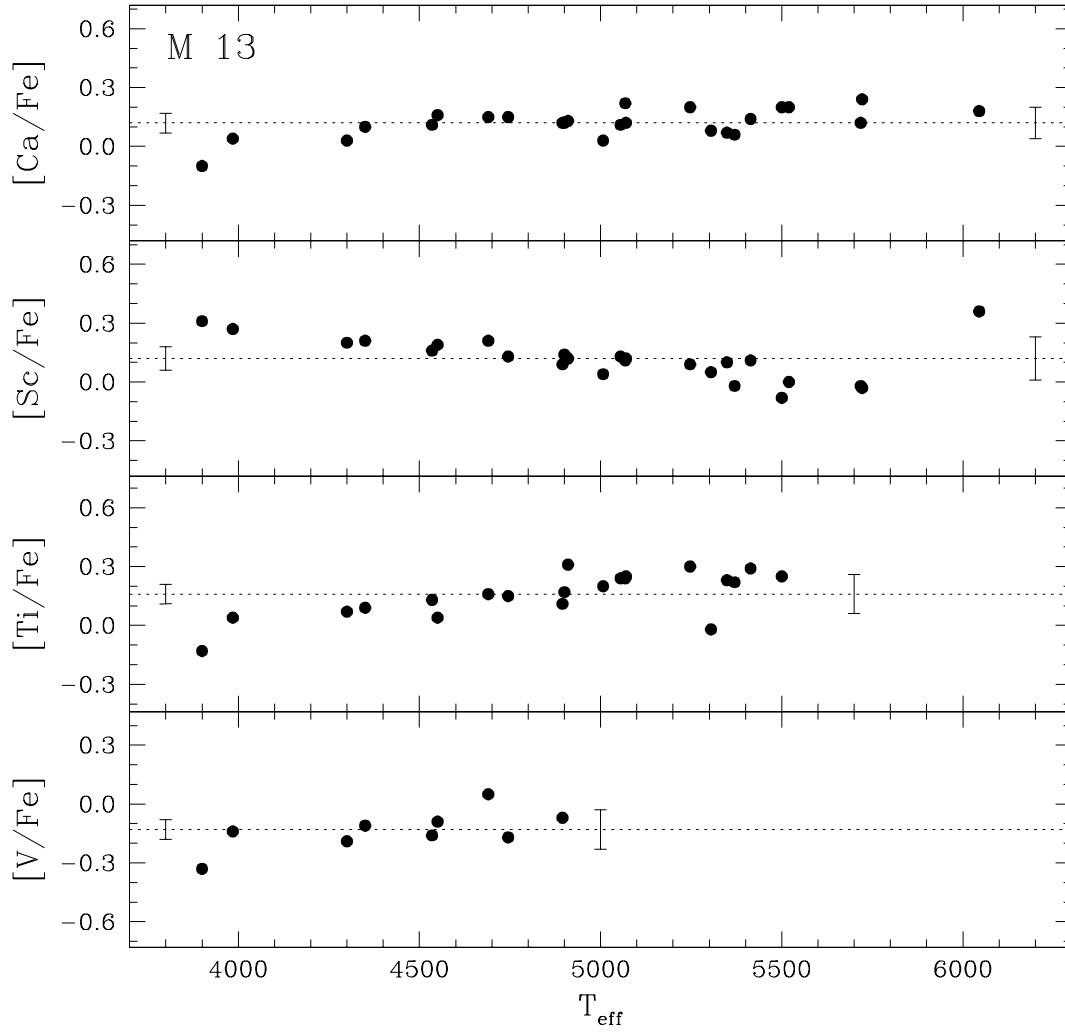


Fig. 11.— Same as Figure 10 for the elements Ca, Sc, Ti and V in M13.

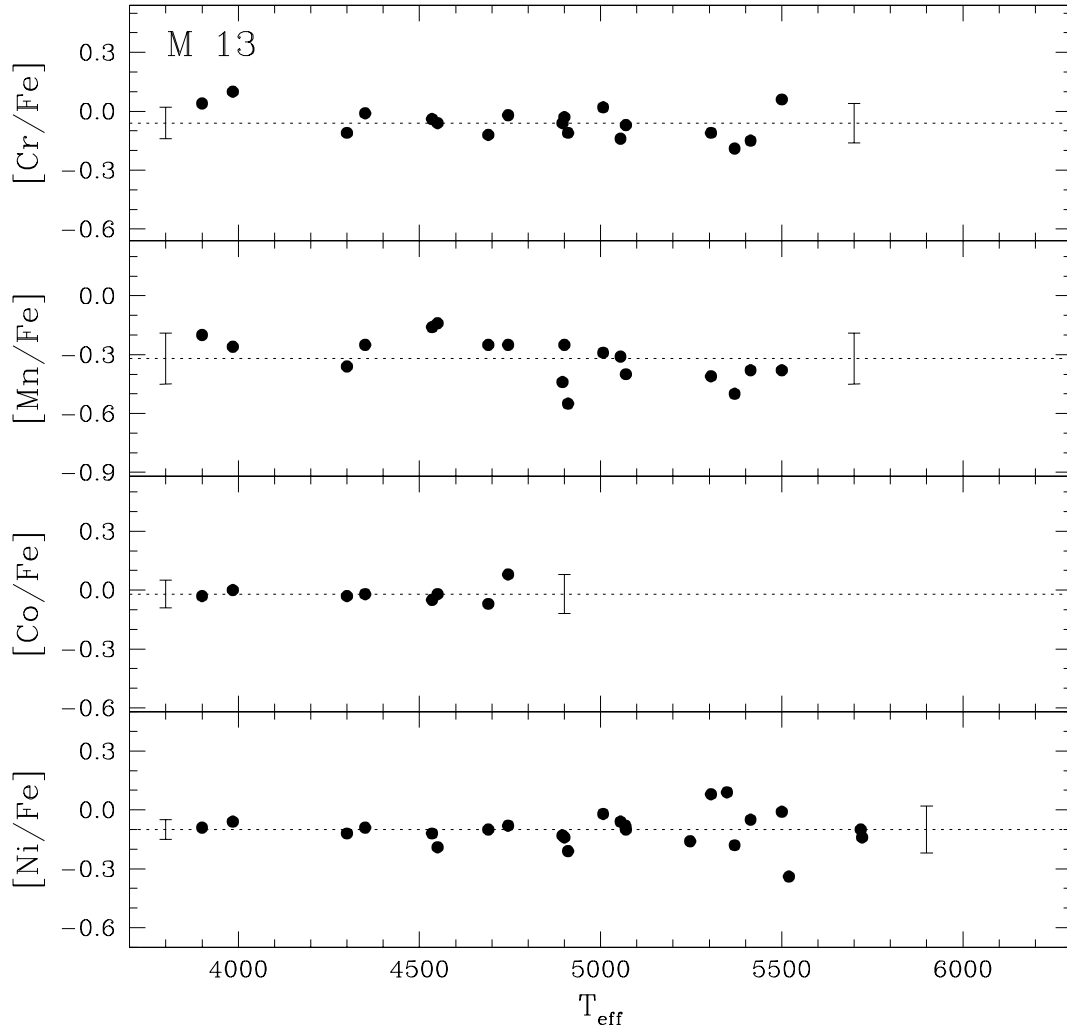


Fig. 12.— Same as Figure 10 for the elements Cr, Mn, Co and Ni in M13.

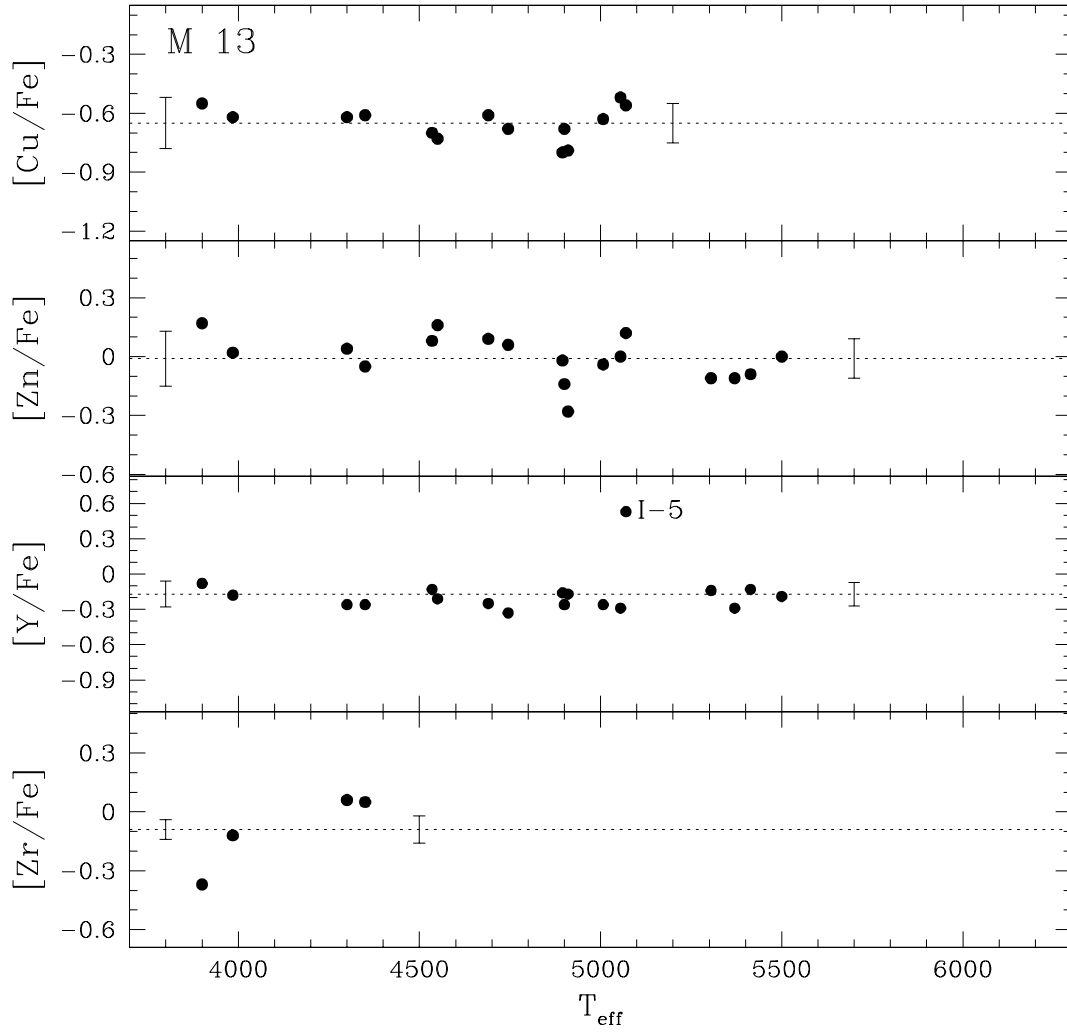


Fig. 13.— Same as Figure 10 for the elements Cu, Zn, Y and Zr for M13.

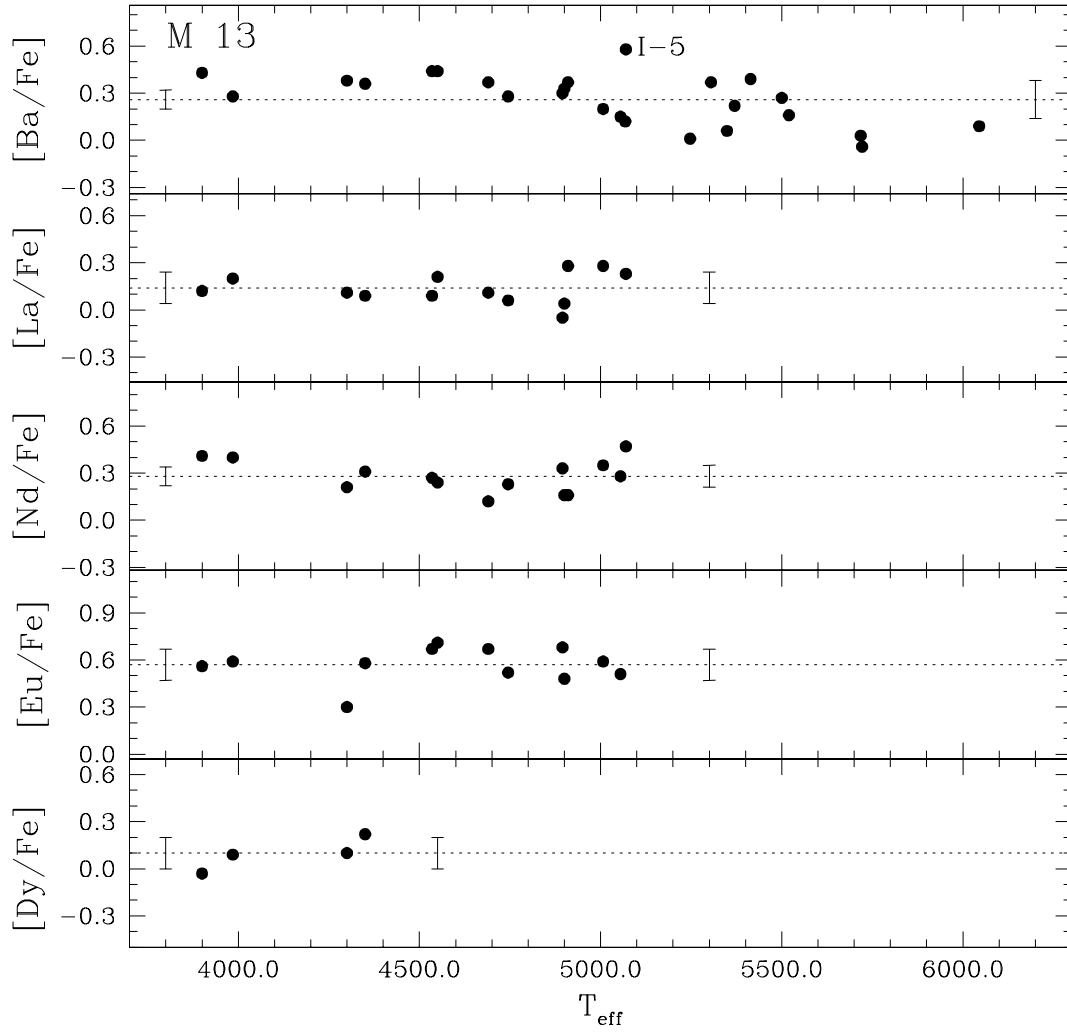


Fig. 14.— Same as Figure 10 for the elements Ba, La, Nd, Eu and Dy in M13.

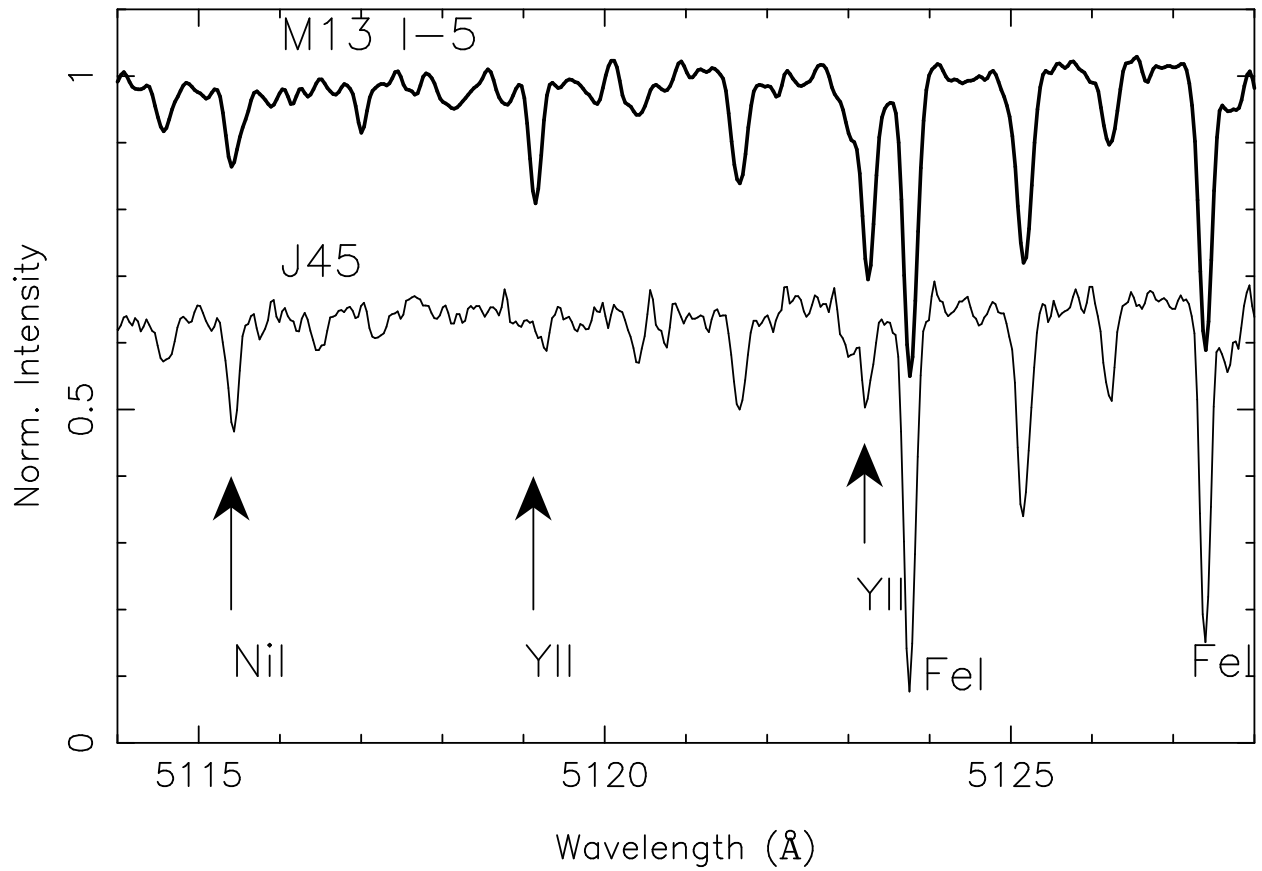


Fig. 15.— A section of the spectrum of the Y-rich star M13 I-5 is shown in the region of several Y II lines. The same region in the spectrum of star M13 J45, a star 0.5 mag brighter in V along the RGB, hence slightly cooler than star I-5, is shown for comparison.

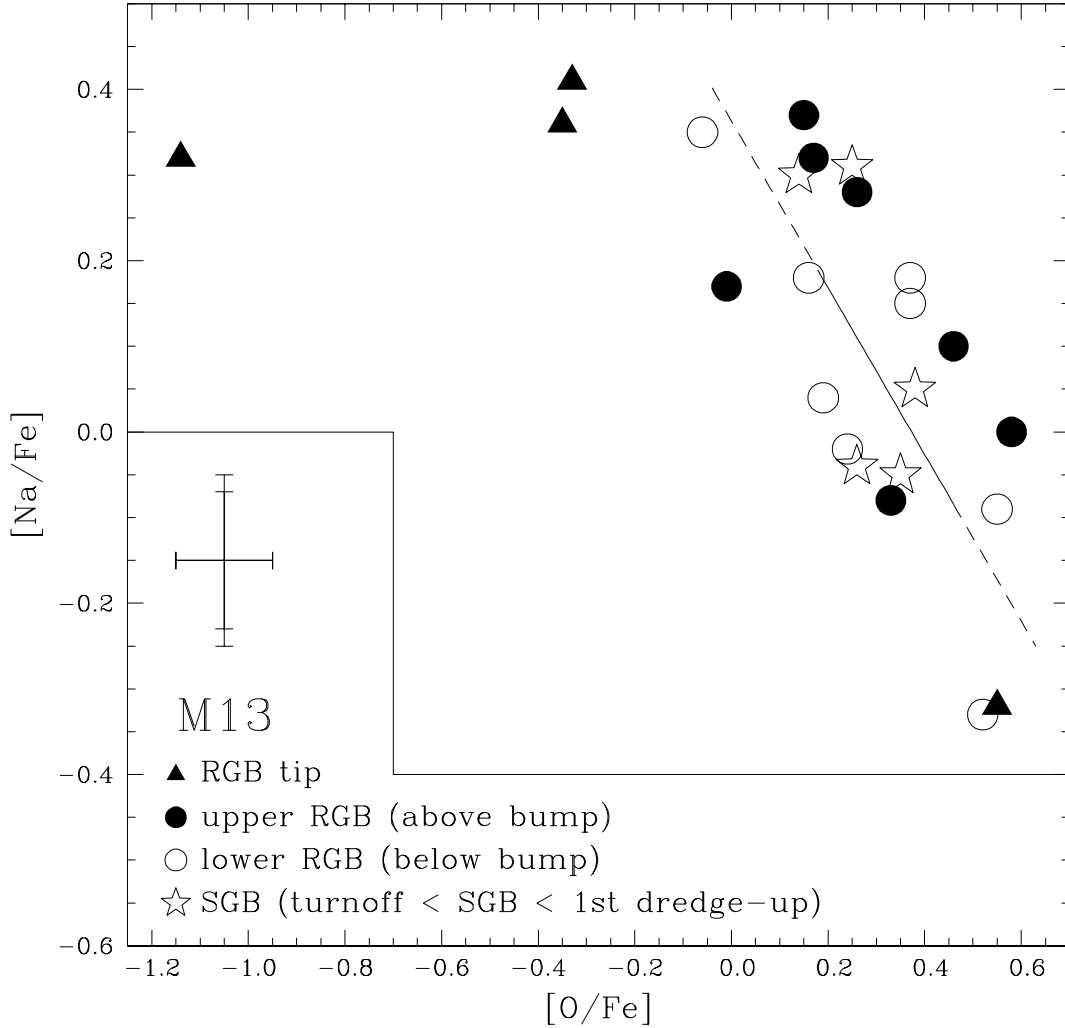


Fig. 16.— The ratio $[Na/Fe]$ is shown as a function of $[O/Fe]$ for 24 of our sample of 25 stars in M13. The error bars typical of the most luminous and least luminous stars in our sample are indicated. The line represents the relationship found for M3, with a vertical offset of +0.22 dex ; the line extends over the range covered by the sample of Sneden *et al.* (2004), it is solid between the first and third quartiles of their sample and is dashed outside that regime. The different symbols denote the luminosity of the star.

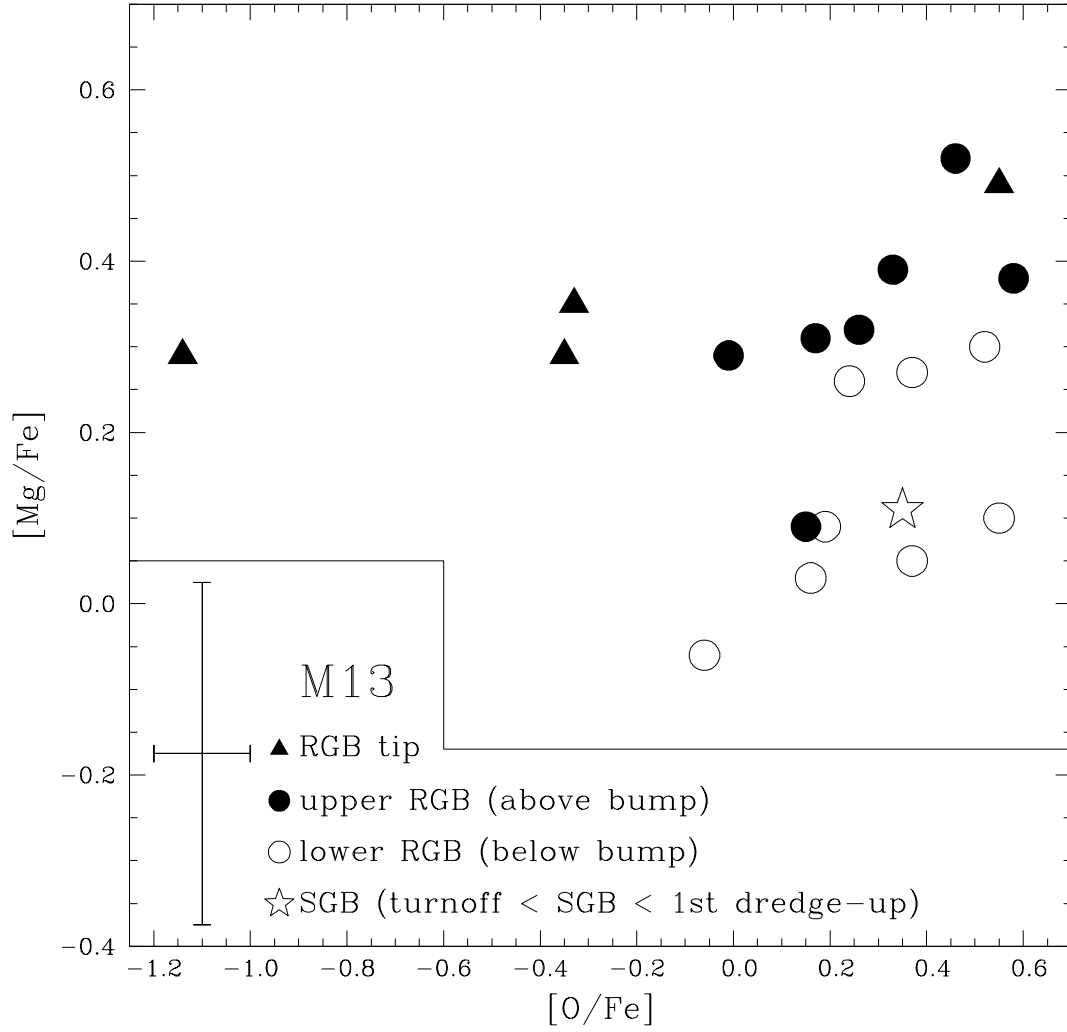


Fig. 17.— The ratio $[Mg/Fe]$ is shown as a function of $[O/Fe]$ for 20 of our sample of 25 stars in M13. The different symbols denote the luminosity of the star. The error bars typical of the most luminous and least luminous stars in our sample are indicated.

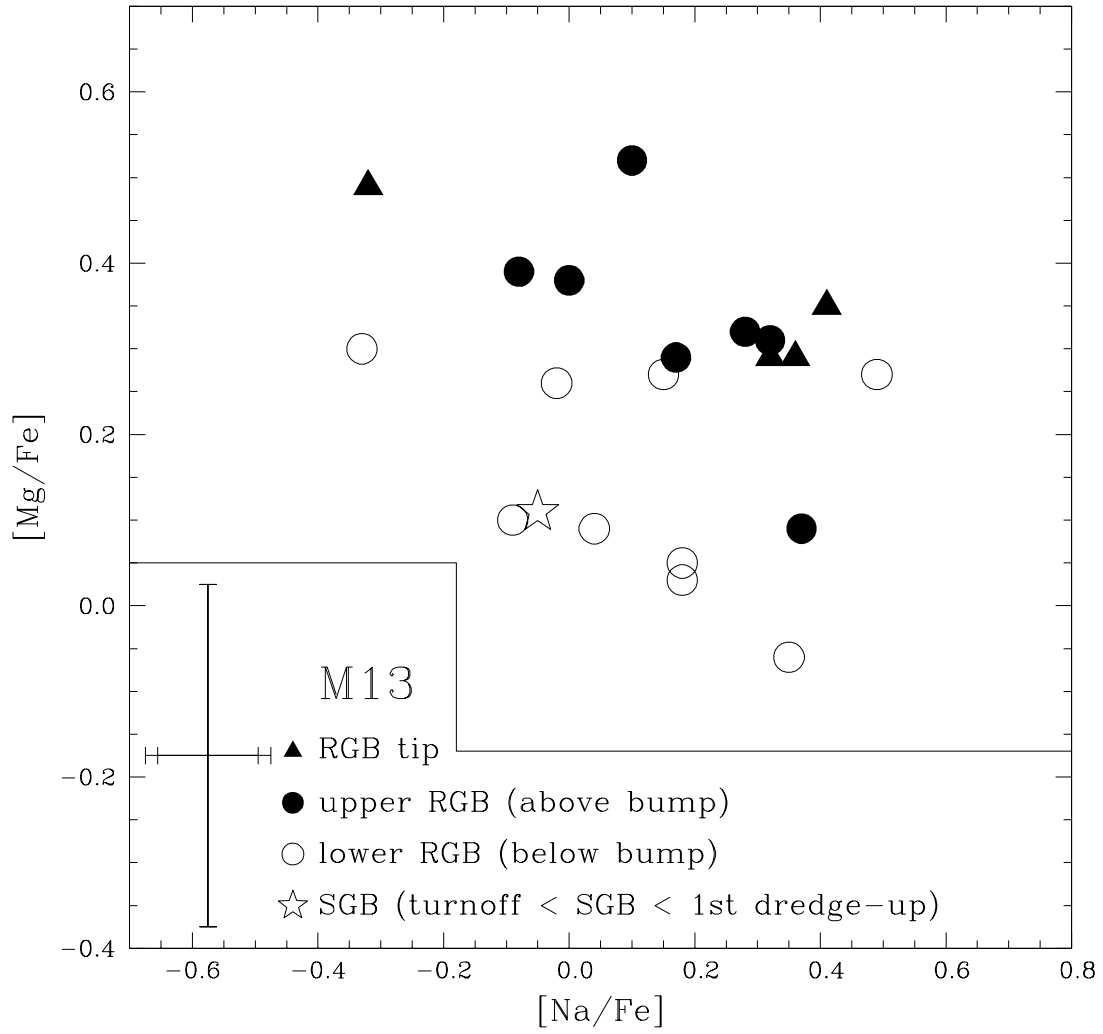


Fig. 18.— The ratio $[Mg/Fe]$ is shown as a function of $[Na/Fe]$ for 21 of our sample of 25 stars in M13. The different symbols denote the luminosity of the star. The error bars typical of the most luminous and least luminous stars in our sample are indicated.

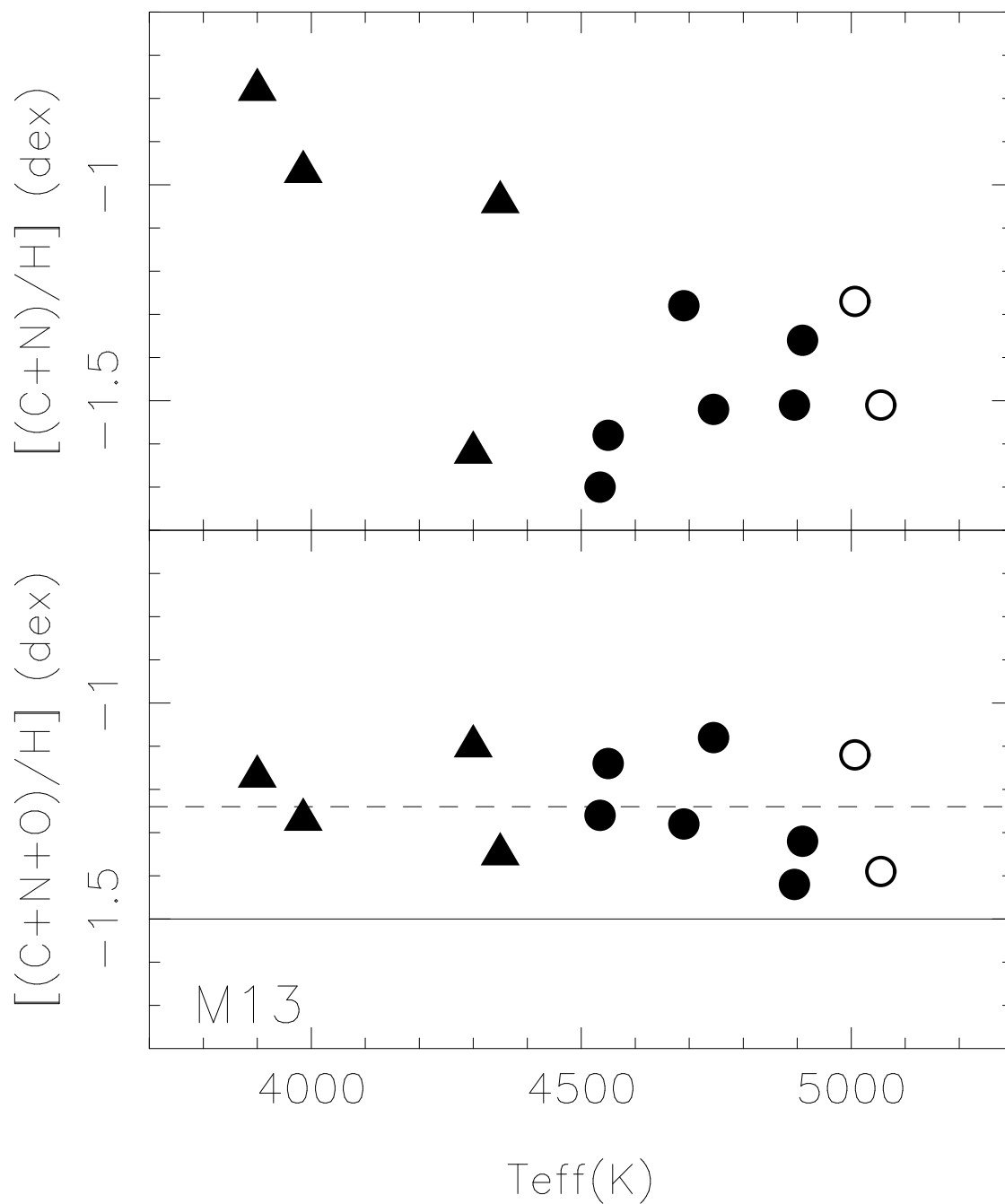


Fig. 19.— The sum of C+N+O (lower panel) and of C+N (upper panel) is shown as a function of T_{eff} for 12 stars in M13. The different symbols denote the luminosity of the star (as in Figure 16). The dashed horizontal line in the lower panel is the mean of $(C+N+O)/H$, while the solid horizontal line is the cluster mean for $[Fe/H]$.

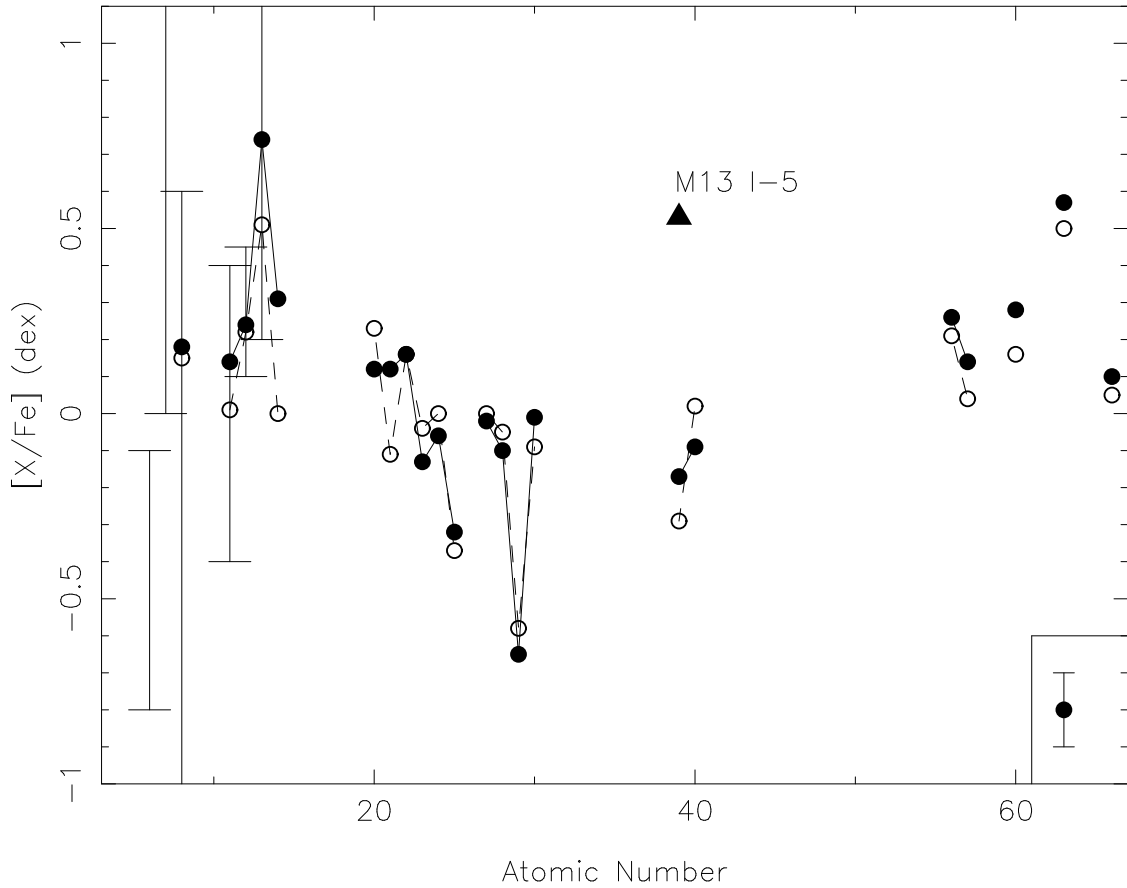


Fig. 20.— The abundance ratios $[X/Fe]$ are shown as a function of atomic number for M3 and for M13. Filled circles are used for M13 and open circles for M3, while a filled triangle denotes the $[Y/Fe]$ for the peculiar star M13 I-5. Elements with consecutive atomic numbers whose abundances have been determined are indicated by solid (dashed) lines. For those elements which show star-to-star variation, ranges are indicated for C, N (both from Briley, Cohen & Stetson 2004), O, Na, Mg, and Al, where the Al range is from Sneden *et al.* (2004). A typical error bar is shown at the lower right.

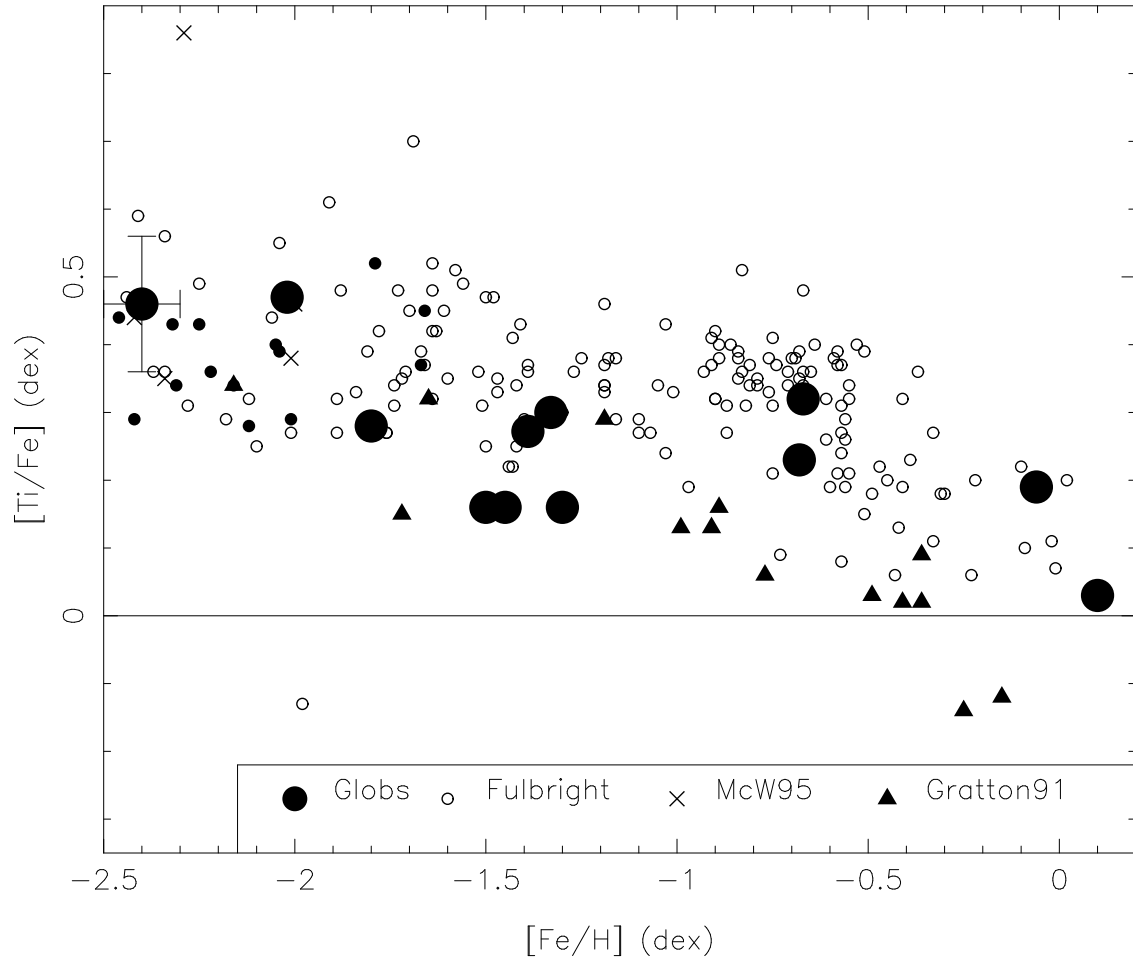


Fig. 21.— The abundance ratio $[\text{Ti}/\text{Fe}]$ is shown as a function of $[\text{Fe}/\text{H}]$ for a sample of 13 Galactic GCs (see text for references), indicated as large filled circles. This is compared to the same relationship for halo field stars (sources and symbols indicated on the figure). An error bar typical of the GCs is shown for the lowest metallicity GC.

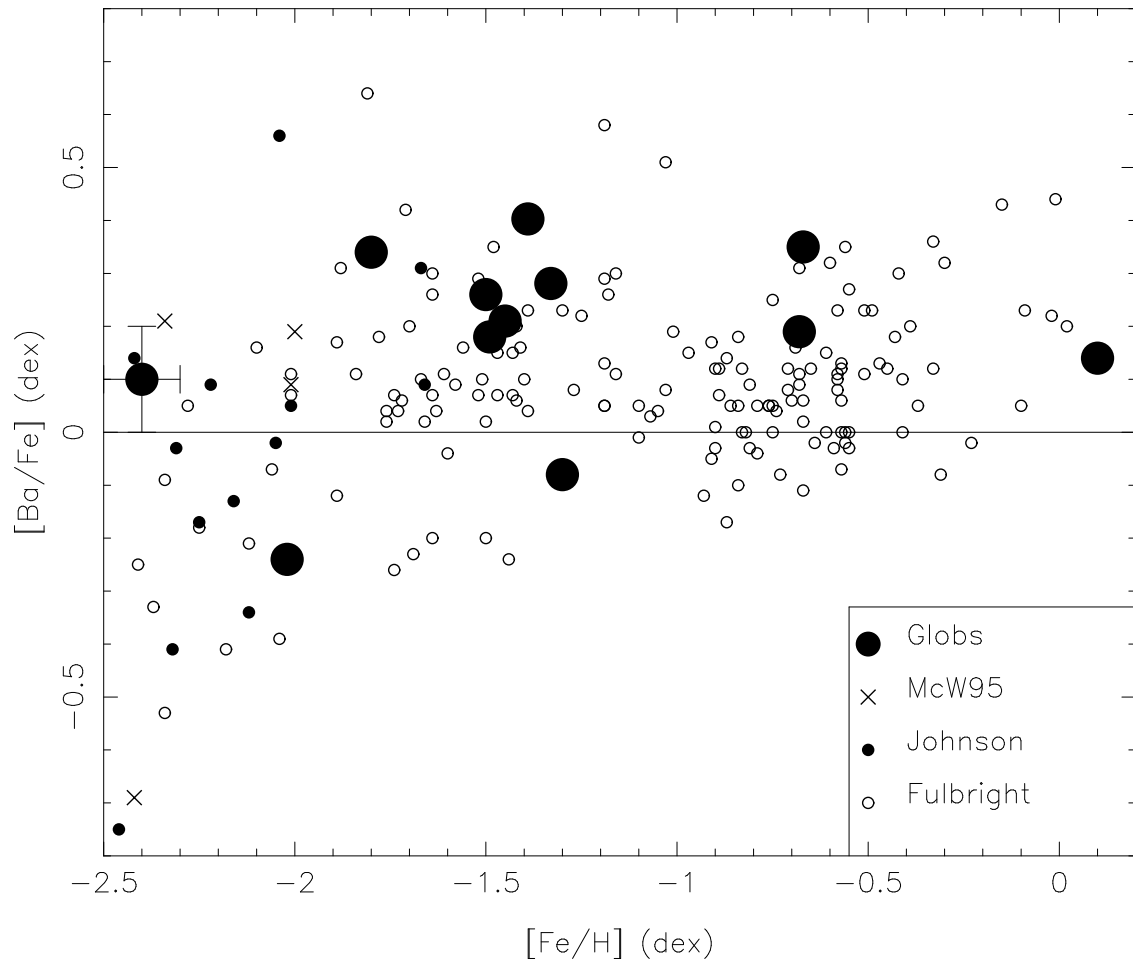


Fig. 22.— The same as Figure 21, but for $[Ba/Fe]$.

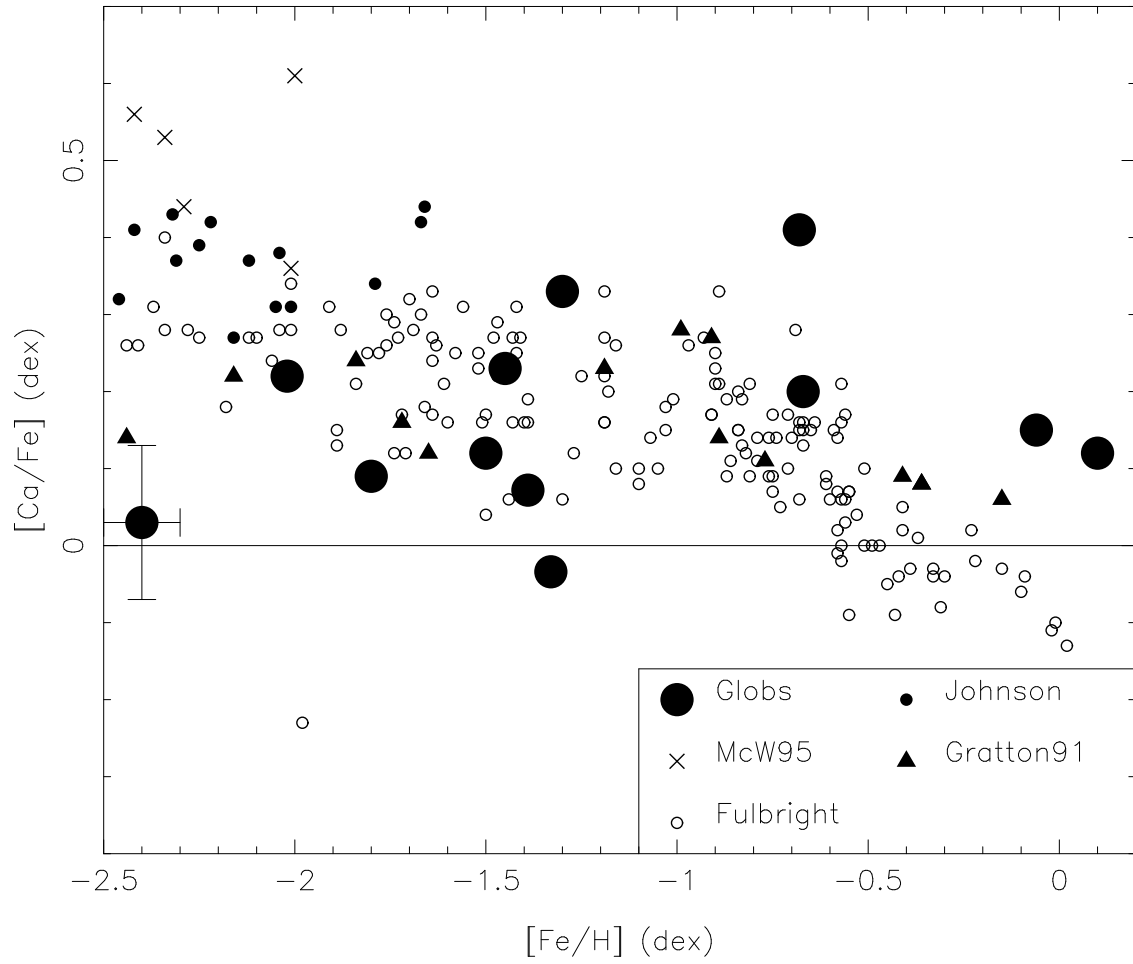


Fig. 23.— The same as Figure 21, but for $[Ca/Fe]$. The gf values adopted by the various groups have been adjusted to a common absolute scale.